

# **Microbial process in organic matter stabilization in agricultural soil**

Von der Naturwissenschaftlichen Fakultät der  
Gottfried Wilhelm Leibniz Universität Hannover

zur Erlangung des Grades

Doktorin der Naturwissenschaften (Dr. rer. nat.)

genehmigte Dissertation

von

Guan Cai, Master Degree of Science (China)

Referent: Prof. Dr. rer. nat. Georg Guggenberger

Korreferent: Prof. Dr. rer. nat. Marcus Andreas Horn

Korreferent: Prof. Tida Ge. PhD

Tag der Promotion: 18.03.2022

## Abstract

Agricultural soils are important C reservoirs that influence global climate change. Plants modulate the soil environment by reduced C release from their roots or through rapid nutrient uptake from the soil by their related microorganisms. Microbial metabolic functions (catabolic and anabolic) are essential control valves for soil organic matter (SOM) turnover and also an essential factor in increasing agricultural soil productivity and decelerated increase in atmospheric CO<sub>2</sub> concentration. However, studies on C and nutrient cycling mostly focus on the effect of organic matter input but rarely combined with their microbial metabolic processes (catabolic and anabolic pathways) in SOM turnover. In this thesis, I have investigated the microbial metabolic processes involved in organic matter decomposition, transformation, and accumulation in agricultural soils, depending on the impact of substrate-nutrient stoichiometry ratios (such as C/N ratios) of organic compounds and the type of organic matter (such as labile root exudates and lignin). This overarching research goal has been explored in three different experiments.

In the first experiment, I investigated the effect of different C/N ratios with low molecular weight and labile plant-derived organic matter (such as root exudates) on microbial activities. I incubated a paddy field soil with three artificial root exudates characterized by different C/N ratios (CN6, CN10, and CN80) using a mixture of glucose, oxalic acid, and alanine. In the second experiment, I focused on the microbial degradation of a complex plant biomacromolecule (lignin), which is considered stable particularly under anaerobic conditions. I incubated the soil for 365 days to investigate the microbial degradation of lignin (<sup>13</sup>C lignin >98 atom%, 80% chemical purity) under anaerobic, followed by aerobic, conditions at different time intervals. While the first two studies dealt with short- and intermediate-term incubation experiments, in a third experiment, I focused on soil samples collected from the field along with from a large-scale area from three primary crops (maize, wheat, and paddy) to investigate the bioavailability of soil organic C (SOC), total N (TN), and organic P concentration in agricultural soils.

In the first experiment, root exudates with low C/N ratios (such as CN6 with high N content) had 2.3-fold higher CO<sub>2</sub> emissions than those with high C/N ratios (such as CN80

with low N content) after 45 days incubation. An associated increased C- to N-hydrolase ratio with increasing substrate C/N ratio suggests that the C/N stoichiometry of root exudates controls SOM mineralization by affecting the specific microbial response through the catabolic activity of C- and N-releasing extracellular enzymes to adjust the microbial C/N ratio. The high C use efficiency (CUE) corresponded to a high C/N ratio of root exudates, indicating that low N-containing root exudates increased the CUE for their biomass synthesis for C accumulation. In the second experiment, the microorganisms degraded lignin under anaerobic and aerobic conditions as indicated by the cumulative CO<sub>2</sub> produced. <sup>13</sup>C lignin degradation contributed about 3.4% CO<sub>2</sub> mineralization during the anaerobic incubation period (1 year). The cumulative lignin-derived C content under aerobic conditions was 11.7% higher than that under anaerobic conditions during four intervals. Lignin-derived microbial biomass C (MBC) accumulation under long-term anaerobic conditions suggests that anaerobic anabolic processes induce an entombing effect, thus promoting SOM accumulation. In the third experiment, SOC, TN, and organic P concentration was significantly related to the diversity of the microbial community and fitted well to linear and quadratic models, suggesting that SOC, TN, and organic P concentration shaped the microbial community (such as *phoD*-harboring bacteria). The organic P concentration (such as enzyme-P, a fraction of organic P) shaped the *phoD*-harboring bacterial diversity and followed the metabolic theory of ecology.

Combined, the results show that labile and stable organic matter (OM) are decomposed, transformed, and accumulated by a microbial metabolic pathway in agricultural soil. The low C/N ratios of labile OM (such as root exudates) followed the catabolism with high soil C mineralization. In contrast, the high C/N ratios of root exudates increased microbial biomass with reduced CO<sub>2</sub> emission, followed by an anabolic activity for soil C sequestration. The stable OM (i.e., lignin) is also degraded under anaerobic conditions through catabolic activity and partly undergoing stabilization reactions by anabolic activity. The SOC, TN, and organic P concentration affected the microbial communities, particularly in the organic P (i.e., enzyme-P) according to the metabolic theory in response to the microbial process in SOM stabilization.

**Keywords:** Soil organic matter, Metabolic process, Root exudates, Lignin, Organic phosphorus

## Zusammenfassung

Landwirtschaftliche Böden sind wichtige C-Speicher, die den globalen Klimawandel beeinflussen. Pflanzen beeinflussen das Bodenmilieu durch eine verringerte C-Freisetzung aus ihren Wurzeln oder durch eine rasche Nährstoffaufnahme aus dem Boden durch ihre verwandten Mikroorganismen. Die mikrobiellen Stoffwechselfunktionen (katabolisch und anabolisch) sind wesentliche Steuerventile für den Umsatz organischer Substanz (SOM) im Boden und auch ein wesentlicher Faktor für die Steigerung der landwirtschaftlichen Bodenproduktivität und die Verlangsamung des Anstiegs der atmosphärischen CO<sub>2</sub>-Konzentration. Studien über den Kohlenstoff- und Nährstoffkreislauf konzentrieren sich jedoch meist auf die Auswirkungen des Eintrags organischer Substanz, werden aber selten mit den mikrobiellen Stoffwechselprozessen (katabole und anabole Wege) beim SOM-Umsatz kombiniert. In dieser Arbeit habe ich die mikrobiellen Stoffwechselprozesse untersucht, die am Abbau, der Umwandlung und der Akkumulation organischer Stoffe in landwirtschaftlich genutzten Böden beteiligt sind, und zwar in Abhängigkeit von den Auswirkungen der Substrat-Nährstoff-Stöchiometrie-Verhältnisse (z. B. C/N-Verhältnisse) der organischen Verbindungen und der Art der organischen Stoffe (z. B. labile Wurzelexsudate und Lignin). Dieses übergreifende Forschungsziel wurde in drei verschiedenen Experimenten untersucht.

Im ersten Experiment untersuchte ich die Auswirkung verschiedener C/N-Verhältnisse mit niedermolekularem und labilen pflanzlichen organischen Stoffen (wie Wurzelexsudaten) auf die mikrobiellen Aktivitäten. Ich bebrütete einen Reisfeldboden mit drei künstlichen Wurzelexsudaten, die sich durch unterschiedliche C/N-Verhältnisse (CN<sub>6</sub>, CN<sub>10</sub> und CN<sub>80</sub>) auszeichneten, unter Verwendung einer Mischung aus Glukose, Oxalsäure und Alanin. Im zweiten Experiment konzentrierte ich mich auf den mikrobiellen Abbau eines komplexen pflanzlichen Biomakromoleküls (Lignin), das insbesondere unter anaeroben Bedingungen als stabil gilt. Ich bebrütete den Boden 365 Tage lang, um den mikrobiellen Abbau von Lignin (<sup>13</sup>C-Lignin >98 Atom-%, 80 % chemische Reinheit) unter anaeroben und anschließend unter aeroben Bedingungen in verschiedenen Zeitabständen zu untersuchen. Während sich die ersten beiden Studien mit kurz- und mittelfristigen Inkubationsexperimenten befassten, konzentrierte ich mich in einem dritten Experiment auf

Bodenproben, die auf dem Feld sowie auf einer großflächigen Fläche aus drei Hauptkulturen (Mais, Weizen und Reis) entnommen wurden, um die Bioverfügbarkeit von organischem C (SOC), Gesamt-N (TN) und der organischen P-Konzentration in landwirtschaftlichen Böden zu untersuchen.

Im ersten Experiment wiesen Wurzelexsudate mit niedrigem C/N-Verhältnis (z. B. CN6 mit hohem N-Gehalt) nach 45 Tagen Inkubation 2,3-fach höhere CO<sub>2</sub>-Emissionen auf als solche mit hohem C/N-Verhältnis (z. B. CN80 mit niedrigem N-Gehalt). Ein damit verbundenes erhöhtes C- zu N-Hydrolase-Verhältnis mit steigendem Substrat-C/N-Verhältnis deutet darauf hin, dass die C/N-Stöchiometrie der Wurzelexsudate die SOM-Mineralisierung steuert, indem sie die spezifische mikrobielle Reaktion durch die katabole Aktivität von C- und N-freisetzenden extrazellulären Enzymen beeinflusst, um das mikrobielle C/N-Verhältnis anzupassen. Die hohe C-Nutzungseffizienz (CUE) entsprach einem hohen C/N-Verhältnis der Wurzelexsudate, was darauf hindeutet, dass niedrige N-haltige Wurzelexsudate die CUE für ihre Biomassesynthese zur C-Akkumulation erhöhten. Im zweiten Versuch bauten die Mikroorganismen Lignin unter anaeroben und aeroben Bedingungen ab, was durch die kumulative CO<sub>2</sub>-Produktion angezeigt wurde. Der <sup>13</sup>C-Ligninabbau trug während der anaeroben Inkubationszeit (1 Jahr) zu einer CO<sub>2</sub>-Mineralisierung von etwa 3,4 % bei. Der kumulative, aus Lignin gewonnene C-Gehalt war unter aeroben Bedingungen um 11,7 % höher als unter anaeroben Bedingungen während vier Intervallen. Die Akkumulation von aus Lignin gewonnenem mikrobiellem Biomasse-C (MBC) unter langfristigen anaeroben Bedingungen deutet darauf hin, dass anaerobe anabole Prozesse einen Einlagerungseffekt induzieren und damit die SOM-Akkumulation fördern. Im dritten Versuch standen die SOC-, TN- und organische P-Konzentration in signifikantem Zusammenhang mit der Diversität der mikrobiellen Gemeinschaft und passten gut zu linearen und quadratischen Modellen, was darauf hindeutet, dass die SOC-, TN- und organische P-Konzentration die mikrobielle Gemeinschaft (z. B. *phoD*-haltige Bakterien) prägte. Die organische P-Konzentration (z. B. Enzym-P, eine Fraktion des organischen P) prägte die Vielfalt der *phoD*-haltigen Bakterien und folgte der metabolischen Theorie der Ökologie.

Zusammengenommen zeigen die Ergebnisse, dass labiles und stabiles organisches Material (OM) durch einen mikrobiellen Stoffwechselweg in landwirtschaftlich genutzten Böden abgebaut, umgewandelt und akkumuliert wird. Die niedrigen C/N-Verhältnisse der

labilen organischen Substanz (z. B. Wurzelexsudate) folgten dem Katabolismus mit hoher C-Mineralisierung im Boden. Im Gegensatz dazu erhöhten die hohen C/N-Verhältnisse von Wurzelexsudaten die mikrobielle Biomasse bei verringerter CO<sub>2</sub>-Emission, gefolgt von einer anabolen Aktivität zur Sequestrierung von C im Boden. Stabiles organisches Material (z. B. Lignin) wird auch unter anaeroben Bedingungen durch katabole Aktivität abgebaut und teilweise durch Stabilisierungsreaktionen durch anabole Aktivität. Die SOC-, TN- und organische P-Konzentration wirkte sich auf die mikrobiellen Gemeinschaften aus, insbesondere auf den organischen P (d. h. Enzym-P) gemäß der Stoffwechseltheorie als Reaktion auf den mikrobiellen Prozess der SOM-Stabilisierung.

**Stichwörter:** Organische Bodensubstanz, Stoffwechselprozess, Wurzelexsudate, Lignin, Organischer Phosphor

---

---

## Table of Contents

<b>Abstract</b> .....	<b>I</b>
<b>Zusammenfassung</b> .....	<b>III</b>
<b>Table of Contents</b> .....	<b>VI</b>
<b>List of Tables</b> .....	<b>VII</b>
<b>List of Figures</b> .....	<b>IX</b>
<b>Abbreviations</b> .....	<b>XIV</b>
<b>1 GENERAL INTRODUCTION</b> .....	<b>1</b>
1.1 THE GLOBAL CARBON CYCLING .....	1
1.2 SOIL ORGANIC MATTER (SOM).....	2
1.3 MICROBES AND METABOLIC PATHWAY ON SOM.....	4
1.4 C USE EFFICIENCY AND ENZYME ACTIVITY .....	7
1.5 MOTIVATION AND GENERAL HYPOTHESES .....	9
<b>2 STUDY 1</b> .....	<b>12</b>
ROOT EXUDATES WITH LOW C/N RATIOS ACCELERATE CO <sub>2</sub> EMISSIONS FROM PADDY SOIL .....	13
<b>3 STUDY 2</b> .....	<b>39</b>
LIGNIN DEGRADATION IN WETLAND SOIL BY ANAEROBIC AND AEROBIC PROCESSE.....	40
<b>4 STUDY 3</b> .....	<b>72</b>
ORGANIC PHOSPHORUS AVAILABILITY SHAPES THE DIVERSITY OF PHOD-HARBORING BACTERIA IN AGRICULTURAL SOIL.....	73
<b>5 GENERAL DISCUSSION</b> .....	<b>110</b>
5.1 MICROBIAL RESPONSES AND ENZYME ACTIVITY ON SOM MINERALIZATION .....	110
5.2 SOM ACCUMULATION UNDER ANAEROBIC CONDITIONS.....	112
5.3 EFFECTS OF NUTRIENTS ON MICROBIAL ACTIVITIES.....	113
<b>6 CONCLUSION AND OUTLOOK</b> .....	<b>116</b>
<b>BIBLIOGRAPHY</b> .....	<b>117</b>
<b>ACKNOWLEDGMENTS</b> .....	<b>136</b>
<b>CURRICULUM VITAE AND PUBLICATIONS</b> .....	<b>137</b>



---

## List of Tables

### Study 1

**Table 1.** Amounts of individual substrates added ( $\text{mg incubation flask}^{-1} \text{ day}^{-1}$ ) to the paddy soil as artificial root exudates in the different treatments.

**Table S1.** Amounts of individual substrates added ( $\text{mg incubation flask}^{-1}$ ) to the paddy soil as artificial root exudates in the different treatments.

**Table S2.** Soil C/N ratios, microbial biomass C (MBC), microbial biomass N (MBN), DOC, and  $\text{NH}_4^+$  at days 3, 12, and 45 during the 45-day incubation period. C-only represents addition of C substrates glucose and oxalic acid only; CN6, CN10, and CN80 represent addition of C substrates glucose and oxalic acid as well as the N substrate alanine at different C/N stoichiometries of CN6, CN10, and CN80, respectively. Different letters indicate significant differences among stoichiometric ratios at the end of cumulative  $\text{CO}_2$  emission (one-way ANOVA and LSD test;  $P < 0.05$  level). Values represent means + standard errors ( $n = 4$ ).

### Study 3

**Table S1.** Second-order Akaike information criterion values (AICc) of the relationship between OTU richness, Faith's phylogenetic diversity and Shannon index of the phoD-harboring bacteria and soil organic carbon (SOC), total nitrogen (TN), pH, available organic P (Enzyme P), and inorganic P extracted by  $\text{CaCl}_2$  ( $\text{CaCl}_2$  P), Citrate (Citrate P), HCl (HCl P) and  $\text{NaHCO}_3$  (Olsen P) fitted to linear, quadratic and Michaelis-Menten models. Significant relationships are bolded.

**Table S2.** Regression coefficient ( $R^2$ ) and significance ( $p$ ) of the optimal models predicting the relationship between OTU richness, Faith's phylogenetic diversity, and Shannon index of the phoD-harboring bacteria and soil organic carbon (SOC), total nitrogen (TN), pH, available organic P (Enzyme P), and inorganic P extracted by  $\text{CaCl}_2$  ( $\text{CaCl}_2$  P), Citrate (Citrate P), HCl (HCl P), and  $\text{NaHCO}_3$  (Olsen P). The superscripts indicate the type of the optimal models: L, linear; Q, quadratic; M, Michaelis-Menten. Significant relationships are bolded.

**Table S3.** Second-order Akaike information criterion values (AICc) of the relationship between node number, edge number, network density, betweenness centrality, average path length, and the ratio of positive edges of the *phoD*-harboring bacteria and soil organic carbon (SOC), total nitrogen (TN), pH, available organic P (Enzyme P), and inorganic P extracted by CaCl<sub>2</sub> (CaCl<sub>2</sub> P), Citrate (Citrate P), HCl (HCl P) and NaHCO<sub>3</sub> (Olsen P) fitted to linear, quadratic and Michaelis-Menten models.

**Table S4.** Regression coefficient ( $R^2$ ) and significance ( $p$ ) of the optimal models predicting the relationship between node number, edge number, network density, betweenness centrality, average path length, and the ratio of positive edges of the *phoD*-harboring bacteria and soil organic carbon (SOC), total nitrogen (TN), pH, available organic P (Enzyme P), and inorganic P extracted by CaCl<sub>2</sub> (CaCl<sub>2</sub> P), Citrate (Citrate P), HCl (HCl P) and NaHCO<sub>3</sub> (Olsen P). The superscripts indicate the type of the optimal models: L, linear; Q: quadratic; M, Michaelis-Menten. Significant relationships are bolded.

## List of Figures

### General Introduction

**Fig. 1.1** Diagram of the global C cycle from 2011 – 2020, modified from Friedlingstein et al. (2020 and 2021). All numbers in the background indicate fluxes and stocks quoted from Ciais et al. (2013), and Friedlingstein et al. (2021 and 2022). The ocean gross fluxes updated with a literature review from Price and Warren (2016) and Friedlingstein et al. (2020 and 2022).

**Fig. 1.2** A conceptual model of organic fragments and potential microbial metabolic processes in agricultural soil organic matter turnover. Modified from Lehmann and Kleber (2015), and Liang et al. (2017)..

### Study 1

**Fig. 1** CO<sub>2</sub> efflux rates (a) and cumulative CO<sub>2</sub> (b) over the 45-day incubation period. The control represents no addition of artificial root exudates to soil; C-only represents addition of C substrates glucose and oxalic acid only; CN6, CN10, and CN80 represent addition of C substrates glucose and oxalic acid as well as the N substrate alanine at different C/N stoichiometries of CN6, CN10, and CN80, respectively. Different letters indicate significant differences among stoichiometric ratios at the end of cumulative CO<sub>2</sub> emission (one-way ANOVA and LSD test; P < 0.05 level). Error bars show standard errors (n = 4).

**Fig. 2** Metabolic quotient of soil microbial biomass (qCO<sub>2</sub>) (a) and carbon use efficiency (CUE) (b) at days 3, 12, and 45 during the 45-day incubation period. C-only represents addition of C substrates glucose and oxalic acid only; CN6, CN10, and CN80 represent addition of C substrates glucose and oxalic acid as well as the N substrate alanine at different C/N stoichiometries of CN6, CN10, and CN80, respectively. Different letters and capital letters indicate significant differences among stoichiometric ratios and sampling periods, respectively (one-way ANOVA and LSD test; P < 0.05 level). Error bars show standard errors (n = 4).

**Fig. 3** Activity of extracellular enzymes  $\beta$ -1,4-glucosidase (BG),  $\beta$ -1,4-xylosidase (XYL), and  $\beta$ -1,4-N-acetyl-glucosaminidase (NAG) at days 3, 12, and 45 during the 45-day incubation period. C-only represents addition of C substrates glucose and oxalic acid only;

CN6, CN10, and CN80 represent addition of C substrates glucose and oxalic acid as well as the N substrate alanine at different C/N stoichiometries of CN6, CN10, and CN80, respectively. Different letters and capital letters indicate significant differences among stoichiometric ratios and sampling periods, respectively (one-way ANOVA and LSD test;  $P < 0.05$  level). Error bars show standard errors ( $n = 4$ ).

**Fig. 4** Relationships between metabolic quotient ( $q\text{CO}_2$ ) and soil enzyme stoichiometry (BG/NAG) (a),  $q\text{CO}_2$  with microbial biomass stoichiometry (MBC/ MBN) (c); carbon use efficiency (CUE) with soil enzyme stoichiometry (BG/NAG) (b), CUE with microbial biomass stoichiometry (MBC/ MBN) (d). Abbreviations are BG,  $\beta$ -1,4-glucosidase; NAG,  $\beta$ -1,4-N-acetyl glucosaminidase. The dots represent data from all treatments in the 45-day incubation period.

**Fig. 5** Structural equation model of the multivariate effects of C/N ratios, leaching water sample  $\text{DOC-L}/\text{NO}_3^-$ -L ratios and  $\text{DOC-L}/\text{NH}_4^+$ -L ratios, soil sample  $\text{DOC}/\text{NO}_3^-$  ratios and  $\text{DOC}/\text{NH}_4^+$  ratios, microbial biomass stoichiometry, and enzyme stoichiometry on the  $\text{CO}_2$  emission. Microbial biomass stoichiometry represents the ratios of microbial biomass C to microbial biomass N; enzyme stoichiometry represents the average ratios of the activity of  $\beta$ -1,4-glucosidase to  $\beta$ -1,4-N-acetyl glucosaminidase and the activity of  $\beta$ -1,4-xylosidase to  $\beta$ -1,4-N-acetyl glucosaminidase. The solid lines indicate positive path coefficients; dashed lines, negative.  $R^2$  values indicate the proportion of variance explained by each variable contribution to the  $\text{CO}_2$  emission from soil application with substrates. The numbers and the width of the arrows indicate the standardized path coefficients.

**Fig. 6** Standardized effect of stoichiometric C/N ratios, leaching water sample  $\text{DOC-L}/\text{NO}_3^-$ -L ratios and  $\text{DOC-L}/\text{NH}_4^+$ -L ratios, soil sample  $\text{DOC}/\text{NO}_3^-$  ratios and  $\text{DOC}/\text{NH}_4^+$  ratios, enzyme stoichiometry, and microbial biomass stoichiometry on  $\text{CO}_2$  emission.

## Study 2

**Fig. 1** Respiration rate of soil-derived C (a), tracer-derived C (b), the percentage of cumulative tracer contribution (c), cumulative  $\text{CO}_2$  emission in tracer labelled soil and control (d), and cumulative priming (e) in anaerobic wetland soil during 360 days of incubation. Values and error bars indicate mean  $\pm$  standard deviation ( $n= 4$ ). Asterisk indicates a significant difference between anaerobic labeled and unlabelled/control treatment ( $P < 0.05$ , Turkey's HSD).

**Fig. 2** Cumulative tracer-respired and lignin respired C (a) proportion of tracer respired C from tracer and pure lignin (b) from wetland soil during 360 days anaerobic incubation.

**Fig. 3** Respiration rate of soil-derived C (a, b, c, d), tracer-derived C (e, f, g, h), the percentage of tracer contribution (i, f, g, h), and priming (m, n, o, p) in the anaerobic and aerobic soil incubation of the wetland soil during the four periods 30-60 d, 90-120 d, 180-210 d, and 335-365 d after which the systems have been sampled. Values and error bars indicate mean  $\pm$  standard deviation (n= 4). Asterisks indicate a significant difference between anaerobic and aerobic treatment ( $P<0.05$ ).

**Fig. 4** The total amount of lignin (a), (Ac/Al)<sub>v</sub> ratios (b), and S/V ratios (c) in the anaerobic and aerobic wetland soil incubations at the four different sampling times. Values and error bars indicate mean  $\pm$  standard deviation (n= 4). Different capital letters and letters indicate significant differences between sampling periods and treatment with anaerobic and aerobic conditions ( $P<0.05$ ).

**Fig. 5** Incorporation of tracer into bulk soil and recovery of tracer-C in the anaerobic and aerobic wetland soil incubations at the four different sampling times. Values and error bars indicate mean  $\pm$  standard deviation (n= 4). Different capital letters and letters indicate significant differences between sampling periods and treatment with anaerobic and aerobic conditions ( $P<0.05$ ).

**Fig. 6** Soil-derived and tracer-derived dissolved organic carbon (DOC) (a, b) and microbial biomass carbon (MBC) (c, d) in the anaerobic and aerobic wetland soil incubations at the four different sampling times. Values and error bars indicate mean  $\pm$  standard deviation (n= 4). Different capital letters and letters indicate significant differences between sampling periods and treatment with anaerobic and aerobic conditions ( $P<0.05$ ).

**Fig. 7.** Relationships between tracer-derived MBC, tracer-derived DOC, and non-crystalline iron oxides (oxalate soluble Fe; Fe<sub>o</sub>) in the anaerobic and aerobic wetland soil incubations at the four different sampling times. The dots represent data from all treatments in the 390-day incubation period.

Graphical abstract: The carbon dioxide (CO<sub>2</sub>) emission in a one-year anaerobic incubation of a wetland soil. The total anaerobic emission rate ( $\mu\text{g CO}_2\text{-C g}^{-1}\text{ soil day}^{-1}$ ) consists of soil-derived C (yellow), tracer-derived C (blue), and lignin tracer-derived C (green) in the top area. The bottom area estimates the CO<sub>2</sub> emission from soil-derived C (yellow numbers) and

tracer-derived C (blue numbers) at the four different sampling periods during anaerobic (blue arrows) and aerobic conditions (red arrows).

**Fig. S1** Experiment design in the anaerobic and aerobic soil incubation of the wetland soil during 365 day incubation.

**Fig. S2** Cumulative tracer-respired C (a), and the tracer recovery % (e) in the anaerobic and aerobic soil incubation of the wetland soil during the four periods 30-60 d, 90-120 d, 180-210 d, and 335-365 d after which the systems have been sampled. Values and error bars indicate mean  $\pm$  standard deviation (n= 4). Asterisks indicate a significant difference between anaerobic and aerobic treatment ( $P<0.05$ ).

**Fig. S3** Activity of peroxidase and polyphenol oxidase in the anaerobic and aerobic wetland soil incubations at the four different sampling times. Values and error bars indicate mean  $\pm$  standard deviation (n= 4). Different capital letters and letters indicate significant differences between sampling periods and treatment with anaerobic and aerobic conditions ( $P<0.05$ ).

**Fig. S4** Activity of extracellular enzymes  $\alpha$ -1,4-glucosidase (AG),  $\beta$ -1,4-glucosidase (BG),  $\beta$ -1,4-cellobioside (Cello),  $\beta$ -1,4-xylosidase (XYL),  $\beta$ -1,4-phosphate (Phos), and  $\beta$ -1,4-N-acetyl-glucosaminidase (NAG) in the anaerobic and aerobic wetland soil incubations at the four different sampling times. Values and error bars indicate mean  $\pm$  standard deviation (n= 4). Different capital letters and letters indicate a significant difference between sampling periods and treatment with anaerobic and aerobic conditions ( $P<0.05$ ).

### Study 3

**Fig. 1** Regressions of the observed OTUs (a-c), Faith's phylogenetic diversity (d-f) and Shannon index (g-i) of the phoD-harboring bacteria to soil organic C (SOC; a, d, g), total nitrogen (TN; b, e, g) and available Po (Enzyme P; c, f, i) as fitted to optimal models suggested by the Second-order Akaike information criterion values (AICc) among linear, quadric and Michaelis-Menten patterns. The AICc values are shown in Table S1.

**Fig. 2** Full (a) and sparse (b) model of random forest analysis predicting the effect of soil properties, climate factors and crop species on the diversity of phoD-harboring bacteria. The bar plot in figure b indicates the explanation on diversity variation of each sparse model; red colored boxes below each bar indicate the variables marked at left are used in the model, while the empty boxes indicate the variables are not used. Significant factors are marked

using the asterisks. \*,  $p < 0.05$ ; \*\*,  $p < 0.01$ .

**Fig. 3** Co-occurrence network between OTUs of phoD-harboring bacteria. The nodes are colored by class. The size of each nodes indicates the number of connections (degree) and the width of the edges indicates the correlation strength of the connection (weight).

**Fig. 4** Regressions of the node number (a1-a3), edge number (b1-b3), network density (c1-c3), betweenness centrality (d1-d3), average path length (e1-e3), and the ratio of positive edges (f1-f3) of the phoD-harboring bacterial network to soil organic C (SOC; a1-f1), total nitrogen (TN; a2-f2) and available organic P (Enzyme P; a3-f3) as fitted to optimal models suggested by the Second-order Akaike information criterion values (AICc) among linear, quadric and Michaelis-Menten patterns. The AICc values are shown in Table S3.

**Fig. 5** Full (a) and sparse (b) model of random forest analysis predicting the effect of soil properties, climate factors and crop species on the network topological features of phoD-harboring bacteria. The bar plot in figure b indicates the explanation on diversity variation of each sparse model; red colored boxes below each bar indicate the variables marked at left are used in the model, while the empty boxes indicate the variables are not used. Significant factors are marked using the asterisks. \*,  $p < 0.05$ ; \*\*,  $p < 0.01$ .

**Fig. S1** Geographical distribution of our sampling sites. The size of the circles indicates the enzyme P content of each site.

**Fig. S2** P value for the KS, SSE, and NNSD tests of the exponential distribution generated by random matrix theory.

**Fig. S3** Five-fold cross-validation error of the diversity of phoD-harboring bacteria as number of variables increasing.

**Fig. S4** Multivariate regression tree (MRT) analysis indicating soil enzyme extractable P content constrains on the diversity indices including OTU richness, phylogenetic diversity and Shannon diversity of phoD-harboring bacteria.

**Fig. S5** Pearson correlation between the relative abundance (abund) and network features including weighted degree, unweighted degree (degree), betweenness centrality (betw.cent), authority centralization (Authority), hub centralization (Hub), clustering centralization (Clustering), eigenvector centrality (eigencentrality), Eccentricity Centrality (Eccentricity), and closeness centrality of phoD-harboring bacteria identified as nodes in the global co-occurrence network.

**Fig. S6** Five-fold cross-validation error of the network topological features of phoD-harboring bacteria as number of variables increasing.

---

## Abbreviations

---

---

AG	$\alpha$ -glucosidase
BG	$\beta$ -glucosidase
BIM	Budget imbalance
C	Carbon
Cello	endocellulase
CO <sub>2</sub>	Carbon dioxide
CUE	Carbon use efficiency
DOC	Dissolved organic carbon
DOM	Dissolved organic matter
EFOS	Fossil CO <sub>2</sub> emissions
ELUC	Land–use change emission
Fe	Iron
GATM	Atmospheric CO <sub>2</sub> growth rate
MBC	Microbial biomass carbon
MBN	Microbial biomass nitrogen
N	Nitrogen
NAG	b-N-acetyl-glucosaminidase
P	Phosphorus
Phos	phosphatase
ppm	Parts per million
SLAND	the terrestrial CO <sub>2</sub> sink
SOCEAN	The ocean CO <sub>2</sub> sink
SOM	Soil organic matter
XYL	$\beta$ -Xylanase

---



# 1 General Introduction

## 1.1 The global carbon cycling

The atmospheric CO<sub>2</sub> concentration has increased from approximately 277 parts per million (ppm) at the beginning of the Industrial Era in 1750 (Joos and Spahni, 2008) to 414 ppm currently (Friedlingstein et al., 2021), and continues to increase rapidly. Anthropogenic emissions are the primary source of these additional atmospheric CO<sub>2</sub> emissions in addition to the active natural C cycle that encompasses C cycling between the atmosphere, oceans, and terrestrial biosphere reservoirs over a historical period (Ballantyne et al., 2012). Friedlingstein et al. (2020) have reported that the global C budget comprises five components: fossil CO<sub>2</sub> emission ( $E_{\text{FOS}}$ ), land-use change emission ( $E_{\text{LUC}}$ ), growth rate of the annual changes in atmospheric CO<sub>2</sub> concentration ( $G_{\text{ATM}}$ ), the ocean CO<sub>2</sub> sink ( $S_{\text{OCEAN}}$ ), and the terrestrial CO<sub>2</sub> sink ( $S_{\text{LAND}}$ ). During the last 10 years (2011–2020, Fig.1.1), the total C budget imbalance ( $B_{\text{IM}}$ ) was  $-0.1 \text{ Gt C yr}^{-1}$  (Friedlingstein et al., 2020). Furthermore, global CO<sub>2</sub> emissions in atmospheric increased by  $5.1 \text{ Gt C yr}^{-1}$  from 2011 to 2020, while terrestrial soil is a major C store (1,500–2,400 Gt C) (Friedlingstein et al., 2021).

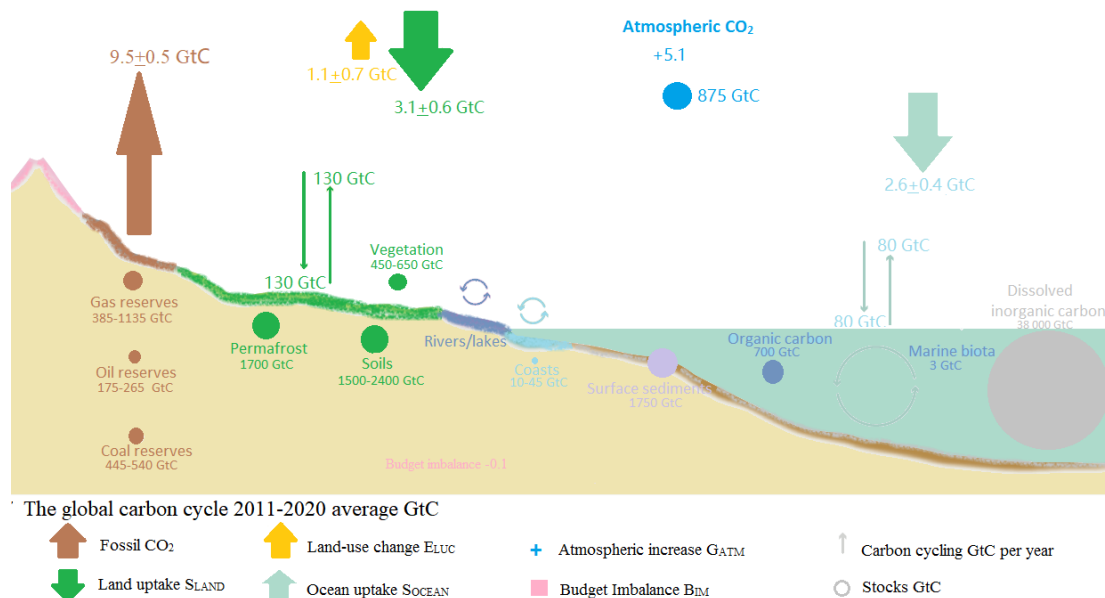


**Fig. 1.1** Diagram of the global C cycle from 2011–2020, modified from Friedlingstein et al. (2020 and 2021). All numbers in the background indicate fluxes and stocks quoted from Ciais et al. (2013), and Friedlingstein et al. (2021 and 2022). The ocean gross fluxes updated according to those reported by Price and Warren (2016) and Friedlingstein et al. (2020 and 2022).

Plant, microorganisms, and animals use various processes to absorb and release C

through photosynthesis and respiration (Lorenz and Lal, 2009; Sperlich et al., 2016). Thus, C can be gained through several pathways at different temporal-spatial scales in the terrestrial ecosystem, such as plant photosynthesis (Austin et al., 2016) and wet–dry deposition (Anderson and Downing, 2006; Lynam et al., 2014; Ossouhou et al., 2021), or lost through volatile organic compound release (Brown et al., 2021), fire (Yu et al., 2021), and dissolved organic C (DOC) and inorganic C (Hafner et al., 2005; Kindler et al., 2011) leaching. The overview of global C cycling has enabled us to understand the importance of terrestrial ecosystem C responses to climate change. For example, soil organic matter (SOM) turnover and stabilization decisively impacts terrestrial C emissions.

To further understand terrestrial C emissions, I have focused on agricultural soils. The storage of soil organic C in agricultural soils depends on their climate (temperature, precipitation), topography (crop type), soil characteristics (texture, aggregation), and land management practices (tillage, irrigation, fertilization, harvest residue return) (Conant, et al., 2001; Kong et al., 2005; Luo et al., 2010; Hasibeder et al., 2015). Two aspects are crucial: C input in agricultural soils and organic matter stabilization. Several studies have demonstrated C substrate (plant-derived C) application in soils, but only few have reported increased C stock (Sohi et al., 2010; Luo et al., 2010; Zhu et al., 2018). Microorganisms play an essential role in C storage; however, analysis of microbial-derived plant C has not fully revealed the mechanisms underlying the differences in organic C content and sequestration potential of agricultural soil. Furthermore, the increased application of organic and inorganic fertilizers, such as N and P, in the agricultural soil significantly changes SOM cycling and affects SOM stabilization (Baldock and Skjemstad, 2000; Chung et al., 2008; Stewart et al., 2008).

## **1.2 Soil organic matter (SOM)**

SOM primarily comprises C (about 58%), O, and H, with organic residues containing trace amounts of other elements such as N and P (Schnitzer and Khan, 1978; Viscarra et al., 2014). SOM turnover is primarily affected by soil type, climate, and land management (Marzaioli et al., 2010; Poeplau et al., 2019; Curtin et al., 2019). Most SOM arises from dead plants and is typically stored in soils for 10 to several thousand years (Spaccini, 2002; Hai et al., 2010). First, plants and animals are converted into SOM as they die (Schnitzer and Khan, 1978; Rimmer, 2006). For instance, plant residues are decomposed into numerous small fragments (<2 mm), such as particulate organic matter; as they are further decomposed, a small amount of organic material is transformed into the stable SOM pool (Sumner, 2000;

Brookes et al., 2008). Then, microorganisms utilize organic (plant) residues and consume SOM (Lal, 1999; Cotrufo et al., 2013). Nutrients not needed by microorganisms are then released and utilized by plants (Kramer and Gleixner, 2006; Tangyu et al., 2019). Thus, the transformation of SOM fractions is widely different and continuously cycled between viable, decomposing, and stable soil components (Tate, 1987; Midwood et al., 2021; La et al., 2021).

Lehmann and Kleber (2015) elaborated on three competing models to differentiate organic matter into the soil: (i) classic ‘humification,’ (ii) selective preservation, and (iii) progressive decomposition, suppose that initial decomposition of plant and soil animal debris into small fragments.

The classic ‘humification’ model is the earliest of the three concepts (Kononova, 1966), initially defining ‘humification’ as the conversion or synthesis of initial decomposition products into decomposition-resistant C and N macromolecules. ‘Humic substances’ can provide cation exchange capacity to interact with Fe, Al, and other metals (Stevenson, 1994). Furthermore, their intrinsic stability prevents further decomposition and is referred to as ‘humification’ or ‘secondary synthesis’ in biogeochemical models (Stevenson, 1994; Burdon, 2001; Guggenberger, 2005). However, there is a lack of evidence for the physical presence of ‘humic substances’ independent of the alkaline extraction process, and no universally accepted interdisciplinary definition of ‘humic substances’ exists (Skjemstad et al., 1996; Rodionov et al., 2010; Lehmann and Kleber, 2015). The second selective preservation model (also known as preferential fractionation) (Sollins et al., 1996) assumes that organic inputs consist of labile and relatively recalcitrant compounds (such as root exudates and lignin) and microorganisms preferentially use the labile components, leading to a relative enrichment of the recalcitrant compounds (Lützow et al., 2006). However, recent research has evidenced that microorganisms can also degrade compounds considered recalcitrant more quickly than previously expected (Wiesenberg et al., 2004; Hamer et al., 2004; Hazen et al., 2010; Yang et al., 2014). The third model of progressive decomposition is also known as the degradative conception (Boodt et al., 1990; Burdon, 2001) or biopolymer degradation (Frimmel et al., 1988). In this model, SOM is composed of organic debris and microbial products that vary among different decomposition stages (Trumbore, 1997; Cotrufo et al., 2013). In contrast to that during the hypothetical classic ‘humification,’ the product size is gradually refined throughout the microbial process during progressive decomposition. The products from plant or microbial fragments under the microbial process were released into the soil for further decomposition after cell death (Kelleher and Simpson, 2006; Gillespie et al., 2011; Mylotte

et al., 2015). Contrary to the previously held model, Lehmann and Kleber (2015) have recently reported a continuum SOM model, where the decomposer community continuously and constantly breaks down organic matter. Increased oxidation status of the remnant molecules (increases in polar and ionizable groups) increases water solubility and decomposes larger plant and animal residues into smaller molecular monomers.

The reactivity of the mineral surface provides an opportunity for DOM to incorporate soil fragments against further decomposition. The microbial decomposition process deposits microbial cells, cell debris, and root exudates on the mineral surface (Miltner et al., 2012; Schurig et al., 2013; Lehmann and Kleber, 2015). Low molecular weight root exudates and stable polymeric lignin biomacromolecules are two typical and abundant SOM. Several studies have reported that the input of labile or stable organic substances affects bulk SOM stabilization and leads to C mineralization or priming (Guenet et al., 2010; Kuzyakov, 2010; Dunham-Cheatham et al., 2020). However, very few studies have compared the composition of labile and stable decomposed organic matter. As microorganisms essential drives SOM turnover, providing conceptual support for further understanding labile and stable organic matter decomposition in the SOM turnover by decomposer organisms and enzymes is needed.

### **1.3 Microorganisms and metabolic pathway on SOM**

Metabolic theory provides a conceptual basis for understanding the microbial energy and nutrient budget in soil (Brown et al., 2004; Sinsabaugh and Follstad Shah, 2012; Vanni and McIntyre, 2016). Soil microorganisms include mainly fungi, bacteria, and archaea (Buée et al., 2009). Fungi and bacteria account for >90% soil microbial biomass (Six et al., 1998). On one hand, microorganisms that continuously modify biomass undergo a catabolic pathway, which partially decomposes their biomass C into catabolic products or mineralizes it into CO<sub>2</sub> and releases into the atmosphere (Spohn et al., 2016). On the other hand, microorganisms continuously assimilate SOM to synthesize biomass C during the anabolic pathway. Microbial biomass C (MBC) refers to the amount of C present in all living microorganisms in the soil, accounting for about 1–5% total soil organic C, and is the most active and unstable SOC component (Carter and Gregorich, 2008). Microbial transformation of organic matter occurs in two distinct microbial metabolic pathways, extracellular enzymatic modification (*ex vivo*) and intracellular (*in vivo*) turnover. Extracellular modification implies reorganization or alteration of molecules in catabolic processes by

microbial degradative enzymes, while intracellular turnover implies a mixture of catabolic and anabolic processes, including the breakdown and resynthesis of molecules in soil C transformation and sequestration (Drotz et al., 2010; Kallenbach et al., 2016; Liang et al., 2017; Zheng et al., 2021). In these two pathways, compounds will be further degraded or readily stabilized by microbial modification of the original compound or microbial synthesis forming new mixtures, such as lignin degradation products or related synthetic polymers (Liang et al., 2017; Fig.1.2). Several studies have described the microbial transformation and deposition of organic compounds (such as root exudates and lignin) focusing on C or C/N combination in these two pathways; however, only few studies have focused on organic P metabolism and the associated environmental factors included in the microbial metabolic process in SOM turnover.

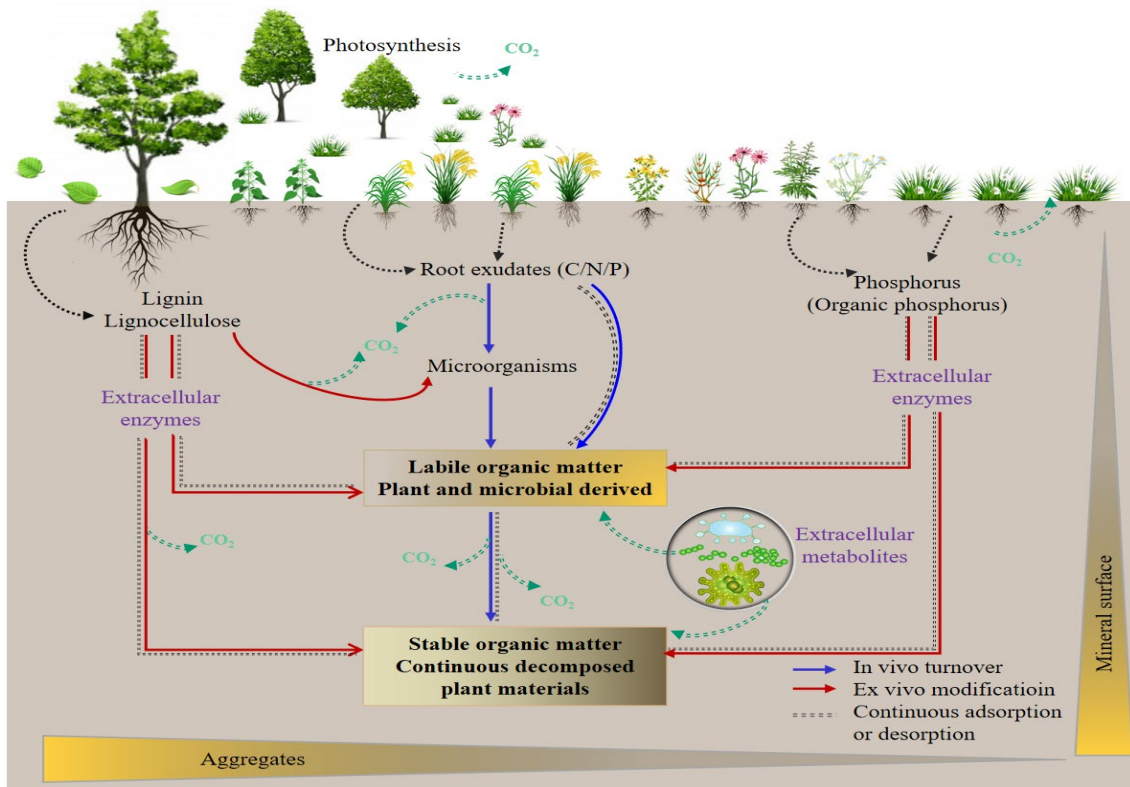


**Fig. 1.2** A conceptual model of organic fragments and potential microbial metabolic processes involved in agricultural soil organic matter turnover. Modified from Lehmann and Kleber (2015) and Liang et al. (2017).

External environmental conditions play an essential role in microbial catabolism for SOM decomposition and transformation. As main driving forces for microorganisms, environmental factors such as soil moisture (which also affects soil aeration status), redox potential, and nutrients (N and P) affect organic matter decomposition and transformation

(Davidson et al., 2000). Soil moisture can modify the microbial activity by changing the soil aeration status, thereby promoting or inhibiting SOM decomposition (Lal, 2002). Several studies showed that SOM mineralization rate under flooded (anaerobic) conditions is significantly lower than that under aerobic conditions (Qiu et al., 2017; Kögel–Knabner et al., 2010), but MBC increased significantly under flooded conditions (Devêvre and Horwáth, 2000). Under flooding conditions, the soil is in a low redox state, which reduces microbial activity and, consequently, SOM decomposition rate (Stevenson and Cole, 1999). In addition, microbial metabolic pathways in paddy field soils (anaerobic environments) differ from those in dryland soils (aerobic environments) because the substrates are partially oxidized in anaerobic environments (Kögel–Knabner et al., 2010).

Moreover, the capacity of sequester C as organic matter in flooded soil (paddy and wetland soil) and non-flooded soil is different. Likewise, the microbial communities in these soils also differ (Chen et al., 2018). Gram-positive and anaerobic gram-negative bacteria predominate in flooded soil, while gram-negative bacteria and fungi dominate in non-flooded soil (Nakamura et al., 2003). Ueki et al. (2018) observed that the soil eliminated soil-borne plant pathogens controlled by anaerobic bacteria and produced mainly antifungal enzymes. Soil flooding followed by drying significantly increased C mineralization rate, while soil drying followed by flooding tended to decrease and then increase C mineralization rate (Devêvre and Horwáth, 2000; Borken and Matzner, 2009; Rodríguez et al., 2019). Qiu et al. (2017) observed a higher mineralization rate in dryland soil than that in paddy field soil, corresponding with reduced organic C content. Alternation of dry and wet conditions affects microbial activity and anaerobic and aerobic microbial communities (Coppens et al., 2006; Kimura and Asakawa, 2006). In contrast, more water-soluble organic matter is produced under reducing conditions, as Suetsugu et al. (2005) observed a substantial increase in DOM during the flooding season. These possibly reflect a link between biodegradation of SOM associated with soil minerals and reducing pH value as an essential stabilization mechanism in C sequestration. However, Hanke et al. (2013) reported that increasing DOM under anoxic conditions does not increase soil respiration, possibly due to poor electron acceptor availability. Repeated anaerobic and aerobic cycles, which continuously change soil solution chemistry and create a temporary oxygen deficiency reflected by the composition and physiological responses of the microbial community (Song et al., 2019). These alterations can strongly affect soil processes, particularly SOM accumulation and mineralization. In submerged soils of paddy fields, lignin generally constitutes a significant portion of SOM,

particularly the young fractions, due to hampered degradation under anaerobic conditions (Olk et al., 2006).

Accompanied with the C cycle, N and P are dominant nutrients for soil microorganisms. Increasing N and P application enhances the microbial biomass that promotes SOM mineralization by microorganisms, which directly affects the microbial community structures (Zhang et al., 2017; Zhu et al., 2018; Ma et al., 2021). Hrynkiewicz et al. (2009) observed that high N supply reduced the diversity of mycorrhizal communities and increased P turnover by soil microbial biomass. Microbial C, N, and P demand induces community shifts that alter microbial-mediated SOM turnover (Mooshammer et al., 2014; Sun et al., 2021; Huang et al., 2021). Zhu et al. (2018) observed positive priming with N and P addition due to straw decomposition and regulated SOM turnover by nutrient stoichiometry. The C:P and N:P ratios of microbes were significantly related to the source C:N:P ratios, indicating that biomass stoichiometry drives microbial demand of C and nutrients, which is regulated by resource stoichiometry (Yao et al., 2019).

#### **1.4 C use efficiency and enzyme activity**

C use efficiency (CUE) and enzyme activities can be powerful indicators of the resource requirements for microbial communities (Schimel, 2003; Hill et al., 2012; Wang et al., 2021). The ratio of the C source taken up by microorganisms to synthesize their cellular material is called CUE (Sinsabaugh et al., 2013). It is a comprehensive soil microorganism catabolism and anabolism indicator, and CUE size determines the fate of SOC (Schimel and Schaeffer, 2012; Chen et al., 2020). Increased CUE indicates decreased basal respiratory consumption and improved efficiency in microbial assimilation and C sequestration. Contrarily, decreased CUE implies low C assimilation and sequestration ability of microorganisms and high CO<sub>2</sub> release (Manzoni et al., 2012b).

Theoretically, the maximum microbial CUE can reach 0.8, implying that no more than 80% C source taken up by microorganisms is used for their growth and microbial biomass synthesis, and at least 20% is needed for basal respiration (Gommers et al., 1988). However, microbial CUE hardly reaches the theoretical value of 0.8 due to environmental conditions limiting the energy required to maintain basal respiration for nutrient acquisition. The magnitude of microbial CUE ranges from 0.3 to 0.8, with a mean value of 0.55 during SOM degradation in the terrestrial ecosystem (Sinsabaugh et al., 2013; Manzoni et al. 2012b). Soil microbial CUE is influenced by external environmental conditions such as temperature,

moisture, substrate type, nutrient effectiveness (particularly soil N and P content), microbial population structure, and biochemical pathways of microbial decomposition and assimilation (Sinsabaugh et al. 2013; Manzoni et al. 2012b). In general, soil microbial respiration rate accelerates with increasing temperature, decreasing microbial CUE (Devêvre and Horwáth 2000). With increased soil C/N ratio, the C source requirement in microorganisms for respiration increases; thus, external nutrients are required, further reducing microbial CUE. Conversely, at low soil C/N ratio, the microbial CUE is high (Ågren et al., 2001; Chen et al. 2020). Manzoni et al. (2012b) observed that although low soil water content increases oxygen transfer rate in the void, it also limits the diffusivity of adequate soil nutrients and their availability to microorganisms, thus reducing microbial CUE.

Extracellular enzyme activities, such as C-, N-, and P-acquiring enzymes, are the most important hydrolytic degradation enzymes, including  $\alpha$ -glucosidase (AG),  $\beta$ -glucosidase (BG),  $\beta$ -xylanase (Xyl), endocellulase (Cello), b-N-acetyl-glucosaminidase (NAG), and phosphatase (Phos). Moreover, peroxidase and polyphenol oxidase represent complex SOM degradation enzymes (Allison and Vitousek, 2005; Sinsabaugh and Follstad Shah, 2012; German et al., 2012; Hettiaratchi et al., 2014; Rosinger et al., 2019). Limited microbial biomass or organic resources in the soil can stimulate enzyme activities (Guan et al., 2022). Xiao et al. (2018) reported that enzymes were sensitive to nutrient addition. The combined addition of N and P increased C-acquiring enzyme activity by 30.7% because microorganisms require more C sources to support their demand (Xu et al., 2020; Li et al., 2021). Simple N addition may trigger microbial demand for C and P supply, resulting in enzymatic hydrolysis of SOM by reducing C- and P-acquiring enzyme activities (Zhang et al., 2019; Silva-Olaya et al., 2021). Yang et al. (2020) reported that the ratio of C-, N-, and P-acquiring enzymes in the soil is 1:1.08:1.28, but only under the experimental conditions.

Anaerobic bacteria such as *Tolomonas ligninolytic* and *Klebsiella* sp. are parthenogenic bacteria that can degrade lignin under anaerobic conditions and use the decomposed monomers as C and energy source (Woo et al., 2014; Billings et al., 2015). Under anaerobic conditions, benzene carboxylases (benzoyl-CoA) degrade benzene gene clusters via anaerobic benzene carboxylation (Atashgahi et al., 2018). Anaerobic gut fungi, such as, *Saccharomyces cerevisiae*, are unique eukaryotic organisms that can adapt to anoxic survival and biosynthesis through gene transfer with coenzyme A metabolic cofactors (Perli et al., 2021). Youssef et al. (2013) observed that anaerobic fungal gut *Orpinomyces* sp. strain C1A could anaerobically degrade plant materials that produce specific extracellular proteases.



While studies focus more on genomes level in microbiology, such strains are less connected with SOM turnover. Therefore, more studies should focus on microbial activities and their related extracellular enzymes to understand the microbial processes involved in SOM turnover in agricultural soils.

## **1.5 Motivation and general hypotheses**

The microbial activity is essential in the agricultural ecosystem, which involves SOM and its elements. Several studies have mainly explained the C budget in agricultural soils by organic residue C input and microbial mineralization (Luo et al., 2010; Tagami et al., 2012; Kirkby et al., 2016). However, as drivers of SOM turnover, microorganisms regulate the decomposition of organic matter while also synthesizing recalcitrant organic matter (Liang et al., 2017). Previous studies have suggested that the contribution of MBC to SOC is relatively small, arguing that microbial biomass contributes less to SOM formation (Dalal, 1998). The latest theoretical framework suggests that two pathways, extracellular enzymatic modification and intracellular turnover, act together in organic matter conversion to form SOM in a microbial metabolic manner (Liang et al., 2017; Sokol and Bradford, 2019; Cotrufo et al., 2021). Microorganisms act as biocatalysts to produce extracellular enzymes that promote the turnover and conversion of plant-derived aromatic macromolecular compounds during growth and activity (Schmidt et al., 2011), thereby indirectly contributing to SOM through the *ex vivo* pathway (Zheng et al., 2021). Moreover, microorganisms actively bind labile organic C into their cells through an *in vivo* pathway, and some microbes die during metabolism and accumulate in the soil (Liang et al., 2017). Labile soil C that includes plant- and microbe-derived C serves as a resource for metabolism, microbial biomass formation, and, consequently, microbial necromass, which is primarily used for further soil microbial loops (Kuzyakov and Mason-Jones, 2018), and finally incorporated into the SOM (Zheng et al., 2021). SOM pool size depends on the balance between microbial C degradation rate (catabolism) and stable C synthesis rate (anabolism) (Liang et al., 2017). Therefore, the strength of microbial catabolism and anabolism is essential in determining the characteristics of SOM as a "source" and "sink." This thesis aimed to assess the microbial activities under catabolism and anabolism for different substrates (root exudates and lignin) under different environmental conditions (anaerobic and aerobic) and the effect of resource supply (C combined with N or P) to identify the factors controlling SOM mineralization and accumulation in agricultural soil; the objectives of my thesis are:

**Objective I** To characterize the difference in the contribution of SOM turnover between low molecular weight compound of root exudates and stable polymeric lignin biomacromolecules in agricultural soil.

**Objective II** To evaluate the microbial biomass turnover and microbial residue stabilization in SOM fraction depending on abiotic conditions.

**Objective III** To quantify the relationship between extracellular enzyme activity and SOM mineralization in agricultural soil.

Based on the research context revealed by literature analysis, I hypothesized that:

**Hypothesis I** Whether maximum C (labile or stable organic C) ends up in microbial biomass with a chance of getting entombed.

**Hypothesis II** Lignin biomacromolecules cannot be effectively stabilized under anaerobic conditions but degraded more slowly than that under aerobic conditions in agricultural soils.

**Hypothesis III** Microorganisms require relatively high N and P contents to meet their demands to enhance microbial growth and promote SOM mineralization in agricultural soils.

To reveal the microbial transformation and accumulation of various SOM forms with environmental changes in agricultural soils, three studies were conducted to achieve the above hypotheses:

**Study I** Different stoichiometric ratios of artificial root exudates were applied to the soil to investigate how they modify microbial activities (including extracellular enzyme production and microbial biomass stoichiometric ratio) and influence SOM mineralization. Stoichiometric ratios of artificial root exudates were regulated by combining different amounts of glucose, oxalic acid, and alanine, which represented low molecular weight organic compounds, namely, sugars, organic acids, and amino acids, respectively. In addition, I determined the extracellular enzymes involved in C and N decomposition, MBC and MBN, and the associated CO<sub>2</sub> emission after adding root exudates.

**Study II** To characterize the stable polymeric lignin decomposition rate in an anaerobic and aerobic environment, wetland soil samples were incubated with 7.5 mg <sup>13</sup>C-lignin (>98 atom%, chemical purity 80%) under anaerobic and aerobic conditions at 15 °C for 365 days. In addition, I determined the fate of lignin, MBC, and related extracellular enzyme activities, along with the associated CO<sub>2</sub> emission after the lignin addition.

**Study III** To evaluate the bioavailability of organic C, N, and organic P to microbial activities, 102 agricultural soil samples (paddy and upland soil) were collected from three

major crop areas (maize, wheat, and paddy) to characterize the bacterial diversity and network of *phoD*-harboring bacteria. First, the contents of organic C, TN, and major organic P species, including CaCl<sub>2</sub>-P, citrate-P, HCl-P, enzyme-P, Olsen-P, and the pH and the soil particle size was determined. Then, we analyzed the diversity and network characteristics of *phoD*-harboring bacteria, and their regressions with organic C, TN, and organic P were calculated for studying the relationship between *phoD*-harboring bacterial network characteristics and the shaping of bulk SOM (such as organic C, TN, and enzyme-P) by the diversity of *phoD*-harboring bacteria.

## **2 Study 1**

### **Root exudates with low C/N ratios accelerate CO<sub>2</sub> emissions from paddy soil**

Contribution: I participated in the experiment incubation, performed most of the analysis in the laboratory, collected and evaluated data, prepared tables and figures, and wrote the manuscript.

Published in Land Degradation and Development (2022)

<https://doi.org/10.1002/ldr.4198>

## **Root exudates with low C/N ratios accelerate CO<sub>2</sub> emissions from paddy soil**

Guan Cai<sup>a,b</sup>, Muhammad Shahbaz<sup>c</sup>, Tida Ge<sup>a,b,d</sup>, Yajun Hu<sup>a</sup>, Baozhen Li<sup>a</sup>, Hongzhao Yuan<sup>a\*</sup>, Yi Wang<sup>a,e</sup>, Yuhuai Liu<sup>a,b</sup>, Qiong Liu<sup>a</sup>, Olga Shibistova<sup>b,f</sup>, Leopold Sauheitl<sup>b</sup>, Jinshui Wu<sup>a</sup>, Georg Guggenberger<sup>b</sup>, Zhenke Zhu<sup>a,d\*</sup>

<sup>a</sup> Key Laboratory of Agro-ecological Processes in Subtropical Region & Changsha Research Station for Agricultural and Environmental Monitoring, Institute of Subtropical Agriculture, Chinese Academy of Sciences, Hunan, 410125, China

<sup>b</sup> Institute of Soil Science, Leibniz Universität Hannover, Hannover 30419, Germany

<sup>c</sup> Centre for Environmental and Climate Research, Lund University, 223 62 Lund, Sweden

<sup>d</sup> State Key Laboratory for Managing Biotic and Chemical Threats to the Quality and Safety of Agro-products, Institute of Plant Virology, Ningbo University, Ningbo 315211, China

<sup>e</sup> College of Resources and Environmental Engineering, Ludong University, Yantai, 264025, China

<sup>f</sup> VN Sukachev Institute of Forest, Siberian Branch of the Russian Academy of Sciences, Krasnoyarsk, 660036, Russian Federation

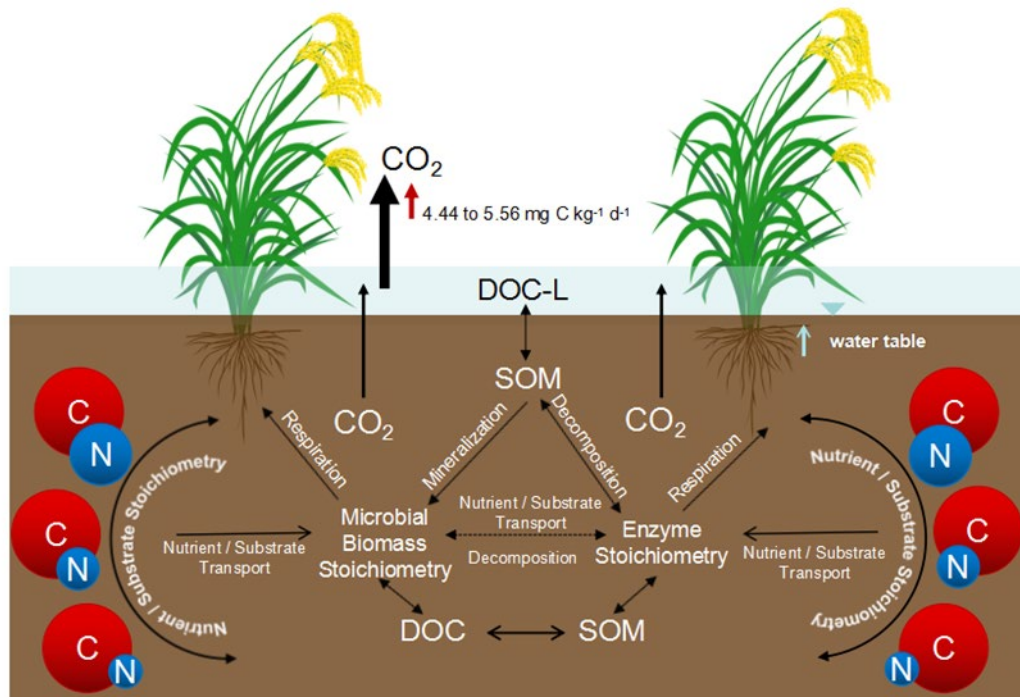
\*Author for Correspondence: Hongzhao Yuan; E-mail: yuanhongzhao@isa.ac.cn; Zhenke Zhu; E-mail: zhuzhenke@isa.ac.cn

**ABSTRACT**

Root exudates can significantly modify microbial activity and soil organic matter (SOM) mineralization. However, how root exudates and their C/N stoichiometric ratios control paddy soil C mineralization is poorly understood. This study used a mixture of glucose, oxalic acid, and alanine as root exudate mimics for three C/N stoichiometric ratios (CN6, CN10, and CN80) to explore the underlying mechanisms involved in SOM mineralization. The input of root exudates enhanced CO<sub>2</sub> emissions by 1.8 – 2.3-fold that of soil with only C additions (C-only). Artificial root exudates with low C/N ratios (CN6 and CN10) increased the metabolic quotient (qCO<sub>2</sub>) by 12% over those with higher stoichiometric ratios (CN80 and C-only), suggesting a relatively high energy demand for microorganisms to acquire organic N from SOM by increasing N-hydrolase production. The increase of stoichiometric ratios of C- to N-hydrolase ( $\beta$ -1,4-glucosidase to  $\beta$ -1,4-N-acetyl glucosaminidase) promoted SOM degradation compared to those involved in organic C- and N- degradation, which had a significant positive correlation with qCO<sub>2</sub>. The stoichiometric ratios of microbial biomass (MBC/MBN) were positively correlated with C use efficiency, indicating root exudates with higher C/N ratios provide an undersupply of N for microorganisms that trigger the release of N-degrading extracellular enzymes. Our findings showed that the C/N stoichiometry of root exudates controlled SOM mineralization by affecting the specific response of the microbial biomass through the activity of C- and N-releasing extracellular enzymes to adjust the microbial C/N ratio.

**KEYWORDS:** Root exudates Stoichiometric ratios Microbial biomass Extracellular enzyme Metabolic quotients Carbon use efficiency

## Graphical abstract



Schematic diagram emphasizing the importance of the stoichiometric control of plants by their release of root exudates of different N contents in the flooded rice-paddy soil system. C and N circles represent artificial root exudates, DOC-W represents dissolved organic C from water solution, SOM represents the soil organic matter, microbial biomass stoichiometry represents the C: N ratios of microbial biomass, and enzyme stoichiometry represents the ratios of the activity of  $\beta$ -1,4-glucosidase to  $\beta$ -1,4-N-acetyl glucosaminidase and the activity of  $\beta$ -1,4-xylosidase to  $\beta$ -1,4-N-acetyl glucosaminidase. The solid lines represent the transportation of active microbial pathways from stoichiometric controls of root exudates.

## 1. INTRODUCTION

Plants modify the soil environment either by releasing C from their roots (e.g., root exudates) or by the rapid uptake of nutrients from the soil by their associated microorganisms. (Kuzyakov, 2002; Jones et al., 2009; Fisk et al., 2015; Liu et al., 2019; Xiong et al., 2019). Across different plant species, around 1 – 10% of photoassimilated C is released into the soil as root exudates (Jones et al., 2004; Phillips et al., 2011; Qiao et al., 2014; Yin et al., 2014), which consist primarily of sugars, but can also include phenolics, amino acids, organic acids, and other metabolite derivatives (Haichar et al., 2014; Yuan et al., 2017). In addition to acting as direct substrates for microorganisms with nutritional value, the stoichiometric ratio of the C- and N-containing compounds is thought to impact their utilization by microorganisms (Wild et al., 2014; Ge et al., 2020). Thus, elucidating the role and underlying mechanisms of exudates with different C/N ratios on microbial substrate utilization is of key importance for understanding soil C and N cycling, as well as soil C sink strength.

Several mechanisms have been proposed to explain how root exudates affect the microbial decomposition of soil organic matter (SOM). It has been hypothesized that (i) root exudates provide energy for stimulating SOM decomposition and changing the chemical and physical characteristics of the soil environment (Qiao et al., 2016; Zhu et al., 2018; Mehnaz et al., 2019; Du et al., 2020)(Liu et al., 2022); (ii) labile C promotes microbial growth, which in turn, increases the N demand and microbial N mining from SOM (Manzoni et al., 2010; Dijkstra et al., 2013; Qiao et al., 2016; Zhu et al., 2018); and (iii) microbial C and N demand causes community shifts that alter microbial-mediated C decomposition (Phillips et al., 2011; Wild et al., 2014; Wei, 2020; Li et al., 2020; Xu et al., 2020). Moreover, the impact of nutrients on C-N stoichiometry need to be considered, such as the addition of C substrates like glucose, and the different several levels of N application, which provide a proportion of C that is integrated into the microbial biomass that becomes stabilized as SOM with the cost of CO<sub>2</sub> emission (Creamer et al., 2014).

Recently, research on the stoichiometry of root exudate compounds combined with mineral N [e.g., (NH<sub>4</sub>)<sub>2</sub>SO<sub>4</sub>] showed that higher C/N ratios increase CO<sub>2</sub> emissions due to high microbial N demand (Du et al., 2020; Liu et al., 2020). Subsequently, resource stoichiometry alters microbial community composition to gain the required elements and increase SOM mineralization (Zhu et al., 2018; Wei, 2020). Extracellular enzyme activities, such as C- and N-acquiring enzymes, can also reflect the resource demands of microbial



communities (Schimel, 2003; Hill et al., 2012; Liu et al., 2021; Wang et al., 2021). For example,  $\beta$ -1,4-glucosidase (BG) and  $\beta$ -1,4-xylosidase (XYL) are the largest contributors to the degradation of cellulose and hemicellulose, respectively. Similarly,  $\beta$ -1,4-N-acetyl glucosaminidase (NAG) plays a major role in chitin degradation and is involved in the organic N pool. These enzyme activities have similar stoichiometries, which could further relate to the elemental stoichiometry of the microbial biomass for microbial nutrient assimilation and growth (Sinsabaugh et al., 2008; Sinsabaugh and Follstad Shah, 2012). To date, the understanding of the influence of root exudates with different stoichiometric compositions on microbial growth and activity is still in its infancy, especially with respect to how root exudate composition affects or contributes to the interactions between microbial biomass and extracellular enzyme stoichiometries.

In the present study, we applied different C/N stoichiometric ratios of artificial root exudates to soil to investigate how they modify microbial activities (including extracellular enzyme production and microbial biomass stoichiometric ratios) and influence SOM mineralization. The stoichiometric ratios of artificial root exudates were regulated by combining different amounts of glucose, oxalic acid, and alanine, which represented low molecular weight organic compounds, such as sugars, organic acids, and amino acids, respectively. We determined the activities of extracellular enzymes involved in C and N decomposition, microbial biomass C (MBC), and N (MBN), along with the associated CO<sub>2</sub> emissions after the addition of root exudates to soil. We hypothesized that (1) the application of C-only artificial root exudates leads to an imbalance in resource stoichiometry that inhibits microbial activity and SOM mineralization; and (2) the inclusion of N-containing root exudates meets microbial stoichiometric demands that enhance microbial growth and improves SOM mineralization.

## **2. MATERIALS AND METHODS**

### **2.1 Study site and soil sampling**

The soil was collected from experimental rice fields in Changsha, Hunan, China (113° 19' 52" E, 28° 33' 04" N). The region has a subtropical climate with an average annual temperature of 16.7C and an estimated annual precipitation of 1457 mm. Moist field soils were collected from the plow layer (0 - 20 cm) with a stainless steel drill (diameter: 5 cm) in September 2019, after the summer growing season. The soil was derived from quaternary red clay and classified as haplic Acrisol according to the IUSS Working Group WRB (WRB,

2015). The soil was supplemented with urea (80 kg ha<sup>-1</sup> yr<sup>-1</sup>), biological fertilizers (livestock manure), and rice plant straw residues (6000 kg ha<sup>-1</sup> yr<sup>-1</sup>) within a rice – rape rotation. Five soil cores were collected and thoroughly mixed, and then promptly stored in a gas-permeable plastic bag and stored at 4°C until further analysis. A batch of soil samples was air-dried and passed through a 2-mm sieve to remove fine roots and other plant residues. The primary chemical properties were presented in a previous report of artificial root exudates (Liu et al., 2020).

## 2.2 Artificial root exudate experiment

The soil samples (3 kg dry weight) were sieved, air-dried, and placed in a 50-L plastic bucket with deionized water to a depth of 2 – 3 cm. The soils were pre-cultured in the dark at 25°C for two weeks. The experiment included five treatments with four replicates organized in a fully randomized design. Subsequently, the soil was mixed well, and 50 g subsamples equivalent to 30 g dry soil were placed in 500-mL incubation serum bottles. Deionized water was added to each serum bottle up to a level of 2 – 3 cm above the soil surface and the bottles were sealed with rubber stoppers. To imitate root exudates, which are mainly dominated by sugars, amino acids, and organic acids (Lopez - Sangil et al., 2017; Xiong et al., 2019), we selected different proportions of glucose (C<sub>6</sub>H<sub>12</sub>O<sub>6</sub>), oxalic acid (H<sub>2</sub>C<sub>2</sub>O<sub>4</sub>), and alanine (C<sub>3</sub>H<sub>7</sub>NO<sub>2</sub>). We adjusted three treatments with different C/N ratios (CN6, CN10, and CN80) by adding different amounts of alanine, along with a treatment without alanine (C-only). Treatment of distilled H<sub>2</sub>O was used as a control. The total amount of added C was maintained at 5% SOC, approximately 0.6 mg C g<sup>-1</sup> soil dry weight. The relative contributions of sugar, amino acids, and organic acid-derived C were within the range of those reported in recent literature (Qiao et al., 2016; Liu et al., 2020).

The solutions were prepared at intervals of 5 days by dissolving these proportions of glucose, oxalic acid, and alanine in 50 mL deionized water. The details are presented in Tables 1 and S1. To mimic a pattern of continuous exudate excretion, we manually injected 0.5 mL of the solution into the soil samples daily with a 10 mL syringe. All samples were cultivated in the dark at 25°C for 45 days. Four sample bottles were randomly chosen and destructively harvested on days 3, 12, and 45 after initial exudate addition. Before harvesting the soil samples, four leachate water samples were collected in a 50-mL centrifuge tube, and the soil samples were then mixed thoroughly. Both leachate water and soil samples were

stored at 4C for additional measurements.

### 2.3 CO<sub>2</sub> efflux measurement

Daily gas samples (15 mL) were collected from 500 mL serum bottles containing the soil samples using a 20-mL syringe before exudate solutions were injected into the soil samples. The serum bottles were then flushed with artificial air for another 10 min and then closed with a rubber stopper. CO<sub>2</sub> measurements were performed using a gas chromatograph (Agilent 7890A, Agilent Technologies, Alto Palo, California, USA) with a thermal conductivity detector.

### 2.4 Soil property analysis

Soil MBC and MBN were estimated using the chloroform fumigation extraction method (Wu et al., 1990; Jenkinson et al., 2004). One subsample (20 g) was directly extracted with 60 mL 0.5 M K<sub>2</sub>SO<sub>4</sub> solution, and another (20 g) was first fumigated with ethanol-free chloroform in darkness for 24 h and then extracted with 60 mL 0.5 M K<sub>2</sub>SO<sub>4</sub> solution. The extracted C from the fumigated and non-fumigated samples was estimated after acidification with a Shimadzu TOC-VWP analyzer (Shimadzu), and inorganic N (NO<sub>3</sub><sup>-</sup> and NH<sub>4</sub><sup>+</sup>) was estimated using 2 M KCl and analyzed with a continuous-flow analyzer (Fiastar 5000; Foss Tecator AB, Höganäs, Sweden). Finally, the TN of the soil samples was estimated with an elemental analyzer (MACRO cube, Elementar, Germany).

MBC and MBN were calculated as the difference in C and N content between fumigated and non-fumigated sample extracts, adjusted by a proportionality coefficient (kEC = 0.45, kEN = 0.54) to account for the extraction efficiency. The 0.5 M K<sub>2</sub>SO<sub>4</sub>-extractable C from the unfumigated sample was considered to be dissolved organic carbon (DOC) (Vance et al., 1987).

The leaching water samples were collected for NO<sub>3</sub><sup>-</sup> (NO<sub>3</sub><sup>-</sup>-L) and NH<sub>4</sub><sup>+</sup> (NH<sub>4</sub><sup>+</sup>-L) analysis with a continuous-flow analyzer (Fiastar 5000; Foss Tecator AB, Höganäs, Sweden). In addition, leaching water DOC (DOC-L) was measured using the Shimadzu TOC-VWP analyzer (Shimadzu).

The metabolic quotient (qCO<sub>2</sub>) and microbial carbon-use efficiency (CUE) were calculated using previously published methods (Anderson and Domsch, 1993; Sinsabaugh et al., 2013). The qCO<sub>2</sub> was defined by the ratio of respired CO<sub>2</sub> to C in the soil microbial biomass (qCO<sub>2</sub>=CO<sub>2</sub>-C/MBC), and the quantity of C defined CUE in the microbial biomass

as the sum of the CO<sub>2</sub>-C and MBC [CUE = MBC/(MBC + CO<sub>2</sub>-C)].

### 2.5 Enzyme activity measurement

Extracellular enzyme activities were measured with a previously established method (Marx et al., 2001). Fluorogenic methylumbelliferone was used as an artificial substrate to estimate the activity levels of BG, XYL, and NAG, which are responsible for the degradation of soil organic C (BG and XYL) and N (NAG) (Sinsabaugh and Follstad Shah, 2012). Fresh soil (1 g) was dissolved in 125 mL 50 mM sodium acetate buffer (pH 5) using low-energy sonication (50 J s<sup>-1</sup>) for 1 min. A 200- μ L aliquot of the slurry was incubated with 50 μ L of the corresponding substrate at 20C for 4 h in the dark. Ten microliters 1 M NaOH solution was added to every plate to stop the reaction before measurement. The fluorescence values were then determined using an automated fluorometric plate reader (Victor3 1420 - 050 Multi-label Counter; PerkinElmer, Waltham, MA, USA) at an excitation wavelength of 365 nm and an emission wavelength of 450 nm. Enzyme activities were expressed as nM g<sup>-1</sup> h<sup>-1</sup>.

### 2.6 Calculations and statistical analysis

Statistical analysis was conducted with R Studio (R version 3.5.2, CDN, Global) using one-way ANOVA with Tukey's post-hoc test to analyze significant differences between single treatments ( $p < 0.05$ ). In addition, structural equation modeling (SEM) was conducted with the Amos 17.0 software package (Smallwaters Corporation, Chicago, IL, USA) to test the hypothesized causal relationships between total C, MBC/MBN, BG/NAG, XYL/NAG, DOC/NH<sub>4</sub><sup>+</sup>, DOC/NO<sub>3</sub><sup>-</sup>, and CO<sub>2</sub> emissions. The log-transformed CO<sub>2</sub>, SOC, DOC/NH<sub>4</sub><sup>+</sup>, DOC/NO<sub>3</sub><sup>-</sup>, MBC/MBN, BG/NAG, and XYL/NAG were used to perform SEM on the data statistics and conceptual assumptions (Hu et al., 2014). The best-fit model was established using a chi-square test ( $\chi^2$ ), P-values, goodness-of-fit index (GEI), root mean square error of approximation (RESEA), and Akaike information criteria (Chen et al., 2016).

## 3. RESULTS

### 3.1 SOM mineralization response to artificial root exudates

The temporal patterns of CO<sub>2</sub> emissions from all artificial root exudate - treated soils were similar. The CO<sub>2</sub> efflux was the highest at the beginning of the incubation (days 1 - 4), and exponentially decreased until day 15. Furthermore, it reached a stable level with only

minor fluctuations at the end of the chasing period (Fig. 1a). Compared with the soil without additions (Control), the input of artificial root exudates increased the cumulative CO<sub>2</sub> emissions by 25%, 25%, 20%, and 19%, as CN6 > CN10 > CN80 > C-only, respectively (Fig 1b).

The input of root exudates with low C/N ratios (CN6 and CN10) significantly increased qCO<sub>2</sub> on day 3. However, the qCO<sub>2</sub> decreased from day 3 to day 45 in all treatments in the following order: CN6 > CN10 > CN80 > C-only > Control (Fig. 2a). In contrast, artificial root exudates decreased the CUE value of the soil samples in the following order: Control > C-only > CN80 > CN10 > CN6 (Fig. 2b). These results suggest a relatively high energy demand for microorganisms to acquire organic N from SOM mineralization.

### 3.2 Enzyme activity and microbial biomass responses to artificial root exudates

Compared with the control, the activities of the three enzymes in the exudate-treated soils were significantly increased. The BG and XYL enzymes increased in the following order: C-only > CN80 > CN10 > CN6 > Control (Fig. 3). Conversely, NAG activity decreased with decreasing N content in the simulated root exudate treatment groups on day 3, following the order of CN 6 > CN10 > CN80 > C-only. Enhancing the BG/NAG ratio increased qCO<sub>2</sub> (R<sup>2</sup> = 0.41, P = 0.01) but decreased the CUE (R<sup>2</sup> = 0.36, P = 0.02) (Fig. 4a and 4b). Compared with the control, MBC and MBN increased in the root exudate treatments, with the exception of the CN6 and C-only treatments on day 3. However, there was a minor increase from day 3 to day 45 in all treatments when compared with the control (Table S2). The C/N ratios of the microbial biomass ranged from 3.2 to 7.8 (Fig. 4c). The MBC/MBN ratio was negatively correlated with qCO<sub>2</sub> (R<sup>2</sup> = 0.29, P = 0.01) but increased the CUE (R<sup>2</sup> = 0.301, P = 0.04) (Fig. 4d).

### 3.3 Structural equation modeling analysis of CO<sub>2</sub> efflux

To quantify the effects of the stoichiometry of root exudates on CO<sub>2</sub> efflux, SEM was constructed based on biotic parameters (microbial biomass and enzyme activity) and products of biological activity (DOC and NH<sub>4</sub><sup>+</sup>) as a proxy of SOM mineralization. The SEM showed a good fit to our hypothesized causal relationships (GEI = 0.98, Chi/DF= 1.00, RESEA < 0.01. Fig. 5) and explained 58% of the variance in CO<sub>2</sub> emissions when all available biotic parameters and the products of biological predictors were analyzed. We found that the increase in C/N ratio had a negative effect on CO<sub>2</sub> emissions (-0.29, P < 0.05,

Fig. 6) and extracellular enzyme stoichiometry (BG/NAG and XYL/NAG ratios) exerted a positive direct effect (+0.39,  $P < 0.001$ ), whereas the DOC/NH<sub>4</sub><sup>+</sup> ratio showed a direct negative effect on CO<sub>2</sub> emissions (-0.30,  $P < 0.001$ ).

## 4. DISCUSSION

### 4.1 Microbial response to the addition of root exudates

Artificial root exudates were designed using three low-molecular weight organic compounds in four different C/N ratios, which are easily degradable and accessible by the microbial community (de Graaff et al., 2010; Bastida et al., 2013). When C and N are sufficient, microorganisms prefer to efficiently utilize compounds from root exudates than from native SOM (Shahbaz et al., 2017; Wei et al., 2019). We found that the addition of root exudates stimulated microbial activity, as indicated by significant accumulative CO<sub>2</sub> emissions. These emissions responded differently to various stoichiometric ratios of root exudates with the same amount of C input, indicating that microbial activity was modified by the N demand. Higher NAG activity was observed in C-rich soil (N limit at high C/N ratio); thus, a continuous supply of low C/N ratio artificial root exudates increased N availability and decreased N-acquiring enzyme activity (Fig. 3). This was consistent with previous studies that applied stoichiometric root exudates to exacerbate CO<sub>2</sub> emissions produced by the microbial demand for N in paddy soils (Liu et al., 2020). However, in contrast to the observations of Liu et al. (2020), we found that a higher proportion of N in artificial root exudates stimulated more CO<sub>2</sub> emission than at high C/N ratios (CN6  $\geq$  CN10 > CN80  $\geq$  C-only) (Fig. 1a, and 1b), and the C-acquiring enzyme activity (BG and XYL) increased in conditions with high C/N ratios of artificial root exudates. These differences were possibly due to the different forms of N nutrients [(NH<sub>4</sub>)<sub>2</sub>SO<sub>4</sub> vs. alanine] added to paddy soils used between the two studies.

Unlike labile inorganic forms of N (NH<sub>4</sub><sup>+</sup> and NO<sub>3</sub><sup>-</sup>), N-containing low-molecular weight organic compounds (e.g., alanine) can decrease microbial nutrient limitations from changes in C/N ratios, and carbohydrate hydrolase has been shown to increase with increasing root exudate C/N stoichiometric ratios due to unbalanced nutrient addition (Allison and Vitousek, 2005; Sinsabaugh et al., 2008). Conversely, higher N-rich artificial root exudates (CN6) showed higher qCO<sub>2</sub> and lower CUE than other treatments on days 3 and 12, whereas the C-only treatment caused low CUE (Fig. 2a, b). A higher proportion of organic N-containing root exudates may have promoted microbial catabolism relative to

anabolism, as there is a higher energy demand for microorganisms in acquiring organic N compared to inorganic N (Näsholm and Persson, 2001; Czaban et al., 2016). Moreover, the positive relationship between BG/NAG ratio and  $q\text{CO}_2$  suggested that microbial catabolism of root exudates that enhanced C- and N-acquiring enzymes can obtain available C and N from both root exudates and SOM. Labile C from root exudates can be quickly utilized by microorganisms as nutrients to enhance microbial consumption of energy and release  $\text{CO}_2$  as a byproduct (Zhu et al., 2018).

Along with the increase in  $\text{CO}_2$  emission, the continuous supply of artificial root exudates lowered microbial CUE in all treated soils when compared with the control. This indicated that the addition of root exudates caused substrate and nutrient uptake by microorganisms (Blagodatskaya et al., 2014; Chen et al., 2020). Additionally, the higher CUE corresponded to a higher C/N stoichiometric ratio in all treatments, except the C-only treatment, indicating that N-containing exudates affected microbial catabolic activity and low N-containing root exudates (i.e., those with high C/N ratios) increased the CUE for SOM accumulation. The positive relationship between the MBC/MBN and CUE (Fig. 4d) suggested that the microbial community with a high C/N ratio biomass had a high potential of C anabolism and induced C accumulation in the soil (Sinsabaugh et al., 2016; Soares and Rousk, 2019). These findings supported our hypothesis that the addition of exudates with a higher C/N ratio increased microbial biomass, lowered  $\text{CO}_2$  emissions, and stimulated soil C sequestration.

#### 4.2 Combining microbial C and N metabolism in the SEM

Root exudates are ubiquitous and quantitatively important drivers of SOM turnover in flooded paddy soil ecosystems. The stoichiometric ratios of resources that are important as energy and nutrients are dominant drivers of the biogeochemical cycles in soil C (McGroddy et al., 2004; Anderson et al., 2005). There are two stoichiometric processes of microbial C and N metabolism of root exudates in paddy soils (Figs. 5 and 6). First, the continuous supply of root exudates caused a C-rich condition and thus, increased microbial activity via overflow respiration of root exudates. The root exudate C/N stoichiometric ratios affected the elemental stoichiometric demands for microorganisms to sustain the C/N stoichiometric balance of microbial biomass (Haichar et al., 2014; Liu et al., 2020; Du et al., 2020; Zhu et al., 2021). A higher energy demand for microorganisms to acquire organic N from amino acids can further increase respiration. In the present study, the root exudate stoichiometric

ratios that lacked N content (e.g., C-only) did not affect microorganism-regulated C mineralization, which were able to allocate energy through lower C mineralization. Second, a combination of exogenous C and N from root exudates by increased C- and N-acquiring enzyme activity caused the catabolism of soil C and was required for microorganism catabolic activity adaptation (Liu et al., 2020; Mori et al., 2021). This was confirmed by our results that identified a significant positive relationship between CO<sub>2</sub> emissions and enzyme stoichiometry. The stoichiometric ratios of root exudates provide a perspective on the microbial stoichiometric requirement for nutrients and help us further understand the root exudate – soil – microorganism interactions that occur in the soil of the rhizosphere.

## **5. CONCLUSIONS**

In this study, we used artificial root exudates with different C/N ratios to investigate the association of the elemental stoichiometric ratios in microbial biomass and extracellular enzyme activities with soil C metabolism. We found that the addition of C-only exudates decreased CO<sub>2</sub> emissions by limiting microbial N metabolism. All three C/N ratios (CN6, CN10, and CN80) of root exudate increased microbial activity and catabolism to meet microorganism demands. The root exudates with lower C/N ratios led to much higher SOM mineralization rates than those with higher C/N ratios. Microorganisms preferred to use easily available low-molecular weight compounds, which led to increased CO<sub>2</sub> emissions and corresponded with increased stoichiometric ratios of C- and N- hydrolases required to meet microbial nutrient demands. Therefore, root exudates with a low C/N stoichiometric ratio stimulates SOM mineralization, while those with a high C/N stoichiometric ratio benefit SOM accumulation. We conclude that root exudate stoichiometric ratios are essential drivers of C cycling in the plant-soil system.

## **CONFLICT OF INTEREST**

The authors declare that they have no known competing financial interests or personal relationships that could have influenced the work reported in this paper.

## **ACKNOWLEDGEMENTS**

This study was supported by the National Natural Science Foundation of China (42177334, 42177330, 41877104), Natural Science Foundation of Hunan Province (2019JJ30028; 2020JJ4653), and Youth Innovation Promotion Association of the Chinese



Academy of Sciences (2019357). We also express gratitude to Alexander von Humboldt Foundation of Germany for their financial support to Tida Ge.

## REFERENCES

- Allison, S.D., Vitousek, P.M., 2005. Responses of extracellular enzymes to simple and complex nutrient inputs. *Soil Biology and Biochemistry* 37, 937–944.
- Anderson, T., Domsch, K., 1993. The metabolic quotient for CO<sub>2</sub> (qCO<sub>2</sub>) as a specific activity parameter to assess the effects of environmental conditions, such as pH, on the microbial biomass of forest soils. *Soil Biology and Biochemistry* 25, 393–395.
- Anderson, T.R., Hessen, D.O., Elser, J.J., Urabe, J., 2005. Metabolic Stoichiometry and the Fate of Excess Carbon and Nutrients in Consumers. *The American Naturalist*, 165, 1–15.
- Bastida, F., Torres, I.F., Hernández, T., Bombach, P., Richnow, H.H., García, C., 2013. Can the labile carbon contribute to carbon immobilization in semiarid soils? Priming effects and microbial community dynamics. *Soil Biology and Biochemistry* 57, 892–902.
- Blagodatskaya, E., Blagodatsky, S., Anderson, T.-H., Kuzyakov, Y., 2014. Microbial Growth and Carbon Use Efficiency in the Rhizosphere and Root-Free Soil. *PLoS ONE* 9, e93282.
- Chen, L., Liang, J., Qin, S., Liu, L., Fang, K., Xu, Y., Ding, J., Li, F., Luo, Y., Yang, Y., 2016. Determinants of carbon release from the active layer and permafrost deposits on the Tibetan Plateau. *Nature Communications* 7, 13046.
- Chen, X., Xia, Y., Rui, Y., Ning, Z., Hu, Y., Tang, H., He, H., Li, H., Kuzyakov, Y., Ge, T., Wu, J., Su, Y., 2020. Microbial carbon use efficiency, biomass turnover, and necromass accumulation in paddy soil depending on fertilization. *Agriculture, Ecosystems & Environment* 292, 106816.
- Creamer, C.A., Jones, D.L., Baldock, J.A., Farrell, M., 2014. Stoichiometric controls upon low molecular weight carbon decomposition. *Soil Biology and Biochemistry* 79, 50–56.
- Czaban, W., Jämtgård, S., Näsholm, T., Rasmussen, J., Nicolaisen, M., Fomsgaard, I.S., 2016. Direct acquisition of organic N by white clover even in the presence of inorganic N. *Plant and Soil* 407, 91–107.

- de Graaff, M.-A., Classen, A.T., Castro, H.F., Schadt, C.W., 2010. Labile soil carbon inputs mediate the soil microbial community composition and plant residue decomposition rates. *New Phytologist* 188, 1055–1064.
- Dijkstra, F.A., Carrillo, Y., Pendall, E., Morgan, J.A., 2013. Rhizosphere priming: a nutrient perspective. *Frontiers in Microbiology* 4.
- Du, L., Zhu, Z., Qi, Y., Zou, D., Zhang, G., Zeng, X., Ge, T., Wu, J., Xiao, Z., 2020. Effects of different stoichiometric ratios on mineralisation of root exudates and its priming effect in paddy soil. *Science of The Total Environment* 743, 140808.
- Fang, Y., Singh, B.P., Collins, D., Armstrong, R., Van Zwieten, L., Tavakkoli, E., 2020. Nutrient stoichiometry and labile carbon content of organic amendments control microbial biomass and carbon-use efficiency in a poorly structured sodic-subsoil. *Biology and Fertility of Soils* 56, 219–233.
- Ge, T., Luo, Y., Singh, B.P., 2020. Resource stoichiometric and fertility in soil. *Biology and Fertility of Soils* 56, 1091–1092.
- IUSS Working Group WRB (2015). World reference base for soil resources 2014. World Soil Resources Reports. No, 106. FAO, Rome
- Fisk, L.M., Barton, L., Jones, D.L., Glanville, H.C., Murphy, D.V., 2015. Root exudate carbon mitigates nitrogen loss in a semi-arid soil. *Soil Biology and Biochemistry* 88, 380–389.
- Haichar, F. el Z., Santaella, C., Heulin, T., Achouak, W., 2014. Root exudates mediated interactions belowground. *Soil Biology and Biochemistry* 77, 69–80.
- Hill, B.H., Elonen, C.M., Seifert, L.R., May, A.A., Tarquinio, E., 2012. Microbial enzyme stoichiometry and nutrient limitation in US streams and rivers. *Ecological Indicators* 18, 540–551.
- Hu, Y., Xiang, D., Veresoglou, S.D., Chen, F., Chen, Y., Hao, Z., Zhang, X., Chen, B., 2014. Soil organic carbon and soil structure are driving microbial abundance and community composition across the arid and semi-arid grasslands in northern China. *Soil Biology and Biochemistry* 77, 51–57.
- Jenkinson, D.S., Brookes, P.C., Powlson, D.S., 2004. Measuring soil microbial biomass. *Soil*

- Biology and Biochemistry 36, 5–7.
- Jones, D.L., Hodge, A., Kuzyakov, Y., 2004. Plant and mycorrhizal regulation of rhizodeposition. *New Phytologist* 163, 459–480.
- Jones, D.L., Nguyen, C., Finlay, R.D., 2009. Carbon flow in the rhizosphere: carbon trading at the soil–root interface. *Plant and Soil* 321, 5–33.
- Kuzyakov, Y., 2002. Separating microbial respiration of exudates from root respiration in non-sterile soils: a comparison of four methods. *Soil Biology and Biochemistry* 34, 1621–1631.
- Li, B., Ge, T., Hill, P. W., Jones, D. L., Zhu, Z., Zhran, M., Wu, J. 2020. Experimental strategies to measure the microbial uptake and mineralization kinetics of dissolved organic carbon in soil. *Soil Ecology Letters* 2, 180-187.
- Liu, Q., Li, Y., Liu, S., Gao, W., Shen, J., Zhang, G., Xu, H., Zhu, Z., Ge, T. and Wu, J., 2022. Anaerobic primed CO<sub>2</sub> and CH<sub>4</sub> in paddy soil are driven by Fe reduction and stimulated by biochar. *Science of The Total Environment* 808: 151911.
- Liu, Y., Ge, T., Zhu, Z., Liu, S., Luo, Y., Li, Y., Wang, P., Gavrichkova, O., Xu, X., Wang, J., Wu, J., Guggenberger, G., Kuzyakov, Y., 2019. Carbon input and allocation by rice into paddy soils: A review. *Soil Biology and Biochemistry* 133, 97–107.
- Liu, Y., Shahbaz, M., Ge, T., Zhu, Z., Liu, S., Chen, L., Wu, X., Deng, Y., Lu, S., Wu, J., 2020. Effects of root exudate stoichiometry on CO<sub>2</sub> emission from paddy soil. *European Journal of Soil Biology* 101, 103247.
- Liu, Y., Shahbaz, M., Fang, Y., Li, B., Wei, X., Zhu, Z., Lynn, T., Lu, S., Shibistova, O., Wu, J., Guggenberger, G., Ge, T., 2021. Stoichiometric theory shapes enzyme kinetics in paddy bulk soil but not in rhizosphere soil (preprint). *Land Degradation & Development*.
- Lopez Sangil, L., George, C., Medina Barcenas, E., Birkett, A.J., Baxendale, C., Bréchet, L.M., Estradera Gumbau, E., Sayer, E.J., 2017. The Automated Root Exudate System (ARES): a method to apply solutes at regular intervals to soils in the field. *Methods in Ecology and Evolution* 8, 1042–1050.
- Lu, R.K., 1999. Soil and agro-chemical analytical methods. *China Agricultural Science and*

- Technology Press, Beijing.
- Manzoni, S., Trofymow, J.A., Jackson, R.B., Porporato, A., 2010. Stoichiometric controls on carbon, nitrogen, and phosphorus dynamics in decomposing litter. *Ecological Monographs* 80, 89–106.
- Marx, M.C., Wood, M., Jarvis, S.C., 2001. A microplate fluorimetric assay for the study of enzyme diversity in soils. *Soil Biology and Biochemistry* 33, 1633–1640.
- McGroddy, M.E., Daufresne, T., Hedin, L.O., 2004. Scaling of C:N:P Stoichiometry in Forests Worldwide: Implications of Terrestrial Redfield-Type Ratios. *Ecology* 85, 2390–2401.
- Mehnaz, K.R., Corneo, P.E., Keitel, C., Dijkstra, F.A., 2019. Carbon and phosphorus addition effects on microbial carbon use efficiency, soil organic matter priming, gross nitrogen mineralization and nitrous oxide emission from soil. *Soil Biology and Biochemistry* 134, 175–186.
- Mori, T., Aoyagi, R., Kitayama, K., Mo, J., 2021. Does the ratio of  $\beta$ -1,4-glucosidase to  $\beta$ -1,4-N-acetylglucosaminidase indicate the relative resource allocation of soil microbes to C and N acquisition. *Soil Biology and Biochemistry* 160, 108363.
- Näsholm, T., Persson, J., 2001. Plant acquisition of organic nitrogen in boreal forests. *Physiologia Plantarum* 111, 419–426.
- Phillips, R.P., Finzi, A.C., Bernhardt, E.S., 2011. Enhanced root exudation induces microbial feedbacks to N cycling in a pine forest under long-term CO<sub>2</sub> fumigation: Rhizosphere feedbacks in CO<sub>2</sub>-enriched forests. *Ecology Letters* 14, 187–194.
- Qiao, N., Schaefer, D., Blagodatskaya, E., Zou, X., Xu, X., Kuzyakov, Y., 2014. Labile carbon retention compensates for CO<sub>2</sub> released by priming in forest soils. *Global Change Biology* 20, 1943–1954.
- Qiao, N., Xu, X., Hu, Y., Blagodatskaya, E., Liu, Y., Schaefer, D., Kuzyakov, Y., 2016. Carbon and nitrogen additions induce distinct priming effects along an organic-matter decay continuum. *Scientific Reports* 6, 19865.
- Schimel, J., 2003. The implications of exoenzyme activity on microbial carbon and nitrogen limitation in soil: a theoretical model. *Soil Biology and Biochemistry* 35, 549–563.

- Shahbaz, M., Kuzyakov, Y., Sanaullah, M., Heitkamp, F., Zelenev, V., Kumar, A., Blagodatskaya, E., 2017. Microbial decomposition of soil organic matter is mediated by quality and quantity of crop residues: mechanisms and thresholds. *Biology and Fertility of Soils* 53, 287–301.
- Sinsabaugh, R.L., Follstad Shah, J.J., 2012. Ecoenzymatic Stoichiometry and Ecological Theory. *Annual Review of Ecology, Evolution, and Systematics* 43, 313–343.
- Sinsabaugh, R.L., Lauber, C.L., Weintraub, M.N., Ahmed, B., Allison, S.D., Crenshaw, C., Contosta, A.R., Cusack, D., Frey, S., Gallo, M.E., Gartner, T.B., Hobbie, S.E., Holland, K., Keeler, B.L., Powers, J.S., Stursova, M., Takacs-Vesbach, C., Waldrop, M.P., Wallenstein, M.D., Zak, D.R., Zeglin, L.H., 2008. Stoichiometry of soil enzyme activity at global scale: Stoichiometry of soil enzyme activity. *Ecology Letters* 11, 1252–1264.
- Sinsabaugh, R.L., Manzoni, S., Moorhead, D.L., Richter, A., 2013. Carbon use efficiency of microbial communities: stoichiometry, methodology and modelling. *Ecology Letters* 16, 930–939.
- Sinsabaugh, R.L., Turner, B.L., Talbot, J.M., Waring, B.G., Powers, J.S., Kuske, C.R., Moorhead, D.L., Follstad Shah, J.J., 2016. Stoichiometry of microbial carbon use efficiency in soils. *Ecological Monographs* 86, 172–189.
- Soares, M., Rousk, J., 2019. Microbial growth and carbon use efficiency in soil: Links to fungal-bacterial dominance, SOC-quality and stoichiometry. *Soil Biology and Biochemistry* 131, 195–205.
- Vance, E.D., Brookes, P.C., Jenkinson, D.S., 1987. An extraction method for measuring soil microbial biomass C. *Soil Biology and Biochemistry* 19, 703–707.
- Wang, Y., Shahbaz, M., Zhran, M., Chen, A., Zhu, Z., Galal, Y. G. M., Ge, T., Li, Y., 2021. Microbial Resource Limitation in Aggregates in Karst and Non-Karst Soils. *Agronomy* 11(8), 1591.
- Wei, L., Razavi, B.S., Wang, W., Zhu, Z., Liu, S., Wu, J., Kuzyakov, Y., Ge, T., 2019. Labile carbon matters more than temperature for enzyme activity in paddy soil. *Soil Biology and Biochemistry* 135, 134–143.
- Wei X, Zhu Z, Liu Y, Luo Y, Deng Y, Xu X, Liu S, Richter A, Shibistova O, Guggenberger G,

- Wu J., 2020. C: N: P stoichiometry regulates soil organic carbon mineralization and concomitant shifts in microbial community composition in paddy soil. *Biology and Fertility of Soils* 56(8).
- Wild, B., Schneckler, J., Alves, R.J.E., Barsukov, P., Bárta, J., Čapek, P., Gentsch, N., Gittel, A., Guggenberger, G., Lashchinskiy, N., Mikutta, R., Rusalimova, O., Šantrůčková, H., Shibistova, O., Urich, T., Watzka, M., Zrazhevskaya, G., Richter, A., 2014. Input of easily available organic C and N stimulates microbial decomposition of soil organic matter in arctic permafrost soil. *Soil Biology and Biochemistry* 75, 143–151.
- Wu, J., Joergensen, R.G., Pommerening, B., Chaussod, R., Brookes, P.C., 1990. Measurement of soil microbial biomass C by fumigation-extraction-an automated procedure. *Soil Biology & Biochemistry* 22, 1167–1169. .
- Xiong, L., Liu, X., Vinci, G., Spaccini, R., Drosos, M., Li, L., Piccolo, A., Pan, G., 2019. Molecular changes of soil organic matter induced by root exudates in a rice paddy under CO<sub>2</sub> enrichment and warming of canopy air. *Soil Biology and Biochemistry* 137,
- Xu, S., Geng, W., Sayer, E. J., Zhou, G., Zhou, P., Liu, C. 2020. Soil microbial biomass and community responses to experimental precipitation change: A meta-analysis. *Soil Ecology Letters* 2(2), 93-103.
- Yin, H., Wheeler, E., Phillips, R.P., 2014. Root-induced changes in nutrient cycling in forests depend on exudation rates. *Soil Biology and Biochemistry* 78, 213–221.
- Yuan, Y., Zhao, W., Xiao, J., Zhang, Z., Qiao, M., Liu, Q., Yin, H., 2017. Exudate components exert different influences on microbially mediated C losses in simulated rhizosphere soils of a spruce plantation. *Plant and Soil* 419, 127–140.
- Zhu, Z., Ge, T., Liu, S., Hu, Y., Ye, R., Xiao, M., Tong, C., Kuzyakov, Y., Wu, J., 2018. Rice rhizodeposits affect organic matter priming in paddy soil: the role of N fertilization and plant growth for enzyme activities, CO<sub>2</sub> and CH<sub>4</sub> emissions. *Soil Biology and Biochemistry* 116, 369-377.
- Zhu, Z., Ge, T., Luo, Y., Liu, S., Xu, X., Tong, C., Shibistova, O., Guggenberger, G., Wu, J., 2018. Microbial stoichiometric flexibility regulates rice straw mineralization and its priming effect in paddy soil. *Soil Biology and Biochemistry* 121, 67–76.

Zhu, Z., Zhou, J., Shahbaz, M., Tang, H., Liu, S., Zhang, W., Yuan, H., Zhou, P., Alharbi, H., Wu, J., Kuzyakov, Y., Ge, T., 2021. Microorganisms maintain C:N stoichiometric balance by regulating the priming effect in long-term fertilized soils. *Applied Soil Ecology* 167, 104033.

Treatment	Glucose (C) (C <sub>6</sub> H <sub>12</sub> O <sub>6</sub> )	Oxalic acid (C) (H <sub>2</sub> C <sub>2</sub> O <sub>4</sub> )	Alanine (C) (C <sub>3</sub> H <sub>7</sub> NO <sub>2</sub> )	Alanine (N) (C <sub>3</sub> H <sub>7</sub> NO <sub>2</sub> )
Control	0	0	0	0
CN6	0.14	0.09	0.17	0.07
CN10	0.22	0.07	0.11	0.04
CN80	0.34	0.05	0.01	0.01
C-only	0.35	0.05	0	0

**Table 1.** Individual substrates added as artificial root exudates (mg incubation flask<sup>-1</sup> day<sup>-1</sup>) to the paddy soil.

## Figures

Fig. 1

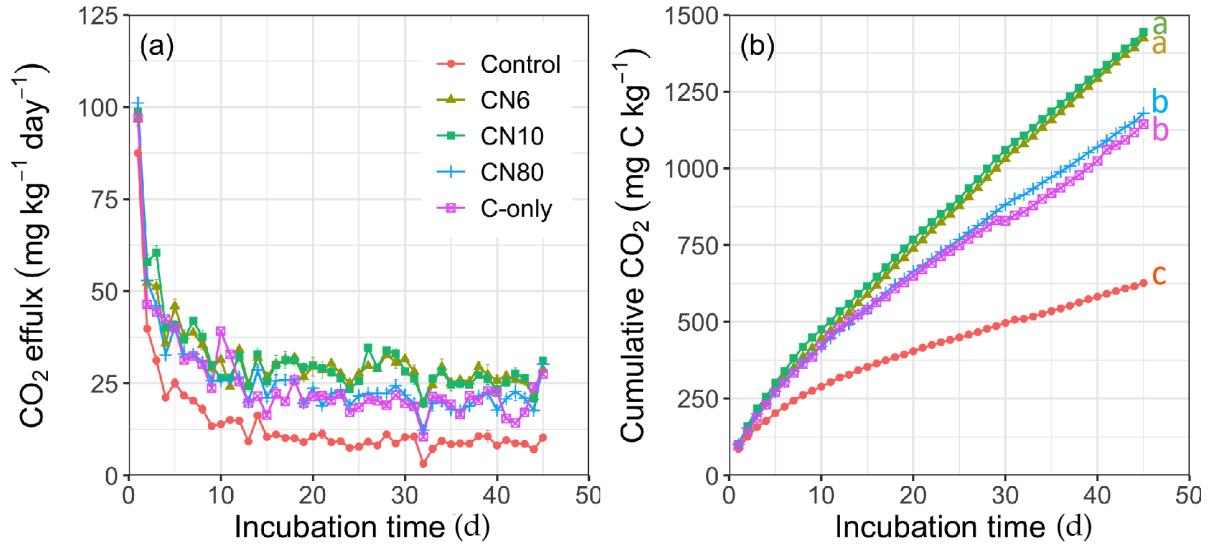
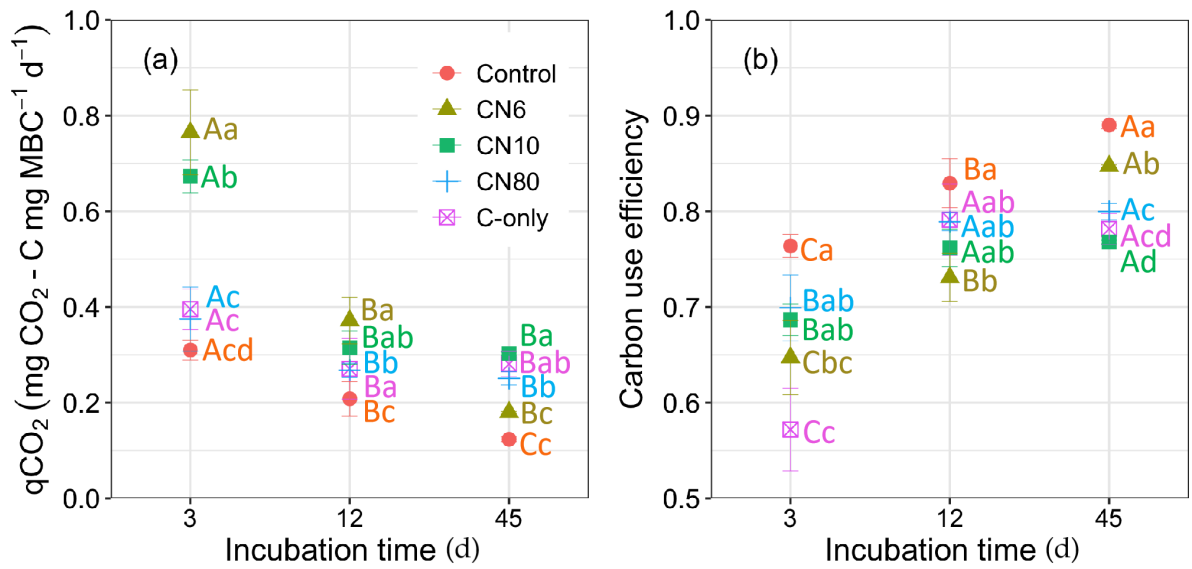
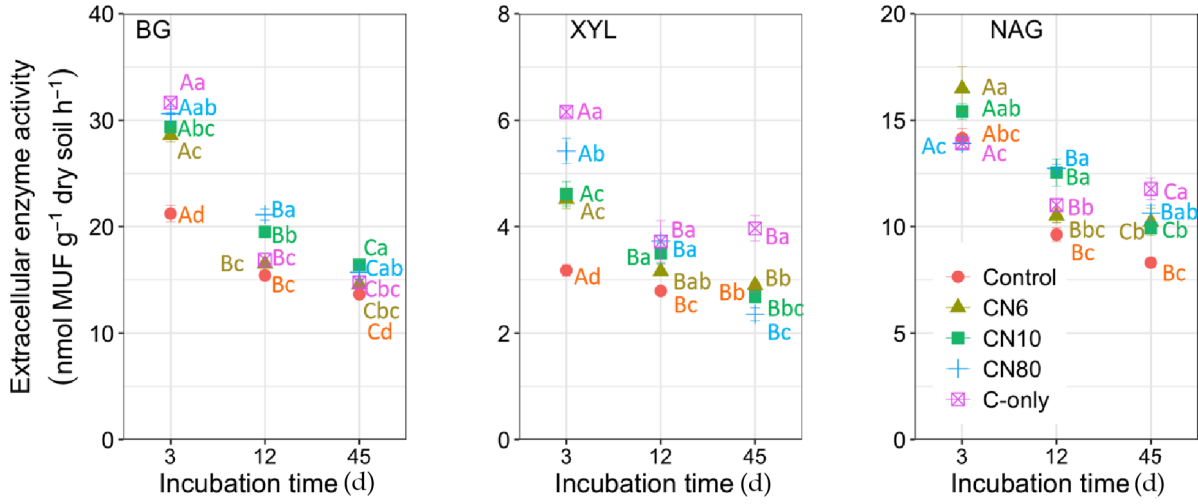


Fig. 2





**Fig. 3**



**Fig. 4**

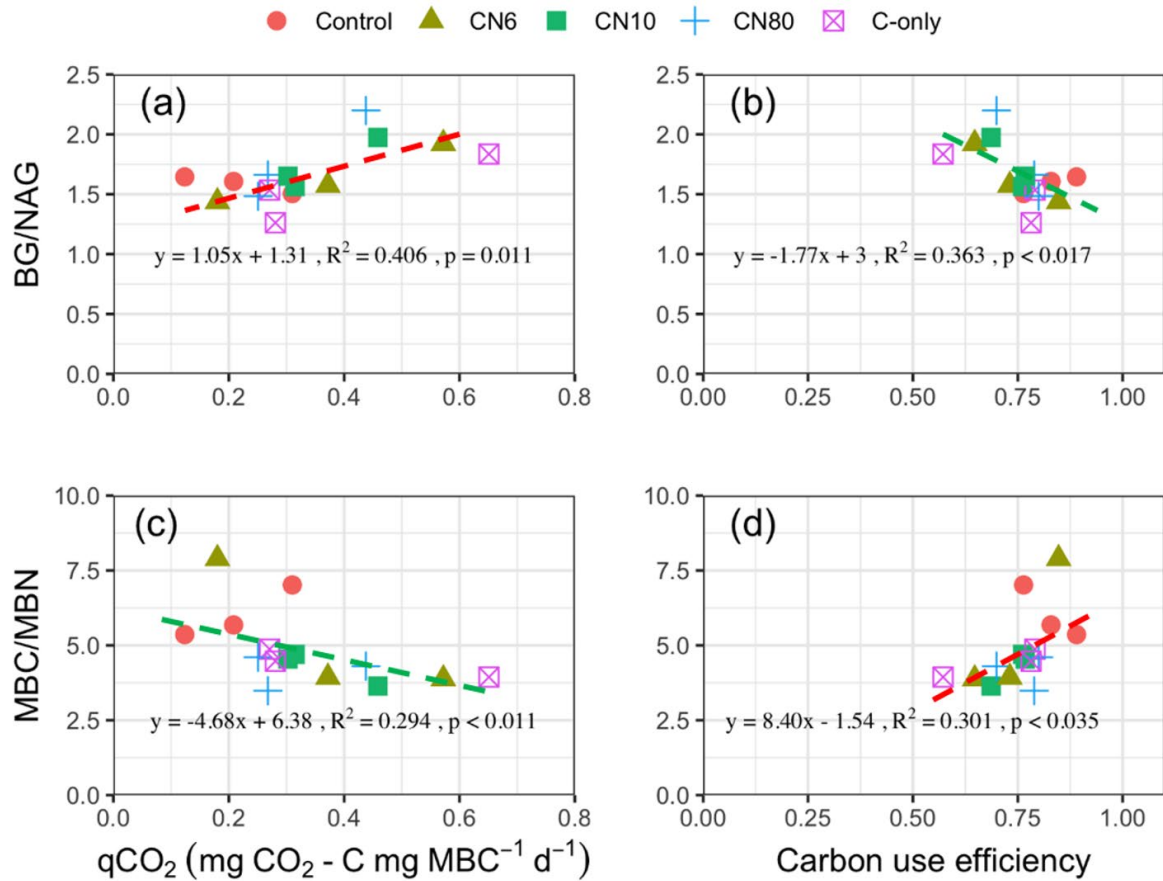


Fig. 5

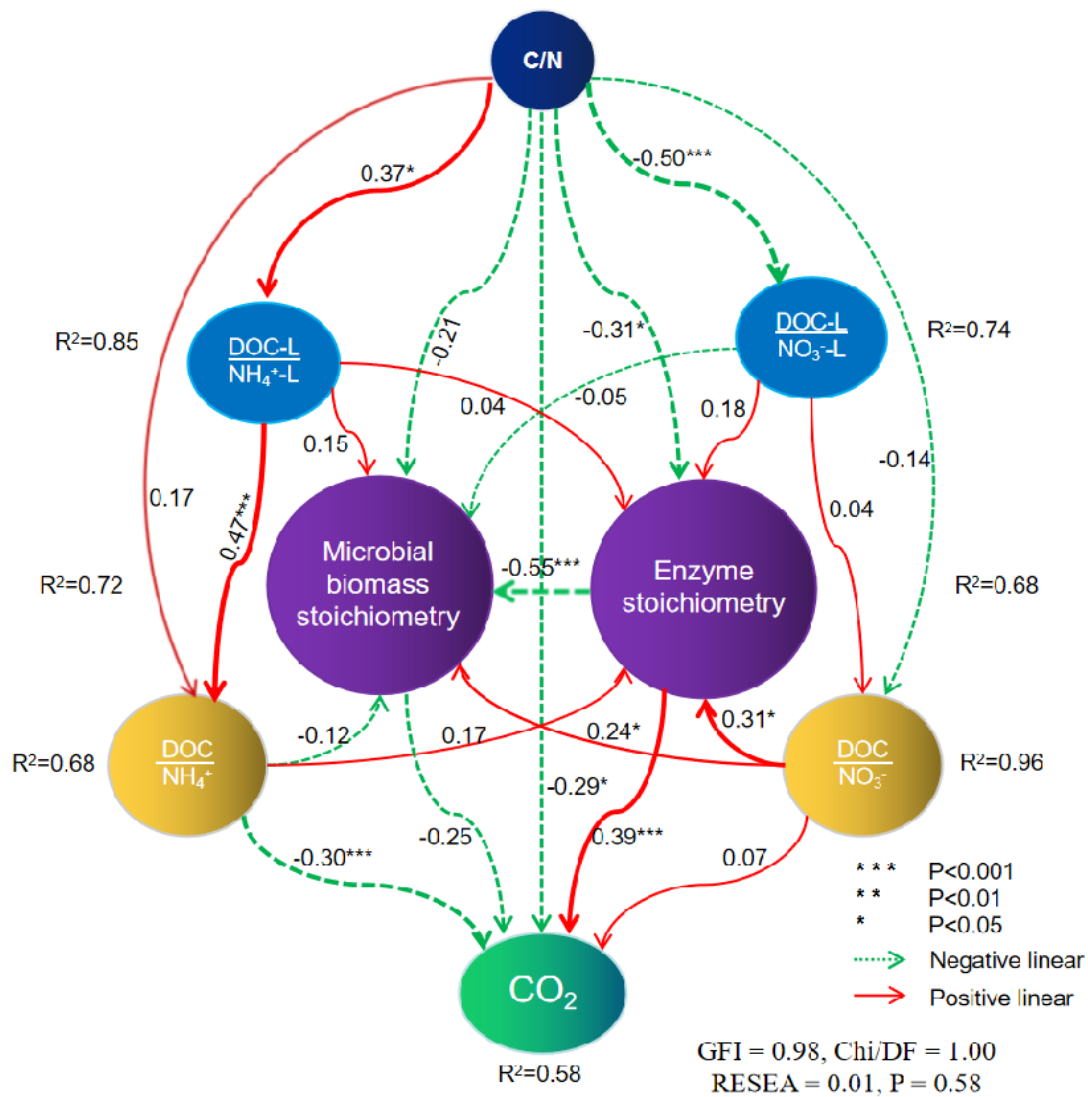
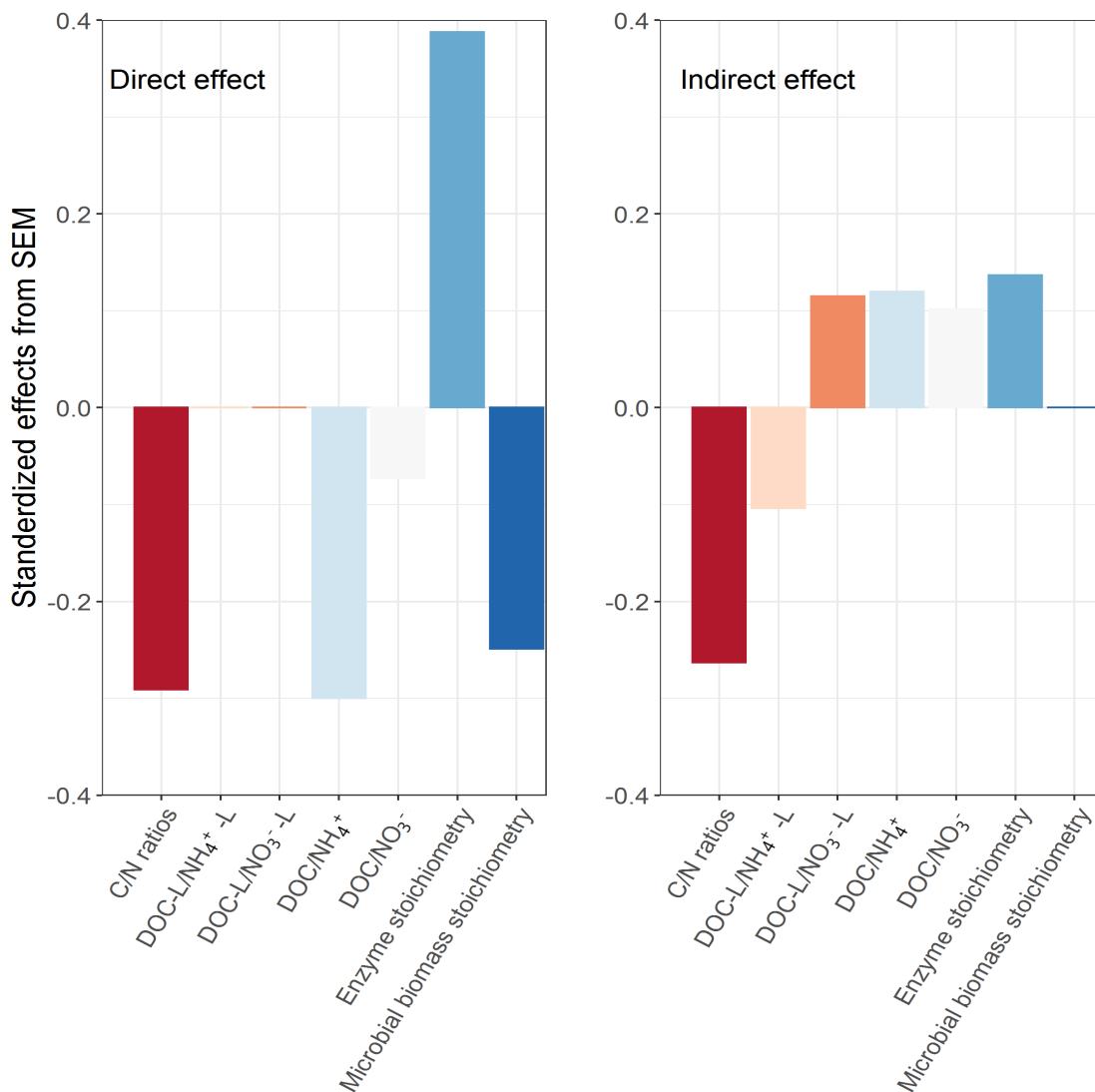


Fig. 6.



### Figure Legends

**Fig. 1** CO<sub>2</sub> efflux rates (a) and cumulative CO<sub>2</sub> (b) over the 45-day incubation period. The control represents no addition of artificial root exudates to soil; C-only represents addition of C substrates glucose and oxalic acid only; CN6, CN10, and CN80 represent addition of C substrates glucose and oxalic acid as well as the N substrate alanine at different C/N stoichiometries of CN6, CN10, and CN80, respectively. Different letters indicate significant differences among stoichiometric ratios at the end of cumulative CO<sub>2</sub> emission (one-way ANOVA and LSD test;  $P < 0.05$  level). Error bars show standard errors ( $n = 4$ ).

**Fig. 2** Metabolic quotient of soil microbial biomass ( $q\text{CO}_2$ ) (a) and carbon use efficiency

(CUE) (b) at days 3, 12, and 45 during the 45-day incubation period. C-only represents addition of C substrates glucose and oxalic acid only; CN6, CN10, and CN80 represent addition of C substrates glucose and oxalic acid as well as the N substrate alanine at different C/N stoichiometries of CN6, CN10, and CN80, respectively. Different letters and capital letters indicate significant differences among stoichiometric ratios and sampling periods, respectively (one-way ANOVA and LSD test;  $P < 0.05$  level). Error bars show standard errors ( $n = 4$ ).

**Fig. 3** Activity of extracellular enzymes  $\beta$ -1,4-glucosidase (BG),  $\beta$ -1,4-xylosidase (XYL), and  $\beta$ -1,4-N-acetyl-glucosaminidase (NAG) at days 3, 12, and 45 during the 45-day incubation period. C-only represents addition of C substrates glucose and oxalic acid only; CN6, CN10, and CN80 represent addition of C substrates glucose and oxalic acid as well as the N substrate alanine at different C/N stoichiometries of CN6, CN10, and CN80, respectively. Different letters and capital letters indicate significant differences among stoichiometric ratios and sampling periods, respectively (one-way ANOVA and LSD test;  $P < 0.05$  level). Error bars show standard errors ( $n = 4$ ).

**Fig. 4** Relationships between metabolic quotient ( $qCO_2$ ) and soil enzyme stoichiometry (BG/NAG) (a), carbon use efficiency (CUE) with soil enzyme stoichiometry (BG/NAG) (b),  $qCO_2$  with microbial biomass stoichiometry (MBC/MBN) (c), CUE with microbial biomass stoichiometry (MBC/MBN) (d). Abbreviations are BG,  $\beta$ -1,4-glucosidase; NAG,  $\beta$ -1,4-N-acetyl glucosaminidase. The dots represent data from all treatments in the 45-day incubation period.

**Fig. 5** Structural equation model of the multivariate effects of C/N ratios, leaching water sample  $DOC-L/NO_3^-$ -L ratios and  $DOC-L/NH_4^+$ -L ratios, soil sample  $DOC/NO_3^-$  ratios and  $DOC/NH_4^+$  ratios, microbial biomass stoichiometry, and enzyme stoichiometry on the  $CO_2$  emission. Microbial biomass stoichiometry represents the ratios of microbial biomass C to microbial biomass N; enzyme stoichiometry represents the average ratios of the activity of  $\beta$ -1,4-glucosidase to  $\beta$ -1,4-N-acetyl glucosaminidase and the activity of  $\beta$ -1,4-xylosidase to  $\beta$ -1,4-N-acetyl glucosaminidase. The solid lines indicate positive path coefficients; dashed lines, negative.  $R^2$  values indicate the proportion of variance explained by each variable contribution to the  $CO_2$  emission from soil application with substrates. The numbers and the width of the arrows indicate the standardized path coefficients.

**Fig. 6** Standardized effect of stoichiometric C/N ratios, leaching water sample  $DOC-L/NO_3^-$ -L ratios and  $DOC-L/NH_4^+$ -L ratios, soil sample  $DOC/NO_3^-$  ratios and  $DOC/NH_4^+$  ratios,

enzyme stoichiometry, and microbial biomass stoichiometry on CO<sub>2</sub> emission.

### Study 1–Supplementary material

**Table S1.** Amounts of individual substrates added (mg incubation flask<sup>-1</sup>) to the paddy soil as artificial root exudates in the different treatment groups.

Treatment	Glucose (C) (C <sub>6</sub> H <sub>12</sub> O <sub>6</sub> )	Oxalic acid (C) (H <sub>2</sub> C <sub>2</sub> O <sub>4</sub> )	Alanine (C) (C <sub>3</sub> H <sub>7</sub> NO <sub>2</sub> )	Alanine (N) (C <sub>3</sub> H <sub>7</sub> NO <sub>2</sub> )
Control	0	0	0	0
CN6	6.17	4.11	7.71	3.00
CN10	9.82	3.27	4.91	1.91
CN80	15.10	2.32	0.58	0.23
C-only	15.60	2.40	0	0

**Table S2.** Soil C/N ratios, microbial biomass C (MBC), microbial biomass N (MBN), DOC, and NH<sub>4</sub><sup>+</sup> at days 3, 12, and 45 during the 45-day incubation period. C-only represents addition of C substrates glucose and oxalic acid only; CN6, CN10, and CN80 represent addition of C substrates glucose and oxalic acid as well as the N substrate alanine at different C/N stoichiometries of CN6, CN10, and CN80, respectively. Different letters indicate significant differences among stoichiometric ratios at the end of cumulative CO<sub>2</sub> emission (one-way ANOVA and LSD test; P < 0.05 level). Values represent means + standard errors (n = 4).

day 3					
Treatment	C/N ratios	MBC (mg/kg)	MBN (mg/kg)	DOC (mg/kg)	NH <sub>4</sub> <sup>+</sup> (mg/kg)
Control	8.71±0.13 <sup>Bab</sup>	101.48±11.00 <sup>Aab</sup>	13.80±1.97 <sup>Ac</sup>	140.02±5.84 <sup>Aa</sup>	84.69±1.49 <sup>Abc</sup>

CN6	8.44±0.49 <sup>Ad</sup>	92.50±20.09 <sup>Bb</sup>	24.25±1.46 <sup>Ab</sup>	153.91±10.06 <sup>Aa</sup>	90.47±2.00 <sup>Aa</sup>
CN10	8.65±0.08 <sup>Bc</sup>	117.23±7.10 <sup>Aa</sup>	22.37±1.66 <sup>Aa</sup>	142.71±4.82 <sup>Aa</sup>	87.03±2.22 <sup>Aab</sup>
CN80	8.88±0.09 <sup>Cab</sup>	111.94±34.90 <sup>Bab</sup>	25.91±0.68 <sup>Bb</sup>	146.17±13.46 <sup>Aa</sup>	82.78±2.59 <sup>Ac</sup>
C-only	9.18±0.11 <sup>Ba</sup>	61.10±15.49 <sup>Cc</sup>	15.70±1.55 <sup>Bc</sup>	152.34±4.51 <sup>Aa</sup>	83.83±1.06 <sup>Abc</sup>
<b>day 12</b>					
<b>Treatment</b>	<b>MBN</b>				
	C/N ratios	MBC (mg/kg)	(mg/kg)	DOC (mg/kg)	NH <sub>4</sub> <sup>+</sup> (mg/kg)
Control	9.40±0.23 <sup>Aa</sup>	74.92±16.25 <sup>Cc</sup>	13.12±1.10 <sup>Ac</sup>	118.26±6.55 <sup>Ba</sup>	87.35±10.92 <sup>Bc</sup>
CN6	8.84±0.22 <sup>Ad</sup>	95.72±23.31 <sup>Bb</sup>	24.25±1.46 <sup>Ab</sup>	107.00±3.72 <sup>Ba</sup>	75.87±7.78 <sup>Aa</sup>
CN10	8.87±0.22 <sup>Bc</sup>	105.86±21.85 <sup>Ba</sup>	22.37±1.66 <sup>Bb</sup>	113.92±5.44 <sup>Ba</sup>	65.09±4.97 <sup>Bab</sup>
CN80	9.18±0.08 <sup>Bab</sup>	100.75±11.83 <sup>Cb</sup>	31.09±2.61 <sup>Aa</sup>	113.92±5.44 <sup>Ba</sup>	65.09±4.97 <sup>Bd</sup>
C-only	9.01±0.20 <sup>Bab</sup>	104.17±34.14 <sup>Aa</sup>	21.85±1.61 <sup>Ab</sup>	114.93±12.59 <sup>Ba</sup>	76.36±6.54 <sup>Bab</sup>
<b>day 45</b>					
<b>Treatment</b>	<b>MBN</b>				
	C/N ratios	MBC (mg/kg)	(mg/kg)	DOC (mg/kg)	NH <sub>4</sub> <sup>+</sup> (mg/kg)
Control	9.59±0.46 <sup>Aa</sup>	82.98±3.31 <sup>ABd</sup>	15.50±0.47 <sup>Ad</sup>	73.94±9.39 <sup>Ca</sup>	19.07±1.15 <sup>Cd</sup>
CN6	8.88±0.26 <sup>Ab</sup>	159.45±2.39 <sup>Aa</sup>	20.24±1.11 <sup>Bc</sup>	68.52±4.92 <sup>Ca</sup>	95.74±3.36 <sup>Aa</sup>
CN10	9.43±0.08 <sup>Aa</sup>	102.82±0.83 <sup>Cc</sup>	22.66±0.87 <sup>Bb</sup>	72.76±2.58 <sup>Ca</sup>	73.22±5.31 <sup>Bb</sup>
CN80	9.65±0.15 <sup>Aa</sup>	121.17±11.54 <sup>Ab</sup>	26.41±1.22 <sup>Ba</sup>	66.49±9.79 <sup>Ca</sup>	36.72±0.97 <sup>Cc</sup>
C-only	9.65±0.08 <sup>Aa</sup>	99.66±13.99 <sup>Bc</sup>	22.25±0.61 <sup>Ab</sup>	74.29±2.78 <sup>Ca</sup>	37.45±1.21 <sup>Cc</sup>

## **3 Study 2**

### **Lignin degradation in wetland soil by anaerobic and aerobic processes**

Contribution: I participated in fieldwork, sampling activities, and the experiment incubation, performed most of the analysis in the laboratory, collected and evaluated data, prepared tables and figures, and wrote the manuscript.

## **Lignin degradation during anaerobic and aerobic processes in wetland**

Guan Cai<sup>a</sup>, Norman Gentsch<sup>a</sup>, Tida Ge<sup>a,b</sup>, Jiří Bárt<sup>c</sup>, Karin Pritsch<sup>d</sup>, Olga Shibistova<sup>ae</sup>, Leopold Sauheitl<sup>a</sup>, Georg Guggenberger<sup>a</sup>

<sup>a</sup> Institute of Soil Science, Leibniz Universität Hannover, Hannover 30419, Germany

<sup>b</sup> State Key Laboratory for Managing Biotic and Chemical Threats to the Quality and Safety of Agro-products, Institute of Plant Virology, Ningbo University, Ningbo 315211, China

<sup>c</sup> Institute of Biochemical Plant Pathology, Helmholtz Zentrum München, Neuherberg 85764, Germany

<sup>d</sup> Department of Ecosystems Biology, University of South Bohemia, České Budějovice, 37005, Czech Republic

<sup>e</sup> VN Sukachev Institute of Forest, Siberian Branch of the Russian Academy of Sciences, Krasnoyarsk, 660036, Russian Federation

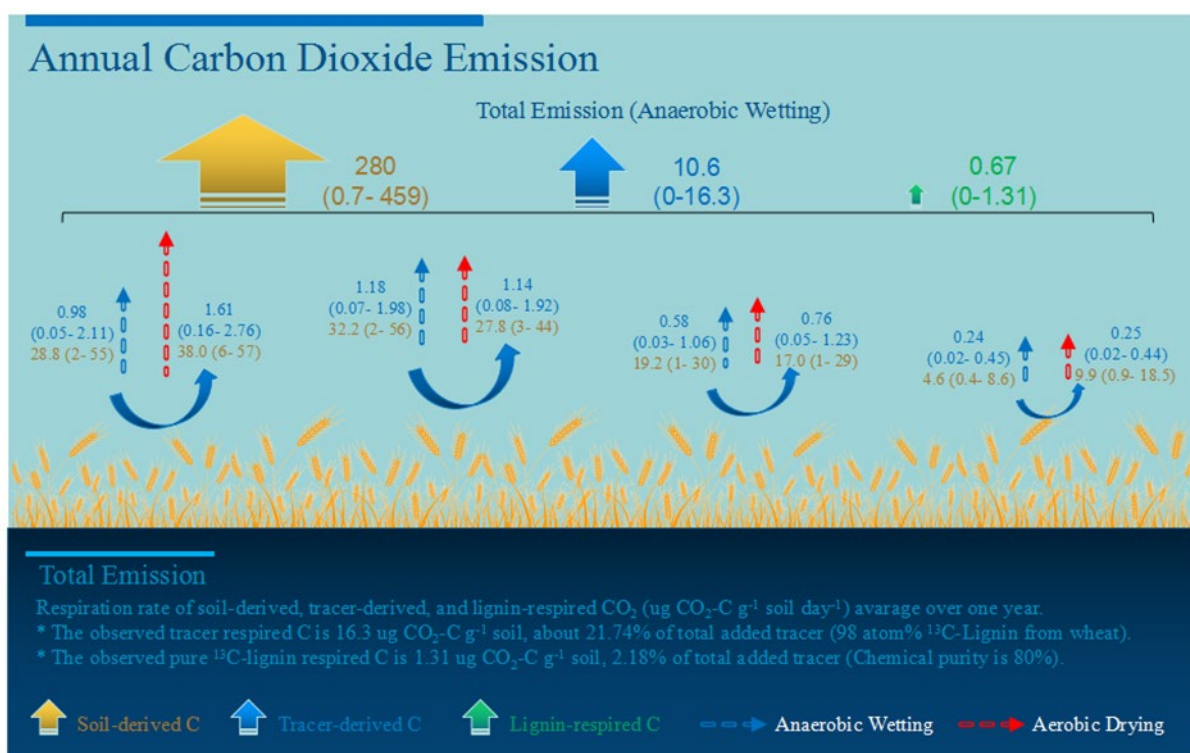


**Abstract**

Lignin is a vital plant residue input to soil and has been a long time thought to play an essential role in the formation of stable soil organic matter (SOM). However, our knowledge on the processing of this macromolecule in the soil is only extensive for aerobic conditions while still in its infancy in an anaerobic environment. But anaerobic soils will undergo dramatic changes during climate change, e.g., melting permafrost or aeration of waterlogged soils. Therefore, exploring the degradation of lignin in soils under anaerobic conditions can help to better understand the carbon (C) sink or source effect of soils in the context of climate change. In this study, a 365-day incubation experiment was performed to investigate the microbial degradation of  $^{13}\text{C}$ -labeled lignin under anaerobic followed by aerobic conditions at different time intervals. The fate of lignin was traced through  $\text{CO}_2\text{-C}$  and microbial biomass C (MBC) in both anaerobic and aerobic soils. Lignin was effectively degraded under aerobic conditions. However, microorganisms also degraded lignin under anaerobic conditions as indicated by  $^{13}\text{C}$  accumulation in microbial biomass and produced  $\text{CO}_2$ . The tracer contributed to about 3.4 % of the total  $\text{CO}_2$  mineralization in one-year of anaerobic incubation. The cumulative tracer-derived C under aerobic conditions was 11.7% larger than under anaerobic conditions during four intervals. These works improve our knowledge that the anaerobic mineralization of lignin can be a significant  $\text{CO}_2$  source, and their anaerobic metabolic process induces an entombing effect for SOM accumulation in anaerobic soil.

Keywords: Anaerobic and aerobic Lignin, Stable-isotope-probing, Soil organic Matter, entombing effect, Carbon recyclingg

## Graphical abstract



Graphical abstract: The carbon dioxide (CO<sub>2</sub>) emission in a one-year anaerobic incubation of a wetland soil. The total anaerobic emission rate (μg CO<sub>2</sub>-C g<sup>-1</sup> soil day<sup>-1</sup>) consists of soil-derived C (yellow), tracer-derived C (blue), and lignin tracer-derived C (green) in the top area. The bottom area estimates the CO<sub>2</sub> emission from soil-derived C (yellow numbers) and tracer-derived C (blue numbers) at the four different sampling periods during anaerobic (blue arrows) and aerobic conditions (red arrows).

## 1. INTRODUCTION

Generally, SOM decomposition in wetlands usually involves a combination of anaerobic and aerobic processes (Bernal and Mitsch, 2008; Song et al., 2019). This is also referred to as lignin, the second most crucial plant input material to the soil, and whose decomposition process will significantly affect CO<sub>2</sub> production and is essential for biogeochemical cycling and climate change (Masai et al., 2007).

Temporal dynamics and fate of lignin decomposition and its mean residence in SOM have been well examined for aerobic soils. Microorganisms control the lignin decomposition through the cooperation of different members of microbial communities (soil bacteria, fungal and archaeal); larger aromatic ring structures are gradually broken down into smaller fragments by microbial activity (Tuomela, 2000; Thevenot et al., 2010; Gittel et al., 2014; Janusz et al., 2017). Fungal is generally considered dominant and fast, but bacteria can also break down the lignin reported recently in aerobic soils, such as  $\alpha$ -Proteobacteria and  $\gamma$  - Proteobacteria (Hu and Bruggen, 1997; Schutter and Dick 2001; Šnajdr et al., 2011; Bugg et al., 2011). Laccase, peroxidase, and polyphenol oxidase play an essential role in the oxidative decomposition of lignin (Bourbonnais and Paice, 1990; Niladevi et al., 2008; Cañas and Camarero, 2010; Song et al., 2019). Biomass amount and thermal conditions were faster-decomposed lignin under aerobic conditions; thus, lignin does not form stable SOM (Torres et al. 2014., Xue et al., 2016; Tao et al., 2020).

A situation may be different for anaerobic soils since oxygen is lacking for regular oxidative decomposition under an extremely waterlogged or frozen environment. Anaerobic conditions and low redox potential modulate the structure and function of the microbial community, thereby affecting the accumulation and stability of SOM (Kögel-Knabner et al., 2010; Hall and Silver 2015; Gentsch et al., 2015; Dao et al., 2018; Xia et al., 2021). Song et al., (2019) observed the anaerobic degradation of specific anaerobic bacteria (*Clostridium*, genus *Sulfuricurvum*, and *Treponema*) and anaerobic fungi (*Chytridia* and *Rhodophyta*) during the biodegradation of lignin in underground sediments. Atkinson et al., (1996) reported about 1% anaerobic bacteria in an anaerobic composting microenvironment, which play an essential role in the degradation of macromolecules, such as mesophilic anaerobic bacteria. Up to 90% of lignin-derived aromatic substrates have been shown to be converted to CH<sub>4</sub> and CO<sub>2</sub> during anaerobic metabolisms, such as aromatics, phenols, and benzoates (Kobayashi et al., 1988). A facultative anaerobe bacterium, *Tolumonas ligninolytic*. and

*Klebsiella sp.* were reported to use lignin as a source of carbon and energy during the lignin depolymerization process under anaerobic conditions through a putative pathway (Woo et al., 2014; Billings et al., 2015). An enzymatic functional nonoxidative gene for the catabolic pathway, namely 5-Carboxyvanillate decarboxylase (LigW, and ligW2), has been observed in *Sphingomonas paucimobilis* SYK-6, which catalyzes the cleavage of the C-C bond of 5-carboxyvanillate to vanillin and release CO<sub>2</sub> and HCO<sub>3</sub><sup>-</sup> (Peng et al., 2002; 2005; Vladimirova et al., 2016; Sheng et al., 2017). Fenner and Freeman (2020) observed that polyphenols inhibit microbial activity by binding additional extracellular hydrolases and substances under anaerobic conditions. Polyphenol oxidase affects metabolite depolymerization and monomer accumulation in soil microbial metabolisms in anaerobic wetland soil (McGivern et al., 2021). Like polyphenol oxidase, peroxidase is a typical aerobic enzyme whose crucial role in anaerobic soil microbial metabolism may also be overlooked, as other aerobic enzymes (DeAngelis et al., 2013; Kuusk et al., 2018; McGivern et al., 2021). Thus, the enzymes involved in soil microbial processes and their contribution to the rate of lignin breakdown metabolism in anaerobic and aerobic soils are still in their infancy.

We aim to investigate the fate of lignin degradation in wetland soil under anaerobic and aerobic conditions and determine the underlying regulations of microbial processes in SOM decomposition. To characterize the detailed lignin degradation, we examined wetland soil samples labeled with <sup>13</sup>C-lignin in a 365-days incubation under anaerobic and aerobic conditions. We hypothesized that (i) lignin decomposition rates are slower under anaerobic than aerobic conditions, (ii) but lignin is also not efficiently stabilized under long-time anaerobic conditions, and (iii) metabolic processes promote biomass accumulation under anaerobic than aerobic conditions

## 2. MATERIALS AND METHODS

### 2.1 Study site and soil sampling

The soil was collected from the Saxony - Thuringian loess hills region 60 km south of the City Leipzig, Germany (50°51'52"N, 12°33'53"E). The climate is Dfb according to Köppen-Geiger climate classification with annual precipitation of 607 mm and annual mean temperature of 8.4 °C. Soils in depressions of the catchments often developed from colluvial deposits and are classified as Eutric Gleysols according to IUSS Working Group WRB (FAO 2015). In April, field moist soils were collected from the oxic part of the Bg horizon

(28–48 cm) using a stainless-steel drill (diameter: 5 cm). This soil horizon undergoes both water-saturated as well as aerated episodes during the year so that the microbial community is supposed to be adapted to the redox fluctuations of the incubation. Soils were thoroughly mixed, then passed through a 2-mm sieve to remove fine roots and other plant residues. Composite soil samples were immediately placed in a gas-free plastic bag and stored at 4 °C until analysis. The sand, silt, and clay content were 2%, 77%, and 21%, respectively. The concentration of organic C was 6.22 g kg<sup>-1</sup> and that of total N 0.25 g kg<sup>-1</sup>. The concentration of soil total pedogenic Fe oxides (dithionite-soluble Fe; Fe<sub>d</sub>) and non-crystalline pedogenic Fe oxides (oxalate-soluble Fe; Fe<sub>o</sub>) was 6.30 g kg<sup>-1</sup> and 9.34 g kg<sup>-1</sup>, respectively. The δ<sup>13</sup>C value of SOM was -28.18 ‰ (vs. VPDB), and pH was 5.71 at soil to water ratio (w:v) of 1:2.5.

## 2.2 Experimental design and soil incubations

A total of 100 g fresh soil was placed in a 75 mL centrifuge tube (diameter 3.5 cm, height 10 cm). A total of 32 tubes were alternately filled with ten layers of soil mixed with a lignin suspension, respectively, to guarantee a homogeneous distribution of the lignin. For preparing the lignin suspension, 7.5 mg <sup>13</sup>C-lignin from wheat (>98 atom%, chemical purity of 80%; Isolife, Wageningen, The Netherlands) was added per tube, which was dissolved in 2 ml distilled H<sub>2</sub>O employing ultra-sonification for 10 min. The amount of added <sup>13</sup>C-lignin (75 µg C g soil) was related to 1 % of soil organic carbon (SOC), and was similar to previous <sup>13</sup>C-lignin isotope labeling experiments (Torres et al., 2014). Each centrifuge tube was placed in a 500 mL gas-tight glass bottle with a screw cap equipped with a connection system for aeration and CO<sub>2</sub> trapping (called incubation system).

After filling, soils were covered with 0.5 cm distilled H<sub>2</sub>O, and the bottles were sealed using a screw cap with coated seals to ensure anaerobic conditions. All these procedures were done in an anaerobic chamber under the flow of helium (BACTRON Anaerobic Chamber, 300 Plate Capacity, Sheldon Manufacturing, Cornelius, OR, USA).

All incubation systems were started at anaerobic conditions (as described above). After 30, 90, 180, and 360 days, the soil of four replicates of the anoxic systems was sampled destructively, respectively. Also, at these time points, another four replicates were oxic conditions for 30 days, respectively, after which they were also sampled destructively (Fig. S1). This design with two incubation conditions, with four replicates, divided into four sampling times, led to a total of 32 incubation vessels. In addition, we had eight systems that

acted as a control, not receiving tracer.

All  $^{13}\text{C}$ -lignin labeled soil samples were incubated under anaerobic conditions at 15 °C under darkness. We flushed the incubation flask with helium (400 ppb He) during the anaerobic water-saturated period. After the anaerobic wetting sample was harvested, another four replicates were switched to anaerobic drying conditions (WHC 40%). After that, the excess soil solution was collected in a 15 ml tube and stored at -20 °C until further analysis. Next, the aerobic samples were flushed with synthetic air (20% O<sub>2</sub>, 80% N<sub>2</sub>, 400 ppb N<sub>2</sub>O) and incubated under darkness at 15 °C. Thirty days after the respective start of the oxic incubation, the soil was sampled. One of the unlabelled control systems was collected at each harvest time point.

### 2.3 Measurements

We continuously measured soil respiration and its isotopic composition from the incubation flasks in order to trace the mineralization of  $^{13}\text{C}$ -lignin. Incubation flasks were first flushed with helium or artificial air for sampling air in the headspace under anaerobic and aerobic soil incubation, respectively. After 10 min flushing, most of the initial CO<sub>2</sub> inside the flask was removed, and soil samples were incubated for CO<sub>2</sub> trapping. A 15 mL gas sample was taken from the incubation flask by using a 20-ml syringe after 24 h (T1), 36 h (T2), and 48 h (T3) for anaerobic samples, and 24 h (T1), 48 h (T2), and 72 h (T3) for aerobic samples. All gas samples (T1, T2, and T3) were transferred to pre-evacuated vials (Exetainers, IVA, Analysentechnik, Meerbusch, Germany). The CO<sub>2</sub> concentration and the  $\delta^{13}\text{C}$  value of each gas sample were analyzed on an isotopic ratio mass spectrometer (Delta Plus, Thermo Scientific, Bremen, Germany) at the Institute of Biochemical Plant Pathology, Helmholtz Centre, Munich (Leiber-Sauheitl et al., 2015).

The C and nitrogen (N) contents, as well as the and the  $\delta^{13}\text{C}$  value of bulk soil samples, were measured in duplicates using an Elementar IsoPrime 100 IRMS (IsoPrime Ltd., Cheadle Hulme, UK) coupled to an elemental analyzer (Vario Isotope Cube, Elementar Analysensysteme GmbH, Hanau, Germany).

Lignin-derived phenols in soil samples were analyzed using alkaline CuO oxidation following the Hedges and Ertel (1982) method with modifications of Kögel and Bochter (1985). Approximately 400 mg of dry soil equivalent to 0.6-0.8% OC were weighed into a teflon vessel. Then 500 mg of CuO together with 100 mg of ammonium iron sulfate hexahydrate [Fe(NH<sub>4</sub>)<sub>2</sub>(SO<sub>4</sub>)<sub>2</sub>·6H<sub>2</sub>O], 50 mg of glucose, 15 mL of 2 M NaOH, and 100 uL of

the internal standard (ethyl vanillin; 10  $\mu\text{g}$  ethyl vanillin in 100  $\mu\text{L}$  2 M NaOH) were added. To remove free  $\text{O}_2$ , the vessel was rinsed with nitrogen gas for a few seconds, then sealed and heated for three hours at 170  $^\circ\text{C}$ . The resulting solution containing the free lignin-derived monomers was then purified by removing humic acids and other impurities using pH adjustment and solid-phase extraction on C18-SPE-columns (Bakerbond<sup>TM</sup> spe Columns, Griesheim, Germany). Finally, samples were derivatized in 5 mL reaction vials by adding 200  $\mu\text{L}$  BSTFA (N, O-bis-(trimethylsilyl)-trifluoroacetamide) and 100  $\mu\text{L}$  pyridine and heating for 20 min at 60  $^\circ\text{C}$  in a derivatization block (C-MAG HS 7, IKA, Staufen, Germany). The derivatized lignin-derived monomers were quantified using a GC-MS (5977 Series GC/MSD system with Agilent 7890B GC, Agilent Technologies, California, USA) (Dao et al., 2018). Calibration was done using nine different standard concentrations containing eight lignin monomers (vanillin, ethyl vanillin, acetovanillin, syringaldehyde, vanillic acid, acetosyringone, syringic acid, p-coumaric acid, and ferulic acid) (50 mg/100 mL MeOH) as well as the two internal standards, ethyl-vanillin and phenyl acetic acid (25  $\mu\text{g}/1$  mL MeOH). The recovery of all samples was  $>70\%$  and averaged to 86%. Vanillyl (V), syringyl (S), and cinnamyl (C) units were calculated as the sum of their aldehyde, acid, and ketone forms. Total lignin-derived phenols were calculated as the sum of individual units ( $\text{VSC} = \text{V} + \text{S} + \text{C}$ ). The mass ratios of phenolic acids over aldehydes for vanillyl units ( $\text{Ac/Al}_\text{V}$ ) and the mass ratio of syringyl to vanillyl (S/V) were calculated following the method of (Hedges and Ertel 1982; Kögel and Bochter 1985).

Soil microbial biomass carbon (MBC) was determined using the chloroform fumigation extraction method (Vance et al., 1987; Wu et al., 1990). One subsample (10 g) was extracted with 40 mL 0.05 M  $\text{K}_2\text{SO}_4$  solution, while another 10 g was first fumigated with ethanol-free chloroform in the dark for 24 h and then extracted with  $\text{K}_2\text{SO}_4$  solution (40 mL; 0.5 M). The extracted C in fumigated and unfumigated samples was measured after acidification using a LiquiTOC analyzer (Elementar Analysensysteme GmbH, Germany). The MBC was calculated as the difference in C content between the fumigated and non-fumigated sample extracts, adjusted by a proportionality coefficient ( $k_{\text{EC}} = 0.45$ ) to account for the extraction efficiency. The remaining extracts were freeze-dried and measured for  $\delta^{13}\text{C}$  on the EA-IRMS mentioned above.

Activities were determined for representative enzymes involved in the turnover of simple SOC, N, P, and complex soil organic matter (SOM). The eight enzyme activities are simple SOC:  $\alpha$ -glucosidase (AG),  $\beta$ -glucosidase (BG),  $\beta$ -Xylanase (Xyl), and endocellulase

(Cello); N: b-N-acetyl-glucosaminidase (NAG); P: phosphatase (Phos); SOM: peroxidase and polyphenol oxidase.

Fluorogenic methylumbelliferone-based artificial substrates were used to estimate the activity levels of AG, BG, Xyl, Cello, Phos, and NAG following the method of Sinsabaugh et al., (1993) and Marx et al., (2001). The fresh soil (1 g) was slurried in 50 mL deionized water using low-energy sonication ( $50 \text{ J s}^{-1}$ ) for 1 min. Next, a 50- $\mu\text{L}$  aliquot of the soil suspension was dispensed in a 96-well black microplate. Subsequently, the same volume of MES buffer (50  $\mu\text{L}$ , pH 6.5) was added. Finally, a serial of increasing concentration of substrate solution (100  $\mu\text{L}$ ) was added to the well. The fluorescence values were then determined with an automated fluorometric plate reader (Victor3 1420–050 Multi-label Counter; PerkinElmer, Waltham, MA, USA) with an excitation wavelength of 365 nm and an emission wavelength of 450 nm. Following the Michaelis- Menten equation, enzyme activities were expressed as  $V_{\text{max}}$  (Dowd and Riggs 1965). Peroxidase and phenol oxidase activities were determined using L-3,4-dihydroxy-phenyl-alanine (L-DOPA) (Sinsabaugh et al., 1993). The fresh soil (1 g) was prepared by dissolving in 50 mM acetate buffer (pH 5) using low-energy sonication ( $50 \text{ J s}^{-1}$ ) for 1 min. To the soil suspension (50  $\mu\text{L}$ ) of peroxidase samples, hydrogen peroxide ( $\text{H}_2\text{O}_2$ ) was added as substrate. The soil slurry was incubated with 50  $\mu\text{L}$  of the substrate (and ten  $\mu\text{L}$  of 0.03%  $\text{H}_2\text{O}_2$  for total oxidase) at  $20^\circ \text{C}$  for one hour. Subsequently, a parallel of substrate and sample controls were included. The samples were measured with an absorbance at 460 nm. Enzyme activities were expressed as  $\mu\text{M}$  substrate  $\text{g}^{-1} \text{h}^{-1}$ . The sum of phenoloxidase activity and the peroxidase activity (total oxidase activity) was determined as the assay for peroxidase (Kourtev et al., 2002).

## 2.4 Calculations

### 2.4.1 Tracer-derived $\text{CO}_2$ -C, soil-derived $\text{CO}_2$ -C, and priming

The soil respiration (in  $\mu\text{g CO}_2\text{-C g}^{-1} \text{ soil day}^{-1}$ ) in each flask was calculated based on the “Keeling plot” method (Keeling, 1958; 1961). A modified version of the Keeling plot was used to calculate the  $\delta^{13}\text{C}$  of soil derived  $\text{CO}_2$  compensating for impurities of ambient  $\text{CO}_2$  at the start of  $\text{CO}_2$  accumulation in the incubation system.

The soil respiration in each serum bottle was separated into tracer-derived  $\text{CO}_2\text{-C}$  and soil-derived  $\text{CO}_2\text{-C}$  (microbial decomposition of SOM) using a two-source mixing model (Gearing, 1991):

$$C_S = C_T \times (at\%^{13}C_T - at\%^{13}C_t) / (at\%^{13}C_S - at\%^{13}C_t) \quad (1)$$



Where  $C_T$ ,  $C_S$ , and  $C_t$  are total flux CO<sub>2</sub>-C, soil-derived CO<sub>2</sub>-C, and tracer-derived CO<sub>2</sub>-C in serum bottles, respectively.  $at\%^{13}C_T$  was measured as the  $at\%^{13}C$  value of total flux CO<sub>2</sub>-C in serum bottles, and  $at\%^{13}C_t$  is the  $at\%^{13}C_{tracer}$  (<sup>13</sup>C-Lignin, >98 atom%) and  $at\%^{13}C_S$  is the  $at\%^{13}C$  value of soil respiration in unlabelled control.

The contribution of soil-derived CO<sub>2</sub>-C in <sup>13</sup>C label efflux from soil respiration was calculated as:

$$C_{SR} = C_S / C_T \times 100(\%) \quad (2)$$

The contribution of tracer-derived CO<sub>2</sub>-C in <sup>13</sup>C label efflux from soil respiration was calculated as:

$$C_{TR} = 1 - C_{SR} \times 100(\%) \quad (3)$$

#### 2.4.2 Cumulative tracer-respired and lignin-respired CO<sub>2</sub>-C

The cumulative tracer-respired CO<sub>2</sub>-C in <sup>13</sup>C label efflux from soil respiration was calculated as:

$$\sum_{i=1}^{n=365} TR = C_{TR} \times \sum CO_2 - C_{efflux} \quad (4)$$

where  $C_{TR}$  is the contribution of tracer-derived CO<sub>2</sub>-C in <sup>13</sup>C label efflux from soil respiration, and  $\sum CO_2 - C_{efflux}$  is the cumulative CO<sub>2</sub>-C efflux.

The cumulative lignin-respired CO<sub>2</sub>-C in <sup>13</sup>C label efflux from soil respiration was calculated as:

$$\sum_{i=1}^{n=365} LR = \sum TR - (1 - 80\%) \times 75 \quad (5)$$

Where  $\sum TR$  is the cumulative tracer-respired CO<sub>2</sub>-C, 80% is the chemical purity of the <sup>13</sup>C-lignin, and the total tracer addition from <sup>13</sup>C-Lignin is 75 ug/g soil. A spline function was used in these equation according to Gentsch et al. (2018).

The priming of soil-derived CO<sub>2</sub>-C between labeled treatments and unlabelled control was calculated as:

$$PE = C_{T(labeled)} - C_{T(unlabelled)} - C_t \quad (6)$$

#### 2.4.3 Tracer-derived MBC and soil-derived MBC

Total MBC (MBC<sub>T</sub>) in each treated soil was separated into tracer-derived MBC (MBC<sub>t</sub>) and soil-derived MBC (MBC<sub>S</sub>) using a two-source mixing model:

$$MBC_S = MBC_T \times (at\%^{13}C_T - at\%^{13}C_t) / (at\%^{13}C_S - at\%^{13}C_t) \quad (7)$$

$$MBC_t = MBC_T - MBC_S \quad (8)$$

Where  $at\%^{13}C_t$  is the  $at\%^{13}C_{tracer}$  of  $^{13}C$ -Lignin,  $at\%^{13}C_s$  is the  $at\%^{13}C$  value of unlabelled soil, and  $at\%^{13}C_T$  is the  $at\%^{13}C$  value of total MBC in treated soil. The  $at\%^{13}C_T$  was the  $^{13}C$  abundance of total MBC calculated as:

$$at\%^{13}C_T = (C_f \times at\%^{13}C_f - C_{uf} \times at\%^{13}C_{uf}) / (C_f - C_{uf}) \quad (9)$$

Where  $C_f$  and  $C_{uf}$  are the total organic C contents of fumigated and unfumigated extracts in treated soils, respectively, and  $at\%^{13}C_f$  and  $at\%^{13}C_{uf}$  were the  $at\%^{13}C$  values of  $C_f$  and  $C_{uf}$ , respectively.

## 2.5 Statistical analyses

Statistical analysis was performed with R Studio (R version 3.5.2, CDN, Global) using one-way ANOVA. The data were normally distributed and variances are homogeneous. Significant differences between single treatments were analyzed using Tukey's post-hoc test. In addition, independent T-test analysis was used to test for the direct and interactive effects of anaerobic and aerobic treatments at each sampling time. All the statistical analyses used the significance level at least  $p < 0.05$ , the \*, \*\*, and \*\*\* represent  $p < 0.05$ ,  $p < 0.01$ , and  $p < 0.001$ .

## 3. RESULTS

### 3.1 Lignin decomposition and priming effect under anaerobic conditions

The respiration rates of SOC-derived C and tracer-derived C peaked at days 15 and 60, respectively, and thereafter both declined at a slow rate (Fig.1a and 1b). As compared with control, the cumulative contribution of tracer led to a significant positive difference in total cumulative  $CO_2$  emission from labeled soils under anaerobic conditions,  $P < 0.05$  (Fig.1c and 1d), i.e., positive priming. The resulting cumulative priming increased sharply from day 0 to day 195, followed by a continuous steady-state, and finally decreased (i.e., a negative priming effect) from day 290 until the end of incubation (Fig.1e).

The used lignin tracer had a purity of 80%, i.e., only 80% of the macromolecular structure was made up of phenol-propane units. To avoid any bias in our data, we thus separately calculated the amount of tracer-derived C (total tracer C including impurities) and the C derived from the pure lignin structure. The conservative assumption was that only the

part of total tracer-derived CO<sub>2</sub>-C, which was >20% of the total added tracer-C amount unambiguously, can be denoted as lignin-derived. During anaerobic conditions, the cumulative amount of respired tracer-C and pure lignin-C after 360 days was 16.31 and 1.31 µg CO<sub>2</sub>-C g<sup>-1</sup> soil, representing approximately 21.7% of the total tracer respired and 2.2% from the pure lignin respired, respectively (Fig.2).

### 3.2 CO<sub>2</sub> emission and priming effect under aerobic and anaerobic conditions

Tracer-derived, SOC-derived CO<sub>2</sub> and priming were significantly affected by the presence of aerobic or anaerobic conditions and the sampling time,  $p < 0.05$  (Fig.3). In the aerobic condition, both soil- and tracer-derived CO<sub>2</sub> declined rapidly at the beginning of incubation day 30; this decline became less pronounced from day 90 onwards, and stagnated on a low level from day 335 until the end of the incubation. In the anaerobic condition, tracer-derived CO<sub>2</sub> was generally decreasing from the first to third sampling interval until day 210, with minor fluctuations, began to level off at day 335 until the end of the experiment (Fig.3e-h).

The contribution of tracer-C to the total CO<sub>2</sub>-flux consistently increased during the first three sampling phases and caused positive priming, showing significant differences between aerobic and anaerobic conditions (Fig.3i-k and 3m-o). However, during the last sampling phase, the contribution of tracer increased only smoothly under anaerobic conditions and reached a stable equilibrium for 335 days producing negative priming, while it decreased slowly under aerobic conditions, producing positive priming ( $p < 0.05$ ) (Fig.3l and 3p).

Tracer respiration C was significantly different between aerobic and anaerobic conditions in the first sampling phase, at 2.77 and 2.11 µg CO<sub>2</sub>-C g<sup>-1</sup> soil, representing approximately 3.69% and 2.81% of the total tracer additions, respectively (Fig. S1). The slope tracer respired C was higher under aerobic than anaerobic conditions (Fig. S1a-d). In addition, the proportion of respired C was higher under aerobic than anaerobic conditions (Fig. S1e-h).

### 3.3 Lignin decomposition and carbon recovery in bulk soil

The total amount of lignin assessed by the CuO method was significantly influenced by the time of harvest (Fig. 4). The contents change from timepoint one to two is higher than between the later time steps under both anaerobic and aerobic conditions (Fig.4a). The (Ac/Al)<sub>v</sub> ratios (Fig. 4b) and S/V ratios (Fig. 4c) increased from the first sampling interval to

the last sampling interval in aerobic conditions while decreasing in anaerobic conditions ( $P < 0.05$ ). A significant difference between anaerobic and aerobic conditions was observed in both (Ac/Al)<sub>v</sub> ratios and S/V ratios at the end of the sampling interval ( $P < 0.05$ ).

The recovery of tracer, tracer-derived DOC, and tracer-derived MBC was significantly affected by anaerobic and aerobic conditions at each sampling time (Fig. 5, Fig.6). Tracer recovery in anaerobic conditions was higher than in aerobic conditions at the first sampling interval and generally decreased from the first sampling interval to the end of the incubation. However, tracer-derived DOC and tracer-derived MBC gradually increased and showed a positive relation with  $Fe_0$  in anaerobic and aerobic conditions (Fig. 7). In addition, tracer-derived-DOC and MBC were significantly higher in anaerobic than in aerobic soil environments (Fig. 6b and 6d). A significant difference between anaerobic and aerobic conditions was observed in peroxidase and polyphenol oxidase (Fig. S3,  $P < 0.05$ ). The peroxidase in anaerobic was higher than aerobic in peroxidase, while polyphenol oxidase in aerobic was higher than in anaerobic. In addition, potential activities of AG, BG, Cello, XYL, and Phos in anaerobic conditions were higher than in aerobic conditions during the incubation period but not in NAG (Fig. S4,  $P < 0.05$ ).

## 4. DISCUSSION

### 4.1 Lignin transformation at aerobic and anaerobic soil conditions

For a long time, lignin has been considered to play an essential role in forming stable SOM. However, recent results indicate that this macromolecule decomposes as fast as other substances in the soil under anaerobic conditions (Kirk, 1971; Tuomela, 2000; DeAngelis et al., 2013; Xue et al., 2016; Khan and Ahring, 2019; Xia et al., 2021), as aerobic conditions can effectively promote the complete degradation of microbial lignin (Torres et al. 2014; Janusz et al., 2017; Dao et al., 2018). Therefore, our study comparatively investigated the rate of lignin transformation at both anaerobic and aerobic conditions.

Few studies have focused on the transformation of lignin under anaerobic conditions. Our study could clearly prove anaerobic lignin degradation in soil and conservatively quantify the amount of tracer respired C in soil mineralization after one year of anaerobic incubation. According to the purity of tracer (98 atom%  $^{13}C$ -lignin, chemical purity 80%), our conservative estimation of pure  $^{13}C$  lignin-derived  $CO_2$ -C indicated that about 2.2% of total added pure  $^{13}C$ -lignin was respired, while the overall tracer mineralization was about 21.7% (Fig. 2). This indicates that pure lignin and even more lignin associations like

lignocellulose could be effectively mineralized by metabolic process under anaerobic conditions. Compared with anaerobic conditions, the contribution of lignin to soil respiration in aerobic soil showed a more active mineralization rate, which was under O<sub>2</sub>-enriched conditions with higher respiration rates and higher cumulative mineralization. Anaerobic and aerobic mineralization is mainly affected by oxygen fluctuations and redox conditions (Hall et al., 2015; Xue et al., 2016; Hall et al. 2016; Song et al., 2019; Xia et al., 2021). Previous results from Torres et al. (2014) who has identified a small amount of <sup>13</sup>C-lignin mineralization through microbial biomass that assimilated the lignin-derived C under aerobic conditions. Merino et al. (2021) observed that Fenton reaction coupled with lignin peroxidase induces C mineralization highly from anaerobic soils. Higher peroxidase activity was observed (Fig. S3a) under anaerobic soils suggested that microorganisms produce more peroxidase requirements in the breakdown of aromatic fragments.

Furthermore, the tracer-derived C content decreased, and the cumulative amount of tracer-derived CO<sub>2</sub>-C increased with the incubation time (also in pure lignin), suggesting degradation of lignin (Fig. 3 and 4). This indicates that part of <sup>13</sup>C lignin was mineralized. The decomposed lignin monomer fragments are more easily used for microbial metabolization than released as CO<sub>2</sub> (Khan and Ahring, 2019; McGivern et al., 2021; Merino et al., 2021). This fits well with the decreasing VSC contents with incubation time, accompanied by decreasing mass ratio of (A<sub>C</sub>/A<sub>I</sub>)<sub>V</sub> and S/V observed in anaerobic conditions, reflecting the selective loss of syringyl units during lignin degradation. The syringyl type has a less crosslinking structure and is more easily decomposed with the breaking of C - O - C links between monolignols, thus releasing the corresponding aromatic aldehydes, e.g., vanillin (Opsahl and Benner, 1995; Pichler and Kögel - Knabner, 2000; Waliszewska et al., 2019). In aerobic conditions, increasing (A<sub>C</sub>/A<sub>I</sub>)<sub>V</sub> and S/V ratios were observed, frequently reported as indicators for lignin degradation in an aerobic environment (Hedges and Ertel 1982; Kögel and Bochter 1985; Thevenot et al., 2010). Therefore, we draw a clear picture of lignin degradation under anaerobic and aerobic conditions, which reflects as abundant natural plant material in the ecosystem.

Despite the observation of lignin-derived C mineralization, we also observed an entombing effect in anaerobic lignin, as the accumulation of <sup>13</sup>C microbial biomass. The amount of <sup>13</sup>C-DOC and <sup>13</sup>C-MBC in anaerobic soil was higher than in aerobic soil, indicating that under anaerobic conditions, relatively more microbial-derived C deposition through the metabolic pathway (e.g., in vivo turnover and ex vivo modification), and thus

likely promotes SOM accumulation more than aerobic environments (Liang et al., 2017). In accordance with the results reported by Lal (2002), water-logging conditions promote a substantial increase in dissolved organic matter (DOM) during flooding. Further, aerobic conditions favor the formation of aggregates as iron hydroxide formation encloses some lignin, while anaerobic conditions prefer to destroy these binding agents, thereby releasing the entrapped lignin (Hall et al., 2016; Chaput et al., 2020). The depolymerization of the lignin macromolecule indicated that part of tracer-derived DOC and MBC probably being a source and finally incorporated into the microbial biomass, which was also significantly enriched in  $^{13}\text{C}$ -MBC. This finding could be explained by several aspects of the inhibition effects of the flooded environment on complete lignin mineralization that dissolved lignin decomposition products can be sorbed to minerals, and more  $^{13}\text{C}$  in MBC indeed suggests a better entombing effect. This possibly reflects a link between the biodegradation of lignin associated with soil minerals as a vital C stabilization mechanism, namely microbial process under an anaerobic and aerobic environment with the physical and the chemical protection for SOM stabilization .

#### 4.2 Priming effect of lignin degradation at aerobic and anaerobic conditions

Overall, priming over the whole incubation is more vital for aerobic than anaerobic conditions. Lignin addition directly resulted in positive priming during the aerobic incubation phases (Fig. 3). While the shift of the community structure or the metabolic strategies differs between the two systems as the observed respired rate of tracer C in aerobic soil was consistently higher than in anaerobic soil (Fig.S2). Indicated that anaerobic condition facilitates the use of tracer-C for anabolic rather than catabolic functions by the microbial community due to the triggered by a lack of electron acceptors. Dunham-Cheatham et al. (2020) reported that Fe reduction modulates the microbial community's structure and function, causing positive priming during the aerobic period, while Feo significantly protected lignin methoxyl compounds (Hanke et al., 2013). Kamimura et al. (2017) reported that the C-C bond cleavage of biphenyl compounds of the lignin macromolecule for the microbes needs to invest more carbon against microbial degradation. A significant positive relationship was observed between Feo to DOC and MBC, and showed anaerobic higher than aerobic condition (Fig.7), suggesting that Feo significantly facilitates lignin-derived C accumulation at anaerobic than aerobic condition. These results indicated that microorganisms adapted to anaerobic condition than aerobic condition that protect lignin stabilization.

During the chasing period, the combined priming effect was observed, turning from the positive priming in the first three intervals to negative in the final stage in anaerobic conditions (Fig. 1). Lignin addition stimulated soil priming (i.e., positive or negative priming) as an abundant OC source by providing fresh OC for soil microorganisms. Blagodatskaya and Kuzyakov (2008) found that priming often follows a two-phase sequence, in which that so-called “apparent priming” and “real priming”. The real priming depicts a change in the microbial community structure or at least a change in the metabolic strategies combined with higher enzyme production for microbes that enhance the degradation of SOM. Due to the long-term incubation in our study and microorganisms preferentially using the energy of complex carbohydrate bindings to synthesize enzymes hydrolyzing the low molecular compounds, a significant increase of hydrolysis enzyme (Fig. S4) and microbial biomass (Fig. 6c and 6d) was observed at anaerobic conditions suggest that a very likely “real priming” was observed in our study. Dunham-Cheatham et al. (2020) observed positive priming by simple glucose addition, a low molecular compound that is easily decomposed during anaerobic-aerobic soil (Bremer and Kuikman 1994; Hamer et al., 2004). Lignin remains in SOM for a more extended period than glucose due to its abundance and resistant properties (Kögel and Bochter 1985; Kiem and Kögel-Knabner 2003). In this study, when during anaerobic incubation, easily degradable carbohydrates are gone, with increase of pure lignin proportion, the negative priming which is observed at last stage (Fig. 1e) suggests that microbes have difficulties covering their C-demand by this source, they can only be able to degrade the side chains or groups of the phenols. Furthermore, the decrease of the priming effect with incubation period indicates that the most substantial priming effects are caused by the more accessible to decompose lignin constituents, e.g., ligno-cellulose, while the pure phenols being degraded in the last phase of the incubation seem to have a small or at even longer incubation times even negative priming effect. This may suggest, that lignin decomposition might reduce the SOC decomposition under anaerobic conditions.

## 5. CONCLUSIONS

In this study, we first proved that pure lignin was effectively degraded at one-year anaerobic conditions. We observed that about 2.2% of pure <sup>13</sup>C-lignin was mineralized, and this number increases to 21.7% when the whole lignin macromolecule, including its lignocellulose moieties, is considered. The priming in both anaerobic and aerobic conditions indicated that microbial biomass was strongly affected by the redox condition. Our study

thus gave an insight into the microbial process for a shift under the anaerobic condition with an anabolic pathway of lignin decomposition and that lignin decomposition at anaerobic conditions also leads to negative priming. Both processes explain that soils under anaerobic conditions (e.g., paddy soils) contain more carbon than their aerobic counterparts. Our results, however, show that the anaerobic mineralization of lignin can be a significant CO<sub>2</sub> source in soils and as, e.g., thawing permafrost soil exactly reflects these conditions should be considered in the future.

### **CONFLICT OF INTEREST**

The authors declare that they have no known competing financial interests or personal relationships that could have appeared to influence the work reported in this paper.

### **REFERENCES**

- Atkinson, C.F., Jones, D.D., Gauthier, J.J., 1996. Putative anaerobic activity in aerated composts. *Journal of Industrial Microbiology* 16, 182–188.
- Bernal, B., Mitsch, W.J., 2008. A comparison of soil carbon pools and profiles in wetlands in Costa Rica and Ohio. *Ecological Engineering* 34, 311–323.
- Billings, A.F., Fortney, J.L., Hazen, T.C., Simmons, B., Davenport, K.W., Goodwin, L., Ivanova, N., Kyrpides, N.C., Mavromatis, K., Woyke, T., DeAngelis, K.M., 2015. Genome sequence and description of the anaerobic lignin-degrading bacterium *Tolomonas lignolytica* sp. nov. *Standards in Genomic Sciences* 10, 106.
- Blagodatskaya, E., Kuzyakov, Y., 2008. Mechanisms of real and apparent priming effects and their dependence on soil microbial biomass and community structure: critical review. *Biology and Fertility of Soils* 45, 115–131.
- Bourbonnais, R., Paice, M.G., 1990. Oxidation of non-phenolic substrates: An expanded role for laccase in lignin biodegradation. *FEBS Letters* 267, 99–102.
- Bremer, E., Kuikman, P., 1994. Microbial utilization of <sup>14</sup>C [U] glucose in soil is affected by the amount and timing of glucose additions. *Soil Biology and Biochemistry* 26, 511–517.
- Bugg, T.D.H., Ahmad, M., Hardiman, E.M., Rahmanpour, R., 2011. Pathways for degradation of lignin in bacteria and fungi. *Natural Product Reports* 28, 1883.



- Cañas, A.I., Camarero, S., 2010. Laccases and their natural mediators: Biotechnological tools for sustainable eco-friendly processes. *Biotechnology Advances* 28, 694–705.
- Chaput, G., Billings, A., DeDiego, L., Orellana, R., Adkins, J.N., Nicora, C., Chu, R., Simmons, B., DeAngelis, K.M., 2020. Iron Chelator-Mediated Anoxic Biotransformation of Lignin by Novel sp., *Tolomonas lignolytica* BRL6-1 (preprint). *Microbiology*.
- Dao, T.T., Gentsch, N., Mikutta, R., Sauheitl, L., Shibistova, O., Wild, B., Schneckner, J., Bárta, J., Čapek, P., Gittel, A., Lashchinskiy, N., Urich, T., Šantrůčková, H., Richter, A., Guggenberger, G., 2018. Fate of carbohydrates and lignin in north-east Siberian permafrost soils. *Soil Biology and Biochemistry* 116, 311–322.
- DeAngelis, K.M., Sharma, D., Varney, R., Simmons, B., Isern, N.G., Markillie, L.M., Nicora, C., Norbeck, A.D., Taylor, R.C., Aldrich, J.T., Robinson, E.W., 2013a. Evidence supporting dissimilatory and assimilatory lignin degradation in *Enterobacter lignolyticus* SCF1. *Frontiers in Microbiology* 4.
- Dowd, J.E., Riggs, D.S., 1965. A Comparison of Estimates of Michaelis-Menten Kinetic Constants from Various Linear Transformations. *Journal of Biological Chemistry* 240, 863–869.
- Dunham-Cheatham, S.M., Zhao, Q., Obrist, D., Yang, Y., 2020. Unexpected mechanism for glucose-primed soil organic carbon mineralization under an anaerobic–aerobic transition. *Geoderma* 376, 114535.
- Fenner, N., Freeman, C., 2020. Woody litter protects peat carbon stocks during drought. *Nature Climate Change* 10, 363–369.
- Gearing, J.N., 1991. The Study of Diet and Trophic Relationships through Natural Abundance  $^{13}\text{C}$ , in: *Carbon Isotope Techniques*. Elsevier 201–218.
- Gentsch, N., Mikutta, R., Alves, R.J.E., Bárta, J., Čapek, P., Gittel, A., Hugelius, G., Kuhry, P., Lashchinskiy, N., Palmtag, J., Richter, A., Šantrůčková, H., Schneckner, J., Shibistova, O., Urich, T., Wild, B., Guggenberger, G., 2015. Storage and transformation of organic matter fractions in cryoturbated permafrost soils across the Siberian Arctic. *Biogeosciences* 12, 4525–4542.

- Gittel, A., Bárta, J., Kohoutová, I., Mikutta, R., Owens, S., Gilbert, J., Schneckner, J., Wild, B., Hannisdal, B., Maerz, J., Lashchinskiy, N., Čapek, P., Šantrůčková, H., Gentsch, N., Shibistova, O., Guggenberger, G., Richter, A., Torsvik, V.L., Schleper, C., Urich, T., 2014. Distinct microbial communities associated with buried soils in the Siberian tundra. *The ISME Journal* 8, 841–853.
- Guenet, B., Leloup, J., Raynaud, X., Bardoux, G., Abbadie, L., 2010. Negative priming effect on mineralization in a soil free of vegetation for 80 years. *European Journal of Soil Science* 61, 384–391.
- Hall, S.J., Silver, W.L., Timokhin, V.I., Hammel, K.E., 2016. Iron addition to soil specifically stabilized lignin. *Soil Biology and Biochemistry* 98, 95–98.
- Hamer, U., Marschner, B., Brodowski, S., Amelung, W., 2004. Interactive priming of black carbon and glucose mineralisation. *Organic Geochemistry* 35, 823–830.
- Hanke, A., Cerli, C., Muhr, J., Borken, W., Kalbitz, K., 2013. Redox control on carbon mineralization and dissolved organic matter along a chronosequence of paddy soils: Redox control on carbon turnover. *European Journal of Soil Science* 64, 476–487.
- Hedges, J.I., Ertel, J.R., 1982. Characterization of lignin by gas capillary chromatography of cupric oxide oxidation products. *Analytical Chemistry* 54, 174–178.
- Hu, S., Bruggen, A.H.C. van, 1997. Microbial Dynamics Associated with Multiphasic Decomposition of <sup>14</sup>C-Labeled Cellulose in Soil. *Microbial Ecology* 33, 134–143.
- Janusz, G., Pawlik, A., Sulej, J., Świdorska-Burek, U., Jarosz-Wilkolazka, A., Paszczyński, A., 2017. Lignin degradation: microorganisms, enzymes involved, genomes analysis and evolution. *FEMS Microbiology Reviews* 41, 941–962.
- Kamimura, N., Takahashi, K., Mori, K., Araki, T., Fujita, M., Higuchi, Y., Masai, E., 2017. Bacterial catabolism of lignin-derived aromatics: New findings in a recent decade: Update on bacterial lignin catabolism. *Environmental Microbiology Reports* 9, 679–705.
- Keeling, C.D., 1961. The concentration and isotopic abundances of carbon dioxide in rural and marine air. *Geochimica et Cosmochimica Acta* 24, 277–298.

- Keeling, C.D., 1958. The concentration and isotopic abundances of atmospheric carbon dioxide in rural areas. *Geochimica et Cosmochimica Acta* 13, 322–334.
- Khan, M.U., Ahring, B.K., 2019. Lignin degradation under anaerobic digestion: Influence of lignin modifications -A review. *Biomass and Bioenergy* 128, 105325.
- Kiem, R., Kögel-Knabner, I., 2003. Contribution of lignin and polysaccharides to the refractory carbon pool in C-depleted arable soils. *Soil Biology and Biochemistry* 35, 101–118.
- Kirk, T.K., 1971. Effects of Microorganisms on Lignin. *Annual Review of Phytopathology* 9, 185–210.
- Kobayashi, T., Hashinaga, T., Mikami, E., Suzuki, T., 1988. Methanogenic degradation of phenol and benzoate in acclimated sludges, in: *Water Pollution Research and Control Brighton*. Elsevier, 55–65.
- Kögel, I., Bochter, R., 1985. Characterization of lignin in forest humus layers by high-performance liquid chromatography of cupric oxide oxidation products. *Soil Biology and Biochemistry* 17, 637–640.
- Kögel-Knabner, I., Amelung, W., Cao, Z., Fiedler, S., Frenzel, P., Jahn, R., Kalbitz, K., Kölbl, A., Schloter, M., 2010. Biogeochemistry of paddy soils. *Geoderma* 157, 1–14.
- Kourtev, P.S., Ehrenfeld, J.G., Huang, W.Z., 2002. Enzyme activities during litter decomposition of two exotic and two native plant species in hardwood forests of New Jersey. *Soil Biology and Biochemistry* 34, 1207–1218.
- Kuusk, S., Bissaro, B., Kuusk, P., Forsberg, Z., Eijsink, V.G.H., Sørli, M., Väljamäe, P., 2018. Kinetics of H<sub>2</sub>O<sub>2</sub>-driven degradation of chitin by a bacterial lytic polysaccharide monooxygenase. *Journal of Biological Chemistry* 293, 523–531.
- Kuzyakov, Y., 2010. Priming effects: Interactions between living and dead organic matter. *Soil Biology and Biochemistry* 42, 1363–1371.
- Lal, R., 2002. Soil carbon dynamics in cropland and rangeland. *Environmental Pollution* 116, 353–362.

- Leiber-Sauheitl, K., Fuß, R., Burkart, St., Buegger, F., Dänicke, S., Meyer, U., Petzke, K.J., Freibauer, A., 2015. Sheep excreta cause no positive priming of peat-derived CO<sub>2</sub> and N<sub>2</sub>O emissions. *Soil Biology and Biochemistry* 88, 282–293.
- Marx, M.-C., Wood, M., Jarvis, S.C., 2001. A microplate fluorimetric assay for the study of enzyme diversity in soils. *Soil Biology and Biochemistry* 33, 1633–1640.
- Masai, E., Katayama, Y., Fukuda, M., 2007. Genetic and Biochemical Investigations on Bacterial Catabolic Pathways for Lignin-Derived Aromatic Compounds. *Bioscience, Biotechnology, and Biochemistry* 71, 1–15.
- McGivern, B.B., Tfaily, M.M., Borton, M.A., Kosina, S.M., Daly, R.A., Nicora, C.D., Purvine, S.O., Wong, A.R., Lipton, M.S., Hoyt, D.W., Northen, T.R., Hagerman, A.E., Wrighton, K.C., 2021. Decrypting bacterial polyphenol metabolism in an anoxic wetland soil. *Nature Communications* 12, 2466.
- Merino, C., Matus, F., Kuzyakov, Y., Dyckmans, J., Stock, S., Dippold, M.A., 2021. Contribution of the Fenton reaction and ligninolytic enzymes to soil organic matter mineralisation under anoxic conditions. *Science of The Total Environment* 760, 143397.
- Niladevi, K.N., Sheejadevi, P.S., Prema, P., 2008. Strategies for Enhancing Laccase Yield from *Streptomyces psammoticus* and Its Role in Mediator-based Decolorization of Azo Dyes. *Applied Biochemistry and Biotechnology* 151, 9–19.
- Opsahl, S., Benner, R., 1995. Early diagenesis of vascular plant tissues: Lignin and cutin decomposition and biogeochemical implications. *Geochimica et Cosmochimica Acta* 59, 4889–4904.
- Peng, X., Masai, E., Kasai, D., Miyauchi, K., Katayama, Y., Fukuda, M., 2005. A Second 5-Carboxyvanillate Decarboxylase Gene, *ligW2*, Is Important for Lignin-Related Biphenyl Catabolism in *Sphingomonas paucimobilis* SYK-6. *Applied and Environmental Microbiology* 71, 5014–5021.
- Peng, X., Masai, E., Kitayama, H., Harada, K., Katayama, Y., Fukuda, M., 2002. Characterization of the 5-Carboxyvanillate Decarboxylase Gene and Its Role in Lignin-Related Biphenyl Catabolism in *Sphingomonas paucimobilis* SYK-6. *Applied and Environmental Microbiology* 68, 4407–4415.

- Pichler, M., Kögel-Knabner, I., 2000. Chemolytic Analysis of Organic Matter during Aerobic and Anaerobic Treatment of Municipal Solid Waste. *Journal of Environmental Quality* 29(4), 1337–1344.
- Schutter, M., Dick, R., 2001. Shifts in substrate utilization potential and structure of soil microbial communities in response to carbon substrates. *Soil Biology and Biochemistry* 33, 1481–1491.
- Sheng, X., Zhu, W., Huddleston, J., Xiang, D.F., Raushel, F.M., Richards, N.G.J., Himo, F., 2017. A Combined Experimental-Theoretical Study of the LigW-Catalyzed Decarboxylation of 5-Carboxyvanillate in the Metabolic Pathway for Lignin Degradation *ACS Catalysis* 7, 4968–4974.
- Sinsabaugh, R.L., Antibus, R.K., Linkins, A.E., McClaugherty, C.A., Rayburn, L., Repert, D., Weiland, T., 1993. Wood Decomposition: Nitrogen and Phosphorus Dynamics in Relation to Extracellular Enzyme Activity. *Ecology* 74, 1586–1593.
- Šnajdr, J., Cajthaml, T., Valášková, V., Merhautová, V., Petránková, M., Spetz, P., Leppänen, K., Baldrian, P., 2011. Transformation of *Quercus petraea* litter: successive changes in litter chemistry are reflected in differential enzyme activity and changes in the microbial community composition: Transformation of *Quercus petraea* litter. *FEMS Microbiology Ecology* 75, 291–303.
- Song, N., Xu, H., Yan, Z., Yang, T., Wang, C., Jiang, H.-L., 2019. Improved lignin degradation through distinct microbial community in subsurface sediments of one eutrophic lake. *Renewable Energy* 138, 861–869.
- Stewart, C.E., Moturi, P., Follett, R.F., Halvorson, A.D., 2015a. Lignin biochemistry and soil N determine crop residue decomposition and soil priming. *Biogeochemistry* 124, 335–351.
- Tao, X., Feng, J., Yang, Y., Wang, G., Tian, R., Fan, F., Ning, D., Bates, C.T., Hale, L., Yuan, M.M., Wu, L., Gao, Q., Lei, J., Schuur, E.A.G., Yu, J., Bracho, R., Luo, Y., Konstantinidis, K.T., Johnston, E.R., Cole, J.R., Penton, C.R., Tiedje, J.M., Zhou, J., 2020. Winter warming in Alaska accelerates lignin decomposition contributed by Proteobacteria. *Microbiome* 8, 84.

- Thevenot, M., Dignac, M.-F., Rumpel, C., 2010. Fate of lignins in soils: A review. *Soil Biology and Biochemistry* 42, 1200–1211.
- Torres, I.F., Bastida, F., Hernández, T., Bombach, P., Richnow, H.H., García, C., 2014. The role of lignin and cellulose in the carbon-cycling of degraded soils under semiarid climate and their relation to microbial biomass. *Soil Biology and Biochemistry* 75, 152–160.
- Tuomela, M., 2000. Biodegradation of lignin in a compost environment: a review. *Bioresource Technology* 72, 169–183.
- Vance, E.D., Brookes, P.C., Jenkinson, D.S., 1987. An extraction method for measuring soil microbial biomass C. *Soil Biology and Biochemistry* 19, 703–707.
- Vladimirova, A., Patskovsky, Y., Fedorov, A.A., Bonanno, J.B., Fedorov, E.V., Toro, R., Hillerich, B., Seidel, R.D., Richards, N.G.J., Almo, S.C., Raushel, F.M., 2016. Substrate Distortion and the Catalytic Reaction Mechanism of 5-Carboxyvanillate Decarboxylase. *Journal of the American Chemical Society* 138, 826–836.
- Waliszewska, H., Zborowska, M., Stachowiak-Wencek, A., Waliszewska, B., Czekala, W., 2019. Lignin Transformation of One-Year-Old Plants During Anaerobic Digestion (AD). *Polymers* 11, 835.
- Woo, H.L., Ballor, N.R., Hazen, T.C., Fortney, J.L., Simmons, B., Davenport, K.W., Goodwin, L., Ivanova, N., Kyrpides, N.C., Mavromatis, K., Woyke, T., Jansson, J., Kimbrel, J., DeAngelis, K.M., 2014. Complete genome sequence of the lignin-degrading bacterium *Klebsiella* sp. strain BRL6-2. *Standards in Genomic Sciences* 9, 19.
- Wu, J., Joergensen, R.G., Pommerening, B., Chaussod, R., Brookes, P.C., 1990. Measurement of soil microbial biomass C by fumigation-extraction-an automated procedure. *Soil Biology and Biochemistry* 22, 1167–1169.
- Xia, S., Song, Z., Li, Q., Guo, L., Yu, C., Singh, B.P., Fu, X., Chen, C., Wang, Y., Wang, H., 2021. Distribution, sources, and decomposition of soil organic matter along a salinity gradient in estuarine wetlands characterized by C:N ratio,  $\delta^{13}\text{C}$ - $\delta^{15}\text{N}$ , and lignin biomarker. *Global Change Biology* 27, 417–434.

Xue, K., M. Yuan, M., J. Shi, Z., Qin, Y., Deng, Y., Cheng, L., Wu, L., He, Z., Van Nostrand, J.D., Bracho, R., Natali, S., Schuur, Edward.A.G., Luo, C., Konstantinidis, K.T., Wang, Q., Cole, J.R., Tiedje, J.M., Luo, Y., Zhou, J., 2016. Tundra soil carbon is vulnerable to rapid microbial decomposition under climate warming. *Nature Climate Change* 6, 595–600.

## Figures

Fig.1

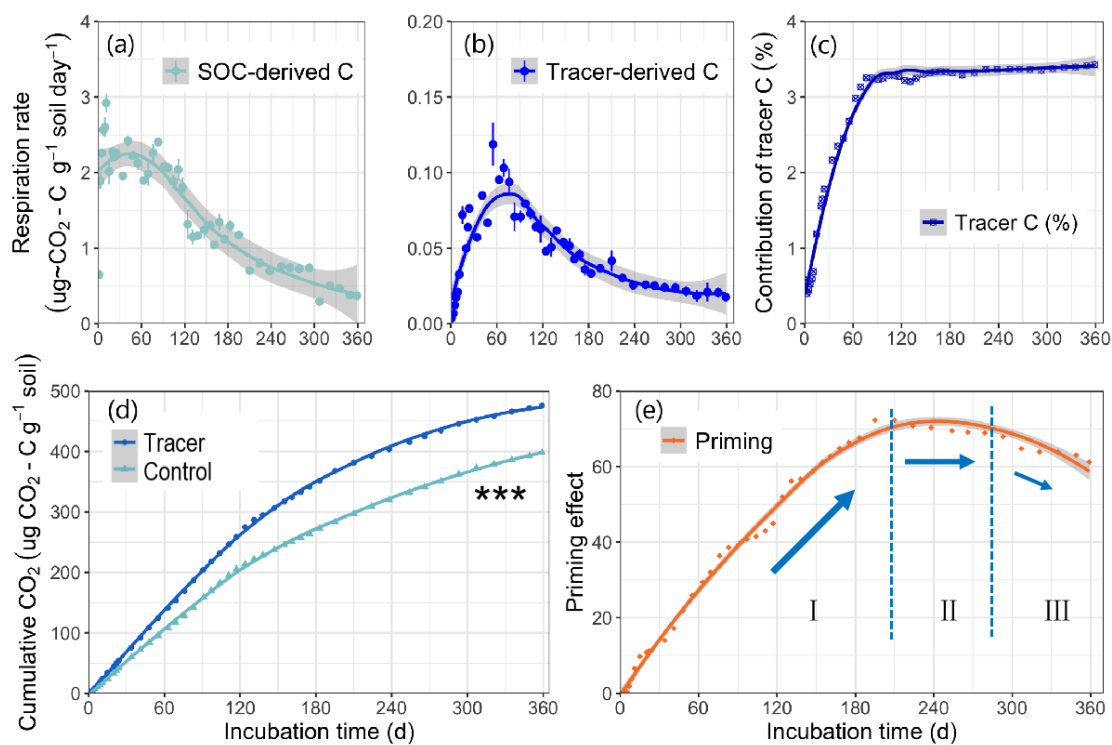


Fig.2

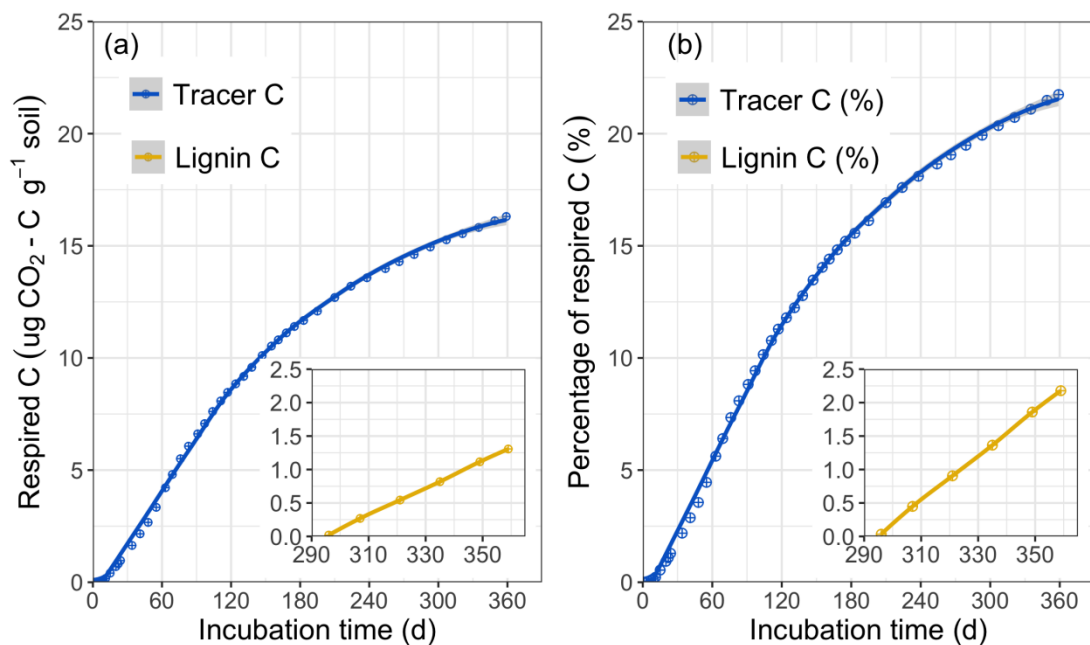




Fig.3

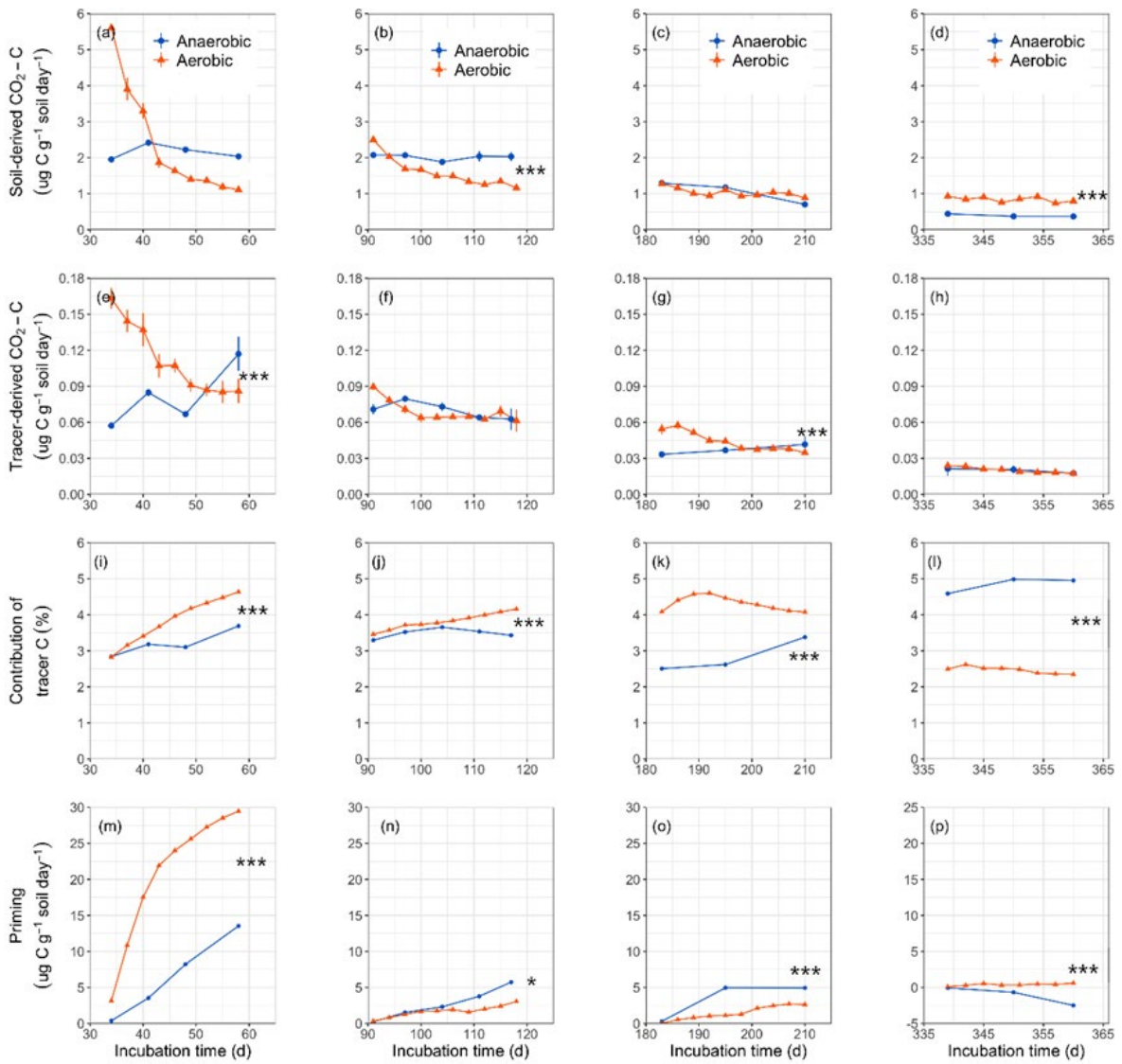
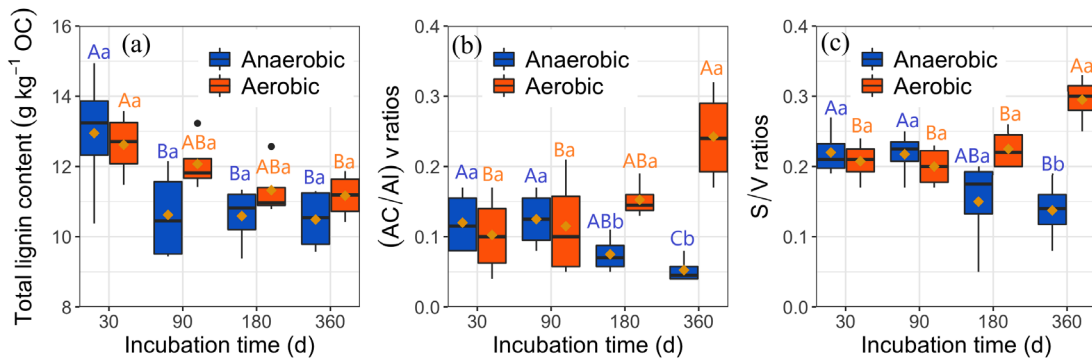
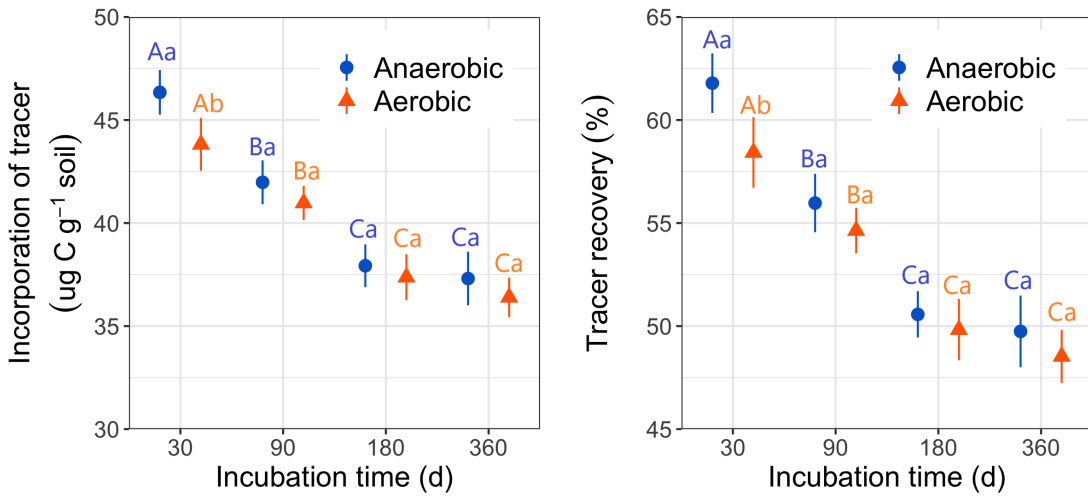


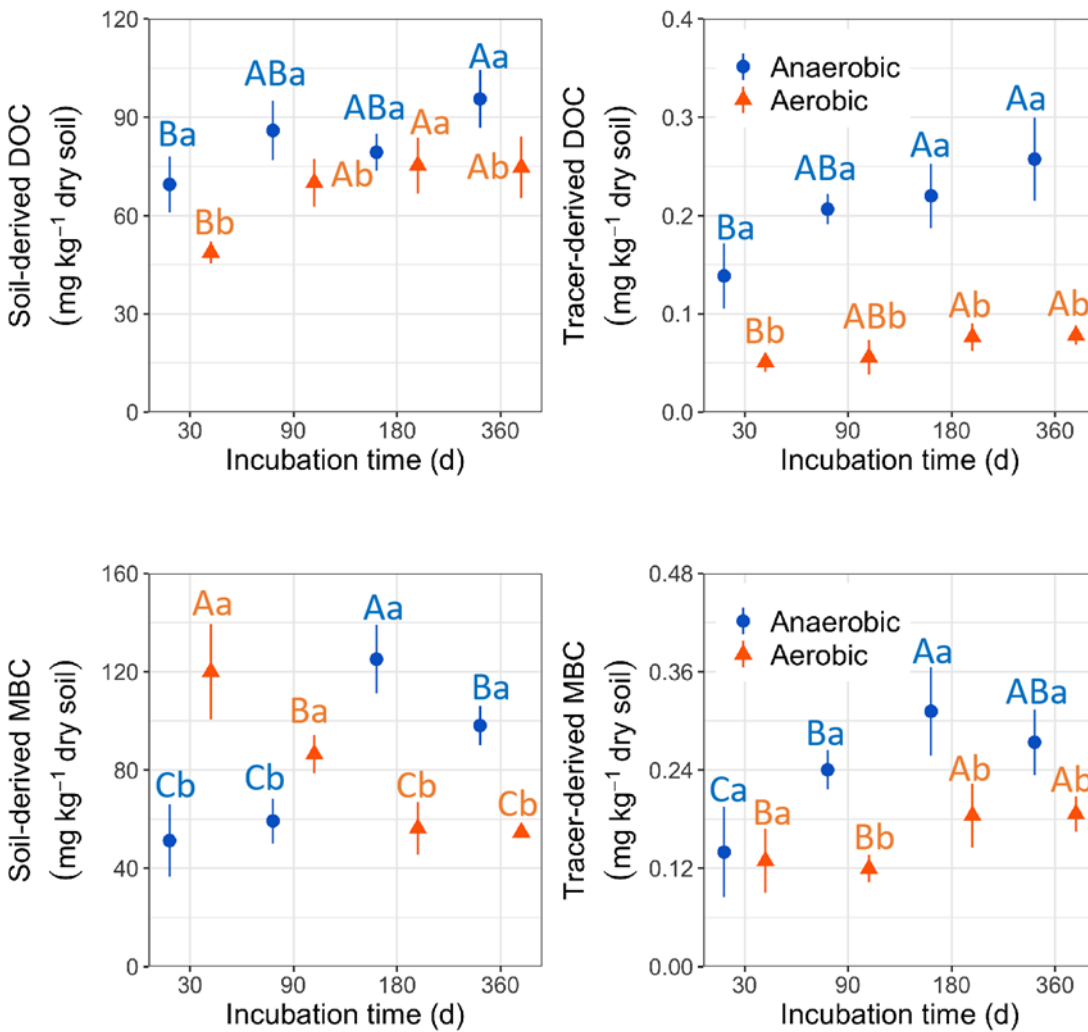
Fig.4



**Fig.5**



**Fig.6**



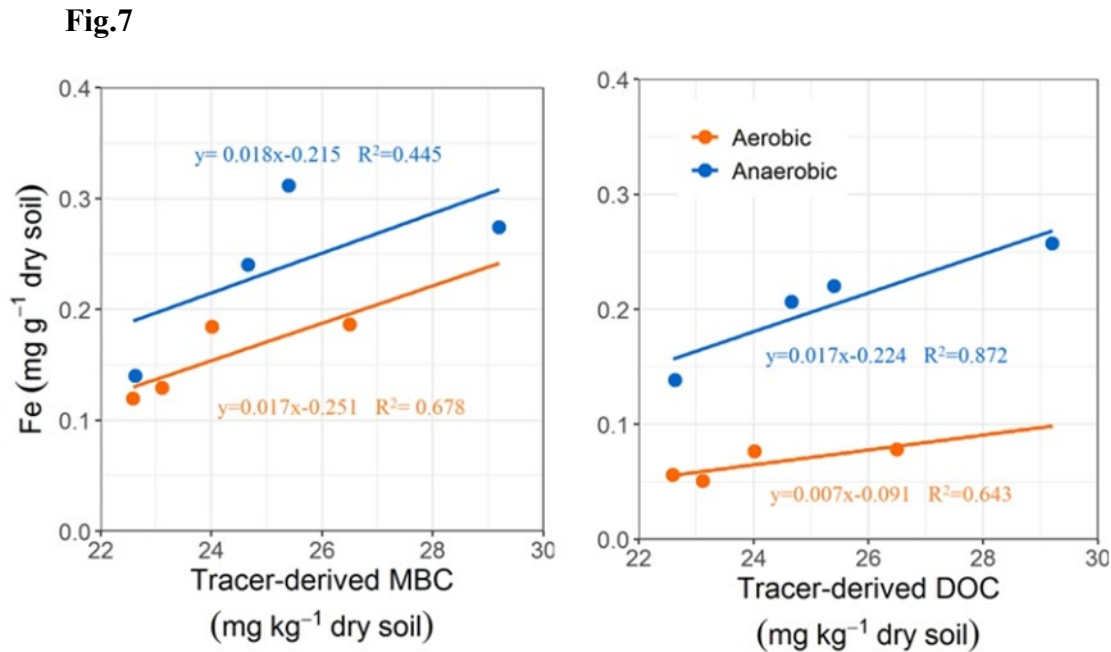


### Figure legends

**Fig. 1** The respiration rate of soil-derived C (a), tracer-derived C (b), the cumulative contribution of tracer (c), cumulative CO<sub>2</sub> emission (d), and cumulative priming (e) in the anaerobic wetland soil under 360 days incubation. Values and error bars indicate mean  $\pm$  standard deviation (n= 4). Asterisk indicates a significant difference between anaerobic labeled and unlabelled/control treatment ( $P<0.05$ , Turkey's HSD).

**Fig. 2** The cumulative tracer-respired and lignin respired <sup>13</sup>CO<sub>2</sub>-C (a) and recovery proportion (b) in the anaerobic wetland soil during 360 days of anaerobic incubation.

**Fig. 3** The respiration rate of soil-derived C (a, b, c, d), tracer-derived C (e, f, g, h), the contribution of tracer (i, f, g, h), and priming (m, n, o, p) in the anaerobic and aerobic treatment during harvest times in which both systems were sampled in parallel. Values and error bars indicate mean  $\pm$  standard deviation (n= 4). Asterisks indicate a significant difference between anaerobic and aerobic treatment ( $P<0.05$ ).

**Fig. 4** The total amount of lignin (a), S/V ratios (b), and (Ac/Al)<sub>v</sub> ratios (c) in the anaerobic and aerobic treated bulk soil during different harvest times. Values and error bars indicate mean  $\pm$  standard deviation (n= 4). Different capital letters and letters indicate significant differences between sampling periods and treatment with anaerobic and aerobic conditions ( $P<0.05$ ).

**Fig. 5** The incorporation and recovery of tracer-C in the anaerobic and aerobic treated bulk soil during different harvest times. Values and error bars indicate mean  $\pm$  standard deviation ( $n=4$ ). Different capital letters and letters indicate significant differences between sampling periods and treatment with anaerobic and aerobic conditions ( $P<0.05$ ).

**Fig. 6** The soil-derived and tracer-derived C of dissolved organic carbon (DOC) (a, b) and microbial biomass carbon (MBC) (c, d) in the anaerobic and aerobic treated bulk soil during different harvest times. Values and error bars indicate mean  $\pm$  standard deviation ( $n=4$ ). Different capital letters and letters indicate significant differences between sampling periods and treatment with anaerobic and aerobic conditions ( $P<0.05$ ).

**Fig. 7** Relationships between tracer-derived MBC, tracer-derived DOC and soil Feo in the anaerobic and aerobic treated bulk soil during different harvest time. The dots represent data from all treatments in the 390-day incubation period.

### Study 2–Supplementary material

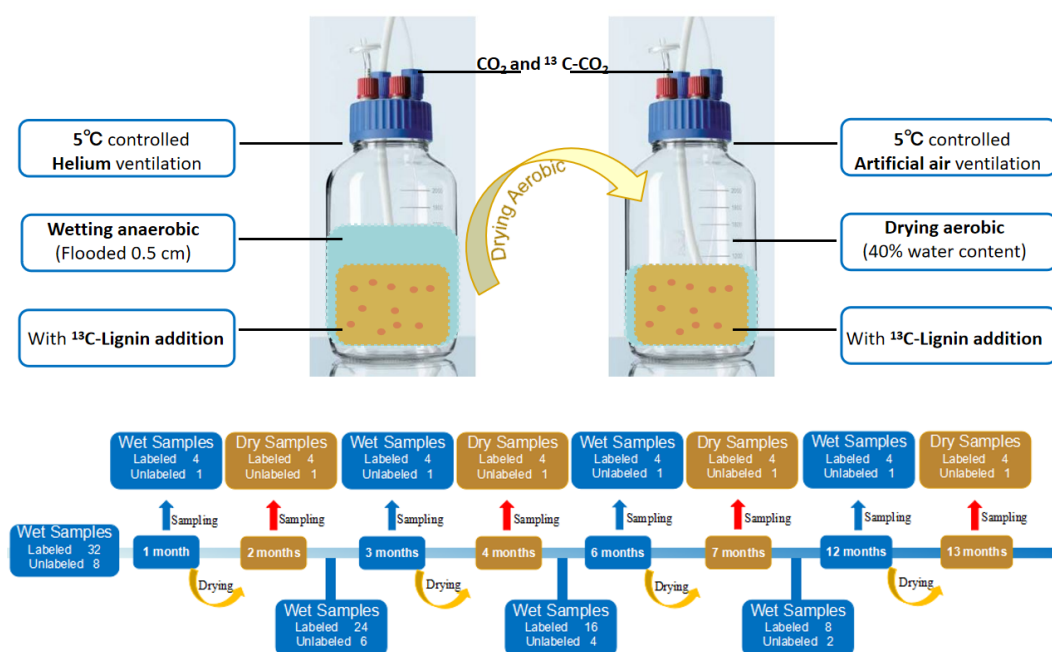


**Fig. S1** Experiment design in the anaerobic and aerobic soil incubation of the wetland soil during 365 day incubation.

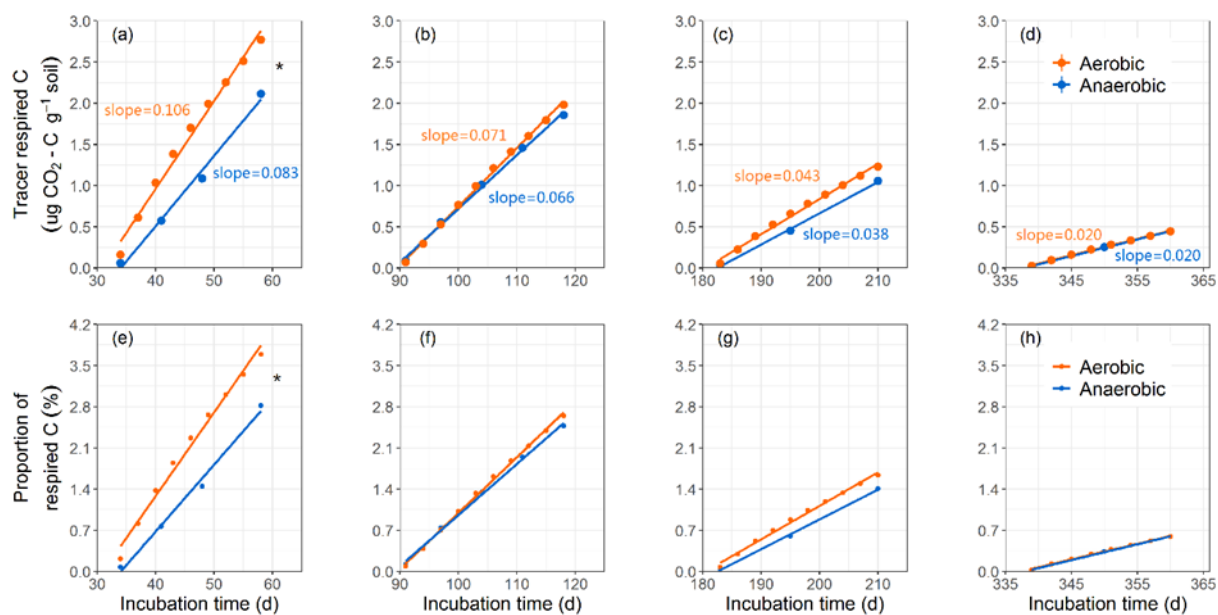


Fig. S2 The cumulative tracer-respired C (a), and the tracer recovery % (e) at different sampling period in anaerobic and aerobic conditions. Values and error bars indicate mean  $\pm$  standard deviation ( $n=4$ ). Asterisks indicate significant difference between anaerobic and aerobic treatment ( $P<0.05$ ).

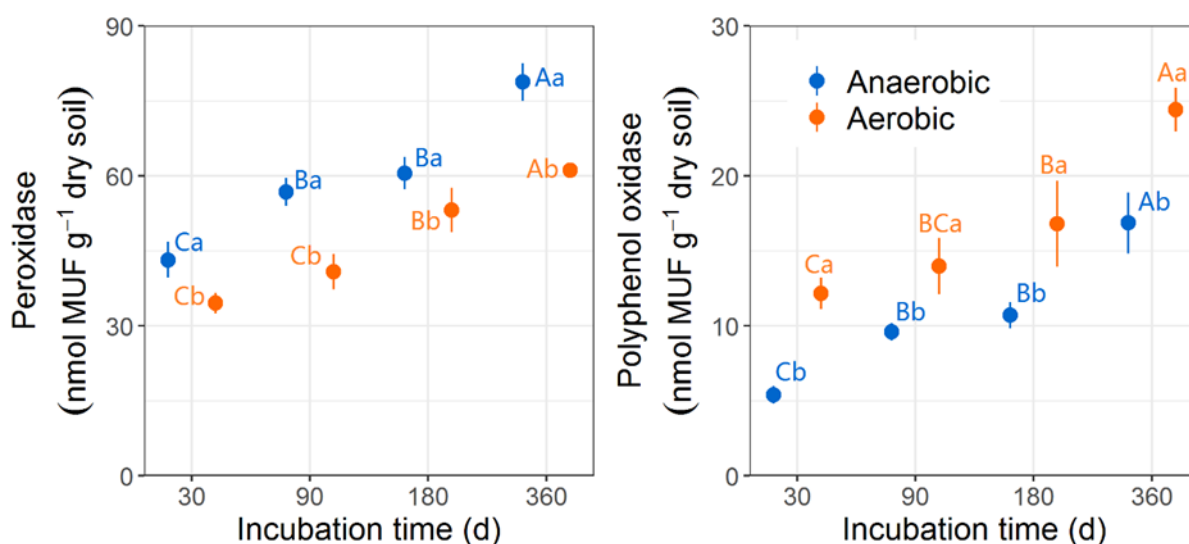


Fig. S3 Activity of peroxidase and polyphenol oxidase in the anaerobic and aerobic treated bulk soil at different sampling period. Values and error bars indicate mean  $\pm$  standard deviation ( $n=4$ ). Different capital letters and letters indicate significant differences between

sampling periods and treatment with anaerobic and aerobic conditions ( $P < 0.05$ ).

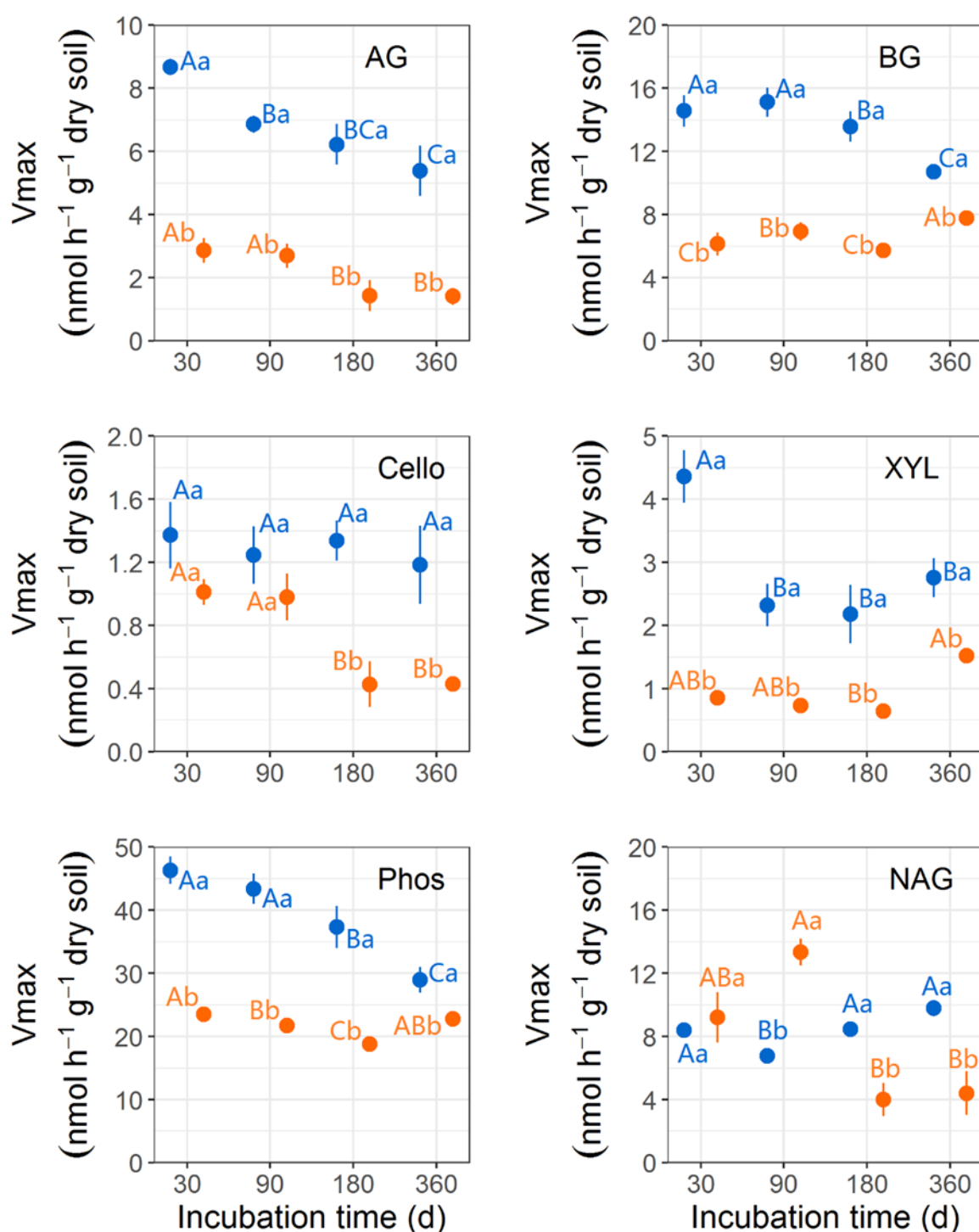


Fig. S4 Activity of extracellular enzymes  $\alpha$ -1,4-glucosidase (AG),  $\beta$ -1,4-glucosidase (BG),  $\beta$ -1,4-cellobioside (Cello),  $\beta$ -1,4-xylosidase (XYL),  $\beta$ -1,4-phosphate (Phos), and  $\beta$ -1,4-N-acetylglucosaminidase (NAG) in the anaerobic and aerobic treated bulk soil during different

harvest time. Values and error bars indicate mean  $\pm$  standard deviation (n= 4). Different capital letters and letters indicate significant difference between sampling periods and treatment with anaerobic and aerobic conditions ( $P<0.05$ ).

## 4 Study 3

### **Organic phosphorus availability shapes the diversity of phoD– harboring bacteria in agricultural soil**

Contribution: I participated in sampling activities and the experiment incubation, performed significant laboratory portions analyses (including CaCl<sub>2</sub>–P, citrate–P, HCl–P, enzyme–P, Olsen–P, SOC, TN, pH, and soil particle–size), and contributed to the manuscript writing.

Published in Soil Biology and Biochemistry 161 (2021) 108364

<https://doi.org/10.1016/j.soilbio.2021.108364>



## **Organic phosphorus availability shapes the diversity of phoD-harboring bacteria in agricultural soil**

Xiaomeng Wei <sup>a,b</sup>, Yajun Hu<sup>a\*</sup>, Guan Cai <sup>b,c</sup>, Huaiying Yaod <sup>e,f</sup>, Jun Ye <sup>g</sup>, Qi Sun <sup>a,b</sup>, Stavros D. Veresoglouh <sup>i</sup>, Yaying Li <sup>d,e</sup>, Zhenke Zhu <sup>a</sup>, Georg Guggenberger <sup>c</sup>, Xiangbi Chen<sup>a</sup>, Yirong Su <sup>a</sup>, Yong Li <sup>a</sup>, Jinshui Wu <sup>a,b</sup>, Tida Ge <sup>a</sup>

<sup>a</sup> Key Laboratory of Agro-ecological Processes in Subtropical Region, Institute of Subtropical Agriculture, the Chinese Academy of Sciences, Changsha 410125, PR China

<sup>b</sup> University of Chinese Academy of Sciences, Beijing 100049, PR China

<sup>c</sup> Institute of Soil Science, Leibniz Universität Hannover, 30419 Hannover, Germany

<sup>d</sup> Key Lab of Urban Environment and Health, Institute of Urban Environment, Chinese Academy of Sciences, Xiamen 361021, PR China

<sup>e</sup> Ningbo Key Lab of Urban Environment Process and Pollution Control, Ningbo Urban Environment Observation and Research Station-NUEORS, Chinese Academy of Sciences, Ningbo 315830, PR China

<sup>f</sup> Research Center for Environmental Ecology and Engineering, Wuhan Institute of Technology, Wuhan 430073, PR China

<sup>g</sup> Australian Centre for Ecogenomics, School of Chemistry and Molecular Biosciences, University of Queensland, Brisbane, QLD 4072, Australia

<sup>h</sup> Freie Universität Berlin-Institut für Biologie, Dahlem Center of Plant Sciences, Plant Ecology, Berlin, Germany

<sup>i</sup> Berlin-Brandenburg Institute of Advanced Biodiversity Research (BBIB), Berlin, Germany (BIBB)

\*Corresponding author: Yajun Hu. Tel.: +86-731-84615244; Fax: +86-731-84612685; E-mail: yjhu@isa.ac.cn

Postal address: Institute of Subtropical Agriculture, Chinese Academy of Sciences, 644 Mapoling, Furong District, Changsha 410125, China

**Abstract**

In light of the limited resources of phosphorus (P) fertilizer, investigating the response of organic P (Po)-mineralizing microbial communities on the resource supply can be an avenue to optimize P recycling in agricultural systems. The alkaline phosphomonoesterase (alkaline P<sub>Ase</sub>)-encoding gene PhoD is universally occurring in soil microorganisms. Here we collected 102 soil samples from Chinese agricultural fields to explore the effect of resource supply on the community of phoD-harboring bacteria. The relationships between the community diversity and soil organic carbon (SOC), total nitrogen (TN) and available Po concentration were fitted to the linear and quadric models suggested by the resource competition theory as well as the Michaelis-Menten model suggested by the metabolic theory of ecology. The results revealed that the response of phoD-harboring bacterial diversity to SOC and TN was likely related to the resource competition theory, with highest diversity at moderate SOC and TN concentration. In contrast, the phoD diversity increased with increasing available Po until the stationary value, which was consistent with the metabolic theory of ecology. Random forest models and multiple regression tree analyses identified the Po availability as the most important predictor on the variation of the phoD-harboring bacterial diversity and network topological features prior to the climate, soil texture, pH and all tested soil nutrient variables. This study highlights the critical role that Po plays in structuring phoD-harboring bacterial communities. Furthermore, for the first time, we correlated functional gene diversity to the corresponding enzymatic substrate availability from a metabolic theory perspective, confirming that the relationship follows the Michaelis-Menten model which was well known to predict the substrate regulation on the rate of enzymatic reactions.

**Keywords:** phoD-harboring bacteria, organic phosphorus availability, community diversity, co-occurrence network

## 1. Introduction

The current mining and usage rates of mineral phosphorus (P) in agriculture are unsustainable (Cordell et al., 2009). Existing projections suggest that in the near future it will become impossible to meet the global P demand, a state referred to as the ‘global P crisis’ (Sattari et al., 2012). Considering that fertilization of soil with P has served as a major component of the agricultural expansion over the last 50 years, any shortages in P could significantly compromise agricultural production and food security (Zhu et al., 2018). Researchers are, therefore, in search of alternative strategies to meet the high P demands of conventional agriculture. These approaches consist not only of ways to use chemical P fertilizers more efficiently, but also increase the mobilization of less available soil P. Mobilizing the mineral-bond P induces a microbial solubilization of mineral phosphate and has been extensively studied since the middle of last century (Alori et al., 2017). An alternative avenue is fostering the reuse of P in organic matter, e.g. via microbial organic P (Po) hydrolysis (Cordell et al., 2011; Richardson and Simpson, 2011). Despite the knowledge on the important contribution of microorganisms to Po mineralization in soil has long been confirmed (Luo et al., 2017; Nannipieri, 2011), we still know little about what and how environmental factors affect the community composition of this functional guild (George et al., 2018).

Following P fertilization in the form of phosphate minerals, a large fraction of bioavailable P is transformed into organic forms by microbial metabolism. Typically, 30%–60% of fertilized P integrated into plant biomass is in organic forms, and the ratio is >90% for microbial biomass (Damon et al., 2014). Organic P is only available after having been transformed to inorganic forms by the mineralization of extracellular phosphatases (enzymes that catalyze the hydrolysis of ester-bond phosphate in soils) and thus represents a renewable P pool in the plant-soil system (Nannipieri et al., 2011). Phosphatases are classified to acid and alkaline phosphatase (PAses) according to the optimal pH. While acid PAses are universally produced by plant, animal and microbes, alkaline PAses are predominantly of bacterial origin in soils (Hui et al., 2013; Chhonkar and Tarafdar, 1981). Alkaline PAses comprise three distinct types: PhoA, PhoD, and PhoX (Tan et al., 2013; Kathuria and Martiny, 2011). These enzymes catalyze the dephosphorylation of mononucleotides, sugar phosphates and lower-order phytates, which account for up to 100% of the total Po compounds (except microbial biomass P) in soil (Nannipieri et al., 2011). Compared to the genes encoding PhoA and PhoX, phoD gene is ubiquitously found across all soil types and

bacterial phyla at high abundances (Tan et al., 2013), and the expression of bacterial *phoD* is strictly regulated by phosphate availability (Apel et al., 2007). Hence, when the mineral P sources in soil become depleted, the *phoD*-harboring bacteria may contribute to the maintenance of soil P availability.

The estimated activity of alkaline PAsE (ALP) in soil generally positively correlates to the *phoD* abundance (Fraser et al., 2015; Hu et al., 2018), but is also influenced by the taxonomic profile of the *phoD*-harboring microbial community (Luo et al., 2017). Several studies have explored the response of *phoD*-harboring bacterial community to anthropogenic and natural disturbances (Fraser et al., 2015; Sun et al., 2019; Wei et al., 2019). Nonetheless, we lack a theoretical background and suitable experimental data at a system-level to explain how biotic and abiotic factors affect the *phoD*-harboring bacterial community in soil. Resource competition (RC) is a core ecological theory routinely used to rationalize the coexistence of plant, microbial and animal species. It postulates that abundant and heterogeneous resources foster a niche differentiation and therefore beget a higher biological diversity. By contrast, a low diversity could be induced by competitive exclusion when limited or excessive resources are provided (Graham and Duda, 2011; Tilman, 1982). Carbon, N and P are the key resources for microorganisms. Previous studies confirmed their potential roles shaping the community of *phoD*-harboring bacteria (Luo et al., 2017; Sun et al., 2019; Wei et al., 2019). However, it is still unknown whether the relationship between the content of these resources and *phoD*-harboring bacterial diversity follows the pattern predicted by RC.

The *phoD*-harboring bacterial community is more related to the  $P_o$  content as compared to total or available P (Liu et al., 2020; Luo et al., 2017). The PAsEs are energy-costing to produce, however are easily released to soil thus benefit also other microorganisms that do not produce the enzymes (cheaters) (Folse & Allison, 2012; Allison, 2005). As a result, the individuals efficient in producing PAsEs and hydrolyzing  $P_o$  may lose in the competition of growth, since they provide for the co-occurring cheaters with P resource, and therefore, may lead to the canceling of RC in predicting the microbial diversity. Michaelis-Menten model is among the most important principles controlling the biological reactions, which describes the relationship between substrate availability and the rate of enzymatic processes (Michaelis and Menten, 1913). According to the metabolic theory of ecology (MTE), which suggests that first principles of physics, chemistry, and biology control the community diversity (Brown et al., 2004; Zhou et al 2016), we would expect the relationship between available

Po and phoD diversity to follow the Michaelis-Menten equation due to the available Po as the enzyme-substrate for the phoD gene. Based on the observation of microbial diversity along temperature gradient, MTE is recently introduced to explain the variation in microbial community composition (Zhou et al., 2016; Wu et al., 2018). However, the theory has not been tested for substrate availability to our best knowledge.

Both RC and MTE explain the variation of community diversity from the perspective of biological interaction. Disentangling the inter-species interactions will increase our insight into the assemblages of phoD-harboring bacterial community, however is difficult to detect in complex soil microbial community. The co-occurrence network provides a tool to approach this issue (Layeghifard et al., 2017; Ponisio et al., 2019). Correlation-based methods are now popular in constructing networks of microbial communities in natural habits, e.g. gut and soil (Deng et al., 2012; Ma et al., 2016). Despite of the limitation of detecting spurious correlations, this method provides new insights into the inter-species interactions (Layeghifard et al., 2017). Mathematic analyses induced a series of network topological features to indicate the complexity, closeness, stability and other properties of a community (Layeghifard et al., 2017). In a weighted network, the negative correlations (edges) are suggested to indicate a potential antagonism (caused by competition or inhibition), while positive correlations indicate facilitation between the linked operational taxonomic units (OTUs). By postulating the relationship between resource and microbial diversity caused by the inter-species interaction, we would expect the network features of phoD-harboring bacteria also shaped by C, N and P contents, following similar patterns as the community diversity.

To test the whether and how the referred ecological theories fit the relationship of phoD-harboring bacterial diversity and network features to C, N and P supply, we carried out amplicon sequencing of phoD in 102 soils samples collected from three main crop areas spanning over a large latitudinal gradient in China. The samples showed large variability in C, N and P content. The diversity and network features of phoD-harboring bacteria were analyzed and their regression to the SOC, TN, and Po were calculated. We hypothesized that (1) the diversity of phoD-harboring bacteria is shaped by SOC and TN following the unimodal pattern suggested by the RC theory; (2) but shaped by the available Po following the metabolic theory of ecology as defined by the Michaelis-Menten equation. Further, we hypothesized that (3) the relationship of phoD-harboring bacterial network features to C, N and P follows a similar pattern as the diversity.

## 2. Material and methods

### 2.1. Soil sampling

The soil samples were collected from 102 small-holder crop fields spanning across the main cereal-producing areas of China, including 36 spring maize sites in Northeast China, 25 wheat-maize rotation sites in the North China Plain, and 41 paddy rice sites in the Yangtze River basin and South China (Fig. S1). Small-holder farmland is the main farming type in China and most developing countries. The peasants operating these farms generally receive little professional training and seldom record the management data. We thus failed to collect the detail management data for every site. Instead, the mean fertilization rates were collected from the agricultural technology demonstration centers of each sampling region. The N and P fertilizers were applied as urea and superphosphate. On average, the N fertilization rate was 220, 251 and 270 kg N ha<sup>-1</sup> for the maize, wheat-maize and double-rice system, and P fertilization rate was 60, 101 and 80 kg P<sub>2</sub>O<sub>5</sub> ha<sup>-1</sup> for the above three crop systems, respectively. The climatic data including mean annual precipitation (MAP) and mean annual temperature (MAT) were collected from climatic stations across the study area in China Meteorological Data Sharing Service System (<http://cdc.cma.gov.cn/>).

At each site, five 1 × 1 m sampling points were assigned in a 20 m × 20 m plot. Three soil cores were randomly collected from the topsoil (0–20 cm, the cultivation layer) at each sampling point during the crop growth season from June to July. All subsamples from the same site (5×3=15) were subsequently combined into one composite sample and transported to the laboratory on ice within 24 hours. The fresh soils were sieved through a 2 mm sieve, and rocks and plant residues were removed by hands. To minimize the instance effect of roots, temperature, soil moisture and other factors, the soils were incubated for 2 weeks at 25°C under controlled water conditions in the laboratory (upland soils were adjusted to 45% water-holding capacity (WHC) moisture, and paddy soils were flooded using deionized water with a 2-cm water layer). After incubation, soil samples were harvested and divided into three fractions: One was frozen in liquid nitrogen and stored at -80°C for DNA extraction, another was stored at 4°C for the determination of P fractions, while the remaining sample was used to analyze the soil organic carbon (SOC), total nitrogen (TN) and pH after air dried.

### 2.2. Analyses of soil properties

SOC and TN were determined using the heat K<sub>2</sub>Cr<sub>2</sub>O<sub>7</sub>-H<sub>2</sub>SO<sub>4</sub> method and Kjeldahl method, respectively, as described by Bao (2000). Soil pH was determined at a water to soil ratio of 1:2.5. The content of available Po as well as inorganic P (Pi) fractions with different mobility were determined using the approach described in DeLuca et al. (2015). Briefly, root and microbial interception of soluble P was mimicked by 10 mM CaCl<sub>2</sub> (CaCl<sub>2</sub>-P). Organic acid release for the exchange of weakly bound P was emulated by 10 mM citrate (citrate-P), while proton exudation to access recalcitrant mineral P was estimated by using 1.0 M HCl (HCl-P). Considering the heterogeneity of soil pH and that alkaline P<sub>ase</sub> also hydrolyze low-order phytate (Li et al., 2011; Nannipieri et al., 2011), also phytates can act as a carbon source affecting the bacterial community. Therefore, biologically accessible Po was simulated using a P<sub>ase</sub> mixture of 0.2 U acid phosphomonoesterase, alkaline phosphomonoesterase, and phytase (enzyme-P). Half a gram of fresh soil was suspended in 10 mL of each extractant in a 15 mL centrifuge tube and shaken at 200 rpm for 3 h. Considering that the method of Deluca et al. (2015) was established just recently and not extensively tested and the pH of our most samples ranged between 5 and 9, Olsen P was extracted with 0.5 M NaHCO<sub>3</sub> to reflect the labile Pi content as a complement (Olsen et al., 1954). The P concentration in the supernatant was determined using the malachite green method after centrifugation at 5000 rpm for 5 min using a PowerWave-XS microplate spectrophotometer (Infinite M200 PRO, Switzerland) at 630 nm (Ohno and Zibilske, 1991).

### 2.3. phoD amplicon sequencing, sequence processing and diversity analyses

Total soil DNA was extracted with the Mobio PowerSoil DNA kit (Mo Bio Laboratories, Inc.; Carlsbad, CA, USA) according to the manufacturer's instructions. DNA quality and concentration were quantified with a NanoDrop spectrophotometer (NanoDrop Technologies; Wilmington, DE, USA) as well as by electrophoresis with a 1% agarose gel. The isolated DNA was stored at -20°C for PCR and sequencing analyses. A region of phoD was amplified by the primer pair ALPS-730F (5'-CAGTGGGACGACCACGAGGT-3') and ALPS-1101R (5'-GAGGCCGATCGGCATGTTCG-3') (Sakurai et al., 2008). PCR products were purified using Tiangen gel extraction kit (Tiangen; Beijing, China) and sequenced with an Illumina Miseq PE250 platform (Illumina; San Diego, CA, UAS). The primers used in this study has an amplicon bias towards  $\alpha$ -Proteobacteria, nevertheless are still widely used because the targeted fragment provided accurate phylogenetic and taxonomic information (Ragot et al., 2015; Bi et al., 2020). Pair-end raw reads were assembled, screened, and

trimmed in Qiime (Caporaso et al., 2010). The sequence assembly was based on 30 bp of overlapping length between the forward and reverse reads. Low quality tags (<Q30) were removed as well as those were less than 250 bp or more than 380 bp. The produced sequences were exposed to chimera filter and frameshift correction in RDP Fungene pipeline (Fish et al., 2013), and subsequently clustered to OTUs at 97% similarity. A representative sequence was selected for each OTU and BLAST against the GenBank non-redundant nucleotide database for taxonomic assignment. All data sets were rarified to the same sequencing depth (3000 sequences per sample) for the following analyses. Three diversity metrics including observed OTU richness, Shannon diversity index and Faith's phylogenetic diversity index were calculated using the libraries picante and vegan. The raw reads were deposited in NCBI Sequence Read Archive under accession number PRJNA577346.

#### 2.4. Network construction

The OTUs, present in less than 10% of the samples, were excluded when constructing the networks to minimize the bias caused by oligotypes (Chafee et al., 2018). A global co-occurrence network was constructed using Sparse Correlations for Compositional data (SparCC) (Friedman and Alm, 2012). Briefly, compositionality-robust Pearson correlations based on the OTU relative abundance were firstly calculated between all filtered OTUs using SparCC.py. The pseudo-P values were then calculated using a two-sided method in SparCC.py with 20 iterations after 100 bootstraps using MakeBootstraps.py. The random matrix-based method was used to identify the appropriate threshold of correlation coefficients between each pair of nodes, and 0.452 was selected as a cutoff (Fig. S2). Compared to a given cutoff applied in other network methods, mathematical modelling is adopted to define the optimal threshold in this method and then produces an unsupervised network (Luo et al., 2006; Ma et al., 2016). Besides, a cutoff of 0.05 was used for P values to remove unsupported correlations. The network was constructed based on the correlation coefficients using the igraph package in R (Csardi and Nepusz, 2006). Nodes in the network represented OTUs and the edges represented correlations between OTU pairs. Single-sample networks were extracted from the global network using the induced\_subgraph function in the igraph package by preserving the OTUs presented in individual samples (Ma et al., 2016). The network visualization was performed using gephi v. 0.9.2 (<http://gephi.github.io/>).

#### 2.5. Calculation of network properties



Nine topological properties of the nodes were calculated in the global network through the integrated software in gephi. These comprised the significance of individual OTUs in the network: the number of links (degree and weighted degree) and link stress (Eigenvector, Authority and Hub centrality) to adjacent nodes, the possibility and closeness of connections passing through a given node (Clustering, Closeness, and Betweenness centrality), and the longest path passing through the node (Eccentricity). Five network-level topological features were calculated for single-sample networks using the igraph package, including the number of nodes and edges, network density, betweenness centrality, and average path length. The former three features indicated complexity, while the latter two indicated tightness of the networks. The correlation coefficients between OTU pairs were taken as the weight of the edges connecting the OTUs (a greater correlation coefficient indicated a stronger edge between the node pair; positive correlation indicated positive edges, and vice-versa), and the ratio of positive edges was calculated for each single-sample network to reflect the facilitation level.

## 2.6. Statistical analyses

Regression of SOC, TN and Enzyme P to the diversity and network topological features were fitted to linear, quadratic and Michaelis-Menten models using the nls function. The model fitness was compared using the second-order Akaike information criterion value (AICc) calculated by the AICc function in AICcmodavg package. A lower AICc indicated a better model, and a  $\Delta AICc > 2$  was used as a threshold to determine a better performing model (Burnham and Anderson, 2002; Burnham et al., 2011). To evaluate the relative importance of measured variables on the diversity and network topological features, random forest model and multivariate regression trees (MRT) analyses were performed using the rfPermute and mvpart packages, respectively. Before constructing the random forest model, PCA analysis was performed based on the matrix of the diversity or network topological features using the rda function in vegan package, and the first axis was introduced as the dependent variable. Instead, the matrix of original diversity indices or network topological features as the response variable was introduced into the MRT because of its capacity to calculate the relationship between variable groups. All collected variables were used to develop a full random forest model, and the significant variables identified in the full model were used to develop more accurate sparse the importance of an individual variable was compared using the increase in mean squared error (IncMSE) of the model and the

significance of IncMSE when it was the randomly replaced. The significant variables were then used to develop a more accurate model. Before the construction of the sparse model, 5-fold cross validation was performed using the `rfvr()` function to determine how many variables should be induced. All statistical analyses were performed using R 3.5.1 (R Core Team, 2019).

### 3. Results

#### 3.1. Diversity of phoD-harboring bacteria

Relationships between SOC and the three calculated diversity indexes were best fitted to the quadratic model (Fig. 1a, d, g and Table S1). With SOC increasing, the OTU richness, Faith's phylogenetic diversity and Shannon diversity increased and then decreased after the peak at respective 29.5, 26.2 and 28.1 g kg<sup>-1</sup>. Soil total nitrogen shaped the OTU richness and Faith's phylogenetic diversity best following the quadratic model, while it shaped the Shannon diversity following the linear model (Table S1). However, only minimum differences were observed between the linear and quadratic model for all the three indexes ( $\Delta IACc = 0.1-2.6$ ). When all fitted to the quadratic model, the peak value was observed at 0.9, 1.2 and 0.7 for OTU richness, Faith's phylogenetic diversity and Shannon diversity, respectively, which was near to or less than the lowest TN in our samples (0.81 g kg<sup>-1</sup>) (Fig. 1b, e and h). Michaelis-Menten model show worst prediction on the response of phoD-harboring bacterial diversity to SOC and TN, whereas best predicted its response to the available organic P (Enzyme P) (Table S1). As Enzyme P increased, the community diversity increased to the maximum and remained relatively stable (Fig. 1c, f and i). Citrate P concentration also significantly correlated with all the three diversity indexes, following either a Michaelis-Menten or a first-order linear pattern. The  $R^2$  values, however, were much lower than those for SOC, TN or Enzyme P (Table S1 and S2).

The full random forest model explained 28.6% of the variation in the diversity of phoD-harboring bacteria. Five significant predictors were identified, among which the Enzyme P was most important (IncMSE = 12.3%), followed by MAT (11.2%), MAP (10.1%) HCl P (7.2%) and TN (6.8%) (Fig. 2a). Five-fold cross validation suggested the minimum cross-validation error appeared when the model contains 3 variables (Fig. S3). We thus excluded the non-significant variables to develop a more accurate model. The result indicated that the optimal containing Enzyme P, MAT and TN as predictors, and explained 35.8% of the total variations (Fig. 2b). The model accuracy was reduced at most if removed the Enzyme P

while minimum impacted by removal of the climate variables. Notably, when the MAT and MAP were exclusively introduced, the model explained only 3.3% of the variation in diversity (Fig. 2b). The importance of Po availability was also validated by the MRT result, in which the Enzyme P concentration was the primary classifier on the phoD-harboring bacterial diversity (Fig. S4).

### 3.2. Co-occurrence network

The co-occurrence network comprised 50 OTUs accounting for 68.2% of the sequences (Fig. 3). Most of the nodes affiliated to  $\alpha$ - (36%) and  $\gamma$ - (38%) Proteobacteria. However, the node with highest degree affiliated to Actinobacteria. Furthermore, 140 edges were detected in the network. Positive connections accounted for 62.1% of the total edges, indicating that there was more facilitation than antagonism across phoD-harboring bacteria. The relative abundance of nodes showed no significant relationship with any topological features other than the betweenness centrality ( $p = 0.025$ ,  $r = 0.317$ ; Fig. S5).

### 3.3. Network-level topological features

Similar to the diversity, all the network-level topological features were influenced by the SOC and Enzyme P following the quadratic and Michaelis-Menten pattern, respectively (Fig. 4a1-f1, Table S3). The node, edge numbers and average path length increased with SOC concentration and peaked at 26.8, 20.5 and 37.3  $\text{g kg}^{-1}$ , respectively. Contrarily, the network density, betweenness centrality and positive edge ratio decreased and then increased with SOC after a valley at 32.5, 1.6 and 14.3  $\text{g kg}^{-1}$ , respectively. Increases in Enzyme P led to more nodes and edges in the network with lower network density and betweenness centralization but higher average path length and negative edge ratio (Fig. 4a3-f3). The TN concentration monotonously influenced the node number (quadratics at the decreasing side), edge number (linear, negatively), betweenness centrality (linear, positively) and positive edge ratio (linear, positively), whereas the network density decreased with TN until a valley at 1.7  $\text{g kg}^{-1}$ , and the average path length showed no significant relationship with TN (Fig. 4a2-f2, TableS3). Beyond SOC, TN and Enzyme P, none of other tested soil properties significantly related to all the network features in the selected regression models (Table S4). Full random forest model indicated MAT and MAP were the most significant impactor on the network features, followed by Enzyme P, crop species, TN and  $\text{CaCl}_2$  P (Fig. 5a). However, the more accurate sparse model generated from the five-fold cross-validation (Fig.

S6) only included MAT, Enzyme P, crop species and TN, among which removal of Enzyme P had greatest impact on the model explanation (Fig. 5b). The results were also supported by the output of MRT, which suggested Enzyme P to be the first classifier on the network features (Fig. S7).

#### 4. Discussion

Organic P mineralizing bacteria are considered critical for the recycling and efficient use of P in agricultural and other terrestrial ecosystems (George et al., 2018). Despite, the factors that shape the community structure of phoD-harboring bacteria are not well known (Luo et al., 2017; Wei et al., 2019). Here for the first time, we investigated how the diversity and co-occurrence network of phoD-harboring bacteria shifted along the resource supply of SOC, TN and available Po, under the framework of two important ecological theories—resource competition vs. metabolic theory of ecology. The results indicated that both the phoD-harboring bacterial diversity and the network topological features related to SOC and TN content following the unimodal model suggested by resource competition, whereas it related to the available Po following the metabolic theory of ecology as evaluated by the Micheal-Menton model. The study highlighted the potential role of Po availability in shaping the community of P mineralizing bacteria.

##### 4.1 Effect of SOC and TN on phoD-harboring bacterial diversity

Consistent with our first hypothesis, the relationships between the SOC concentration and all calculated diversity indexes of phoD-harboring bacteria in the investigated soils were best predicted by the quadric model (Fig. 1, Table S1). As suggested by the resource competition theory, the phoD-harboring bacterial diversity peaked at a moderate SOC level (26.2–29.5 mg kg<sup>-1</sup>). The theory postulates that resource limitation selects for only oligotrophic species, while a high resource availability favors interspecific competition, selecting for most competitive species for these resources (Tilman, 1982). Acidobacteria have been considered to following the oligotrophic life strategy (Fierer et al., 2012), and this phylum negatively correlated to the SOC concentration in our study (Fig. S8). By contrast, Proteobacteria, which are considered copiotrophic, were positively correlated to SOC (Fig. S8) (Bastida et al., 2015). This phenomenon further supports our hypothesis that SOC would be a key resource influencing the diversity of phoD-harboring bacteria, and functions through the resource competition theory. The result is not surprising because SOC provides

C and energy for all heterotrophic bacteria thus is the most essential resource (Bastida et al., 2016). Previous studies suggested that soil microorganisms produce phosphatases not only for P acquisition but also to mitigate the C limitation, because organic phosphates serve as both P and C pools (Luo et al 2017). This may further underline the role of SOC in the community assembly of phoD-harboring bacteria. Many studies that investigated the assembly of phoD-harboring bacterial community highlighted the significance of SOC, however the underlying mechanism is yet to be revealed (Ragot et al., 2015; Sun et al., 2020). Our results provide an empirical evidence for a theoretical explanation of this observation.

As with SOC, the quadric model showed also a good performance at predicting the relationship between TN and the diversity of phoD-harboring bacteria. The results indicated that the effect of TN on phoD-harboring bacterial diversity might also adapt to the resource competition theory. However, the fitness was minimally different from the linearly decreasing model (Table S1). We attribute this to the high TN concentration in our soils (0.81–4.01 g kg<sup>-1</sup>), where the increasing side of the quadric curve was missing. Soil pH is among the most significant factors regulating microbial community at large scales (Fierer and Jackson, 2006; Shi et al., 2018; Wu et al., 2017). However, a decrease of phoD-harboring bacterial diversity with decreasing pH is not likely in our study, since no relationship between pH and OTU richness, Shannon diversity or Faith's phylogenetic diversity was found (Table S1 and S2). In the study of Dai et al (2018), the decrease in bacterial diversity was combined with the enrichment of the copiotrophs (Proteobacteria) and a depletion of oligotrophs (Acidobacteria), and the authors attributed the results to the direct effect of nutrient availability more than pH. Similar correlations were detected in our study (Fig. S8). Phosphatases are N-rich molecules (Olander et al., 2000). If phoD-harboring bacteria benefit from ALP production, they will have to compete for N. Therefore, we suggest that soil nitrogen would affect the diversity of phoD-harboring bacteria also due to resource competition.

#### 4.2 Effect of available organic P on phoD-harboring bacterial diversity

The most interesting finding in this study is the relationship between available organic P (Enzyme P) and phoD-harboring bacterial diversity, which can be described by a Michaelis-Menten model (Fig. 1 and Table S1). The Michaelis-Menten equation is a universal law, which is used to describe substrate regulation on the rate of enzymatic reactions (German et al., 2012). The organic P measured in this study represented the readily

available substrate of phosphomonoesterase, the enzyme group which the *phoD*-encoding protein belongs to (Nannipieri et al., 2011). Consistent with the hypothesis of the metabolic theory of ecology, our results suggested that the first principle of enzymatic reactions likely also works on the community assembly of bacteria driving these reactions (Brown, 2004). As expected, OTU richness, Shannon diversity and Faith's polygenetic diversity increased and remained steady from low to high organic P availability (Fig. 1). The decline of diversity at low Enzyme P is likely because the limitation of organic P allows only the colonization of populations producing PAse with high substrate affinity and not sufficient to support the individuals with low substrate affinity (Straka et al., 2019; Thingstad et al., 1993). The Michaelis-Menten constant ( $K_m$ ) of PAse varied from  $\mu\text{g l}^{-1}$  to  $\text{mg l}^{-1}$  P as affected by the taxa of the producers, indicating different phosphate-affinity of different P-mineralizing bacteria (Nedoma et al., 2007; Pilar et al., 2003). We fitted enzyme kinetic analysis on 20 randomly chosen samples, and found a positive relationship between the  $K_m$  and  $P_o$  availability (Enzyme P concentration) (Fig. S9). The results further supported our hypothesis that substrate affinity may be a determinant for the colonization of *phoD*-harboring bacteria. However, instead of the decrease at high concentration of SOC and TN, the diversity remained steady at high  $P_o$  availability. An increase in  $K_m$  is generally accompanied with a decrease in  $V_{\text{max}}$  (maximal enzymatic velocity) (Hui et al., 2013). In fact, an increased  $K_m$  indicates an overall depletion in the enzyme function (German et al., 2012). As a result, despite the fact that high  $P_o$  availability would allow the colonization of bacteria producing PAse with high  $K_m$ , they are not likely to outcompete the fellows with better substrate affinity. While the guilds producing PAse with low  $K_m$  win in substrate competition, the  $\text{PO}_4$  they hydrolyzed is also available for other populations, thus is not likely to outcompete in growth, neither (Allison et al., 2005). Moreover, we found a negative correlation between Enzyme P and TN (Fig. S8). The results indicated the increase in *phoD*-harboring bacterial diversity possibly met a N limitation, which would counteract the positive effect of organic P availability and lead to a plateau.

Many studies found that the P availability relates less with the community composition of *phoD*-harboring bacteria than with other soil properties across field experiments (Hu et al., 2018; Liu et al 2021; Xie et al., 2020). These results raise the question of whether P conditions matter for the P-mineralizing bacterial community, which is essential for the development of microbe-mediated P mobilizing technologies in agricultural production (Richardson and Simpson, 2011). Our study suggested that soil P condition plays a role in

the composition of phoD-harboring bacterial community. However, instead of the inorganic P or total P which was previously focused on (Hu et al., 2018; Ragot et al., 2017; Xie et al., 2020), the availability of Po most likely functions in this process. Through the random forest model and multiple regression tree analysis, we found the available Po is the most important factor influencing the diversity features of phoD-harboring bacteria prior to all other soil properties, climate factors and crop species (Fig. 2 and 5). Despite we pre-incubated the soils to mitigate the effect of climate variation, MAP and MAT were among the most important impactors on the diversity of phoD-harboring bacteria following organic P availability (Fig. 2 and 4). This might be due to the historical effect on climate on the soil properties (Hou et al., 2018; Sun et al., 2020). We found significant correlation between soil properties and the MAT and MAP (Fig. S8), which may support the hypothesis. Anyway, relationships between environmental factors and soil microbial features are affected by the investigating scale, and in most cases MAT, MAP and pH is related to microbial community composition at large spatial scales (Fierer and Jackson, 2006; Matsuoka et al., 2019; Shi et al., 2018; Tu et al., 2016). In our study, however, pH had no effect on the diversity of phoD-harboring bacteria. The result was consistent with previous reports that labile organic P had stronger effects than pH on phoD diversity (Luo et al., 2017; Ragot et al., 2017).

#### 4.3 Network features of phoD-harboring bacteria responding to resource availability

The network features of phoD-harboring bacterial community changed with the concentration of SOC, TN and Enzyme P in the same pattern as that of the diversity (Fig. 4). Lower nodes and edge numbers at low SOC and Enzyme P concentration may indicate a decline in the network complexity because of resource limitation, but also possible imply a lower OTU richness (Butler and Dwyer, 2020). We observed less tightly woven network of interactions (indicated by lower network density and higher average path length) with increasing resource availability to the valley and then increased for SOC and TN while remained steady for Enzyme P (Fig. 4c1, 2 and c3). We attributed this to the changes in phylogenetic similarity of the community. As shown in Fig. 1d-f, close relatives were more common at low resource availability (smaller Faith's phylogenetic diversity), which were suggested to share conserved interactions (Kinkel et al., 2014). In complex ecological networks, higher tightness likely indicates a loss in the stability and robustness (Allesina and Tang, 2012; Butler and O'Dwyer, 2018). Increases in the betweenness centralization with larger SOC and TN concentrations suggested that the relationship between phoD-harboring

bacteria had been more mutually depended, which also led to a higher sensitivity to disturbances (Ma et al., 2016). However, the results do not necessarily imply a monotonous response of betweenness centralization to the resource availability at any range, since - as claimed above - the model fitness of linear and unimodal functions were similar, and the SOC and TN concentrations in our agricultural soils were relatively high. Accordingly, organic P limitation led to higher betweenness centralization (Fig. 4d3). Our results overall suggested that most complex and robust interactions among phoD-harboring bacteria in agriculture soil may occur at moderate resource supply rates. Positive co-occurrence pattern would indicate facilitation between the OTUs, whereas negative co-occurrence indicates antagonism (Harris, 2016). As reported across many microbial communities, facilitation seemed to dominate in our networks (Gu et al., 2019; Tao et al., 2018; van der Gast et al., 2011). A high positive edge ratio in soils with high SOC and TN concentrations was consistent with the reports that oligotrophic bacterial communities favor antagonistic interactions (Ponce-Soto et al., 2015; Pérez-Gutiérrez et al., 2013). However, an increase in Enzyme P seemed to have led to increased antagonism (Fig. 4f3). The results were likely due to the competition for organic P between species with low and high substrate affinity (Martens-Habbena et al., 2009). Unlike the diversity, variation in network features was less explained organic P availability than climate factors and significant effect of crop types was observed (Fig. 5). The results indicate that the historical effect more worked on the interaction among phoD-harboring bacteria than their diversity. Plant roots produce and release acid Pases to soil, and compete for organic P with the bacteria producing PAsE, which would impact the network relationship of phoD-harboring bacterial community (Neal et al., 2017; Tarafdar et al., 2001).

## 5. Conclusions

In conclusion, we showed that the diversity and network topological features of phoD-harboring bacteria related to the concentration of SOC and TN in unimodal or linear pattern, while related to the Po availability it followed the Michaelis-Menten model. The two patterns could be explained by the resource competition and metabolic theory of ecology, respectively, which were likely related to the interactions among species, as indicated by the co-occurrence network. Organic P availability was the most important soil property shaping the community of phoD-harboring bacteria, which was little studied in previous studies. Other factors significantly influencing the phoD-harboring bacterial community included



MAT, MAP and crop types, however not pH. Our study provides a clear empirical evidence supporting the crucial role of organic P on the community of phoD-harboring bacteria. Nevertheless, because of the complexity in soil, further studies are needed to confirm the patterns figured in this study, and to clarify other confounding factors influencing the community of phoD-harboring bacteria.

### **Acknowledgements**

This study was supported by the National Key Research and Development program (2017YFD0800104), the National Natural Science Foundation of China (41601260, 41761134095); the Natural Science Foundation of Hunan Province (2019JJ10003; 2019JJ30028); the Youth Innovation Team Project of the Institute of Subtropical Agriculture, Chinese Academy of Sciences (2017QNCXTD\_GTD) and the Hunan Province Base for Scientific and Technological Innovation Cooperation (2018WK4012). We thank anonymous reviewers for their careful and patient work that have helped to improve the quality of this manuscript.

### **References**

- Allesina, S., Tang, S., 2012. Stability criteria for complex ecosystems. *Nature* 483(7388), 205–208.
- Allison, S.D., 2005. Cheaters, diffusion and nutrients constrain decomposition by microbial enzymes in spatially structured environments. *Ecology Letters* 8(6), 626–635.
- Alori, E.T., Glick, B.R., Babalola, O.O., 2017. Microbial phosphorus solubilization and its potential for use in sustainable agriculture. *Frontiers in microbiology* 8, 971.
- Apel, A.K., Sola-Landa, A., Rodríguez-García, A., Martín, J.F., 2007. Phosphate control of phoA, phoC and phoD gene expression in *Streptomyces coelicolor* reveals significant differences in binding of PhoP to their promoter regions. *Microbiology* 153(10), 3527–3537.
- Bao, S.D., 2000. *Soil Agro-Chemistry Analysis*. Chinese Agriculture Press, Beijing (in Chinese).

- Bastida, F., Selevsek, N., Torres, I.F., Hernández, T., García, C., 2015. Soil restoration with organic amendments: linking cellular functionality and ecosystem processes. *Scientific Reports* 5(1), 1–12.
- Bastida, F., Torres, I.F., Moreno, J.L., Baldrian, P., Ondoño, S., Ruiz-Navarro, A., Hernández, T., Richnow, H.H., Starke, R., García, C., Jehmlich, N., 2016. The active microbial diversity drives ecosystem multifunctionality and is physiologically related to carbon availability in Mediterranean semi-arid soils. *Molecular Ecology* 25(18), 4660–4673.
- Bi, Q.F., Li, K.J., Zheng, B.X., Liu, X.P., Li, H.Z., Jin, B.J., Ding, K., Yang, X.R., Liu, X.R., Zhu, Y.G., 2020. Partial replacement of inorganic phosphorus (P) by organic manure reshapes phosphate mobilizing bacterial community and promotes P bioavailability in a paddy soil. *Science of The Total Environment* 703, 134977.
- Brown, J.H., Gillooly, J.F., Allen, A.P., Savage, V.M., West, G.B., 2004. Toward a metabolic theory of ecology. *Ecology* 85(7), 1771–1789.
- Burnham, K.P., Anderson, D.R., 2002. A practical information-theoretic approach. *Model selection and multimodel inference*, 2. New York.
- Burnham, K.P., Anderson, D.R., Huyvaert, K.P., 2011. AIC model selection and multimodel inference in behavioral ecology: some background, observations, and comparisons. *Behavioral Ecology and Sociobiology* 65(1), 23–35.
- Butler, S., O’Dwyer, J.P., 2018. Stability criteria for complex microbial communities. *Nature Communications* 9(1), 1–10.
- Butler, S., O’Dwyer, J.P., 2020. Cooperation and stability for complex systems in resource-limited environments. *Theoretical Ecology* 13(2), 239–250.
- Caporaso, J.G., Kuczynski, J., Stombaugh, J., Bittinger, K., Bushman, F.D., Costello, E.K., Fierer, N., Peña, A.G., Goodrich, J.K., Gordon, J.I., Huttley, G.A., Kelley, S.T., Knights, D., Koenig, J.E., Ley, R.E., Lozupone, C.A., McDonald, D., Muegge, B.D., Pirrung, M., Reeder, J., Sevinsky, J.R., Turnbaugh, P.J., Walters, W.A., Widmann, J., Yatsunencko, T., Zaneveld, J., Knight, R., 2010. QIIME allows analysis of high-throughput community sequencing data. *Nature Methods* 7(5), 335–336.

- Chafee, M., Fernández-Guerra, A., Buttigieg, P.L., Gerdt, G., Eren, A.M., Teeling, H., Amann, R.L., 2018. Recurrent patterns of microdiversity in a temperate coastal marine environment. *The ISME Journal* 12(1), 237–252.
- Chhonkar, P.K., Tarafdar, J.C., 1981. Characteristics and location of phosphatases in soil-plant system. *Journal of the Indian Society of Soil Science* 29(2), 215–219.
- Cordell, D., Drangert, J.O., White, S., 2009. The story of phosphorus: global food security and food for thought. *Global Environmental Change* 19(2), 292–305.
- Cordell, D., Rosemarin, A., Schröder, J.J., Smit, A.L., 2011. Towards global phosphorus security: A systems framework for phosphorus recovery and reuse options. *Chemosphere* 84(6), 747–758.
- Csardi, G., Nepusz, T., 2006. The igraph software package for complex network research. *InterJournal, Complex Systems* 1695(5), 1–9.
- Dai, Z., Liu, G., Chen, H., Chen, C., Wang, J., Ai, S., Wei, D., Li, D., Ma, B., Tang, C., Brookes, P.C., Xu, J., 2020. Long-term nutrient inputs shift soil microbial functional profiles of phosphorus cycling in diverse agroecosystems. *The ISME Journal* 14(3), 757–770.
- Dai, Z., Su, W., Chen, H., Barberán, A., Zhao, H., Yu, M., Brookes, P.C., Schadt, C.W., Chang, S.X., Xu, J., 2018. Long-term nitrogen fertilization decreases bacterial diversity and favors the growth of Actinobacteria and Proteobacteria in agroecosystems across the globe. *Global Change Biology* 24(8), 3452–3461.
- Damon, P.M., Bowden, B., Rose, T., Rengel, Z., 2014. Crop residue contributions to phosphorus pools in agricultural soils: A review. *Soil Biology and Biochemistry* 74, 127–137.
- DeLuca, T.H., Glanville, H.C., Harris, M., Emmett, B.A., Pingree, M.R., de Sosa, L.L., Cerdá-Moreno, C., Jones, D.L., 2015. A novel biologically-based approach to evaluating soil phosphorus availability across complex landscapes. *Soil Biology and Biochemistry* 88, 110–119.
- Deng, Y., Jiang, Y.H., Yang, Y.F., He, Z.L., Luo, F., Zhou, J.Z., 2012. Molecular ecological network analyses. *BMC Bioinformatics* 13: 113.

- Fierer, N., Jackson, R.B., 2006. The diversity and biogeography of soil bacterial communities. *Proceedings of the National Academy of Sciences* 103(3), 626–631.
- Fierer, N., Lauber, C.L., Ramirez, K.S., Zaneveld, J., Bradford, M.A., Knight, R., 2012. Comparative metagenomic, phylogenetic and physiological analyses of soil microbial communities across nitrogen gradients. *The ISME Journal* 6(5), 1007–1017.
- Fish, J.A., Chai, B., Wang, Q., Sun, Y., Brown, C.T., Tiedje, J.M., Cole, J.R., 2013. Funene: the functional gene pipeline and repository. *Frontiers in Microbiology* 4, 291.
- Folse, H.J., Allison, S.D., 2012. Cooperation, competition, and coalitions in enzyme-producing microbes: social evolution and nutrient depolymerization rates. *Frontiers in Microbiology* 3: 338.
- Fraser, T., Lynch, D.H., Entz, M.H., Dunfield, K.E., 2015. Linking alkaline phosphatase activity with bacterial *phoD* gene abundance in soil from a long-term management trial. *Geoderma* 257, 115–122.
- Friedman, J., Alm, E.J., 2012. Inferring correlation networks from genomic survey data. *PLoS Computational Biology* 8(9), e1002687.
- George, T.S., Giles, C.D., Menezes-Blackburn, D., Condrón, L.M., Gama-Rodrigues, A.C., Jaisi, D., Lang, F., Neal, A.L., Stutter, M.I., Almeida, D.S., Bol, R., Cabugao, K.G., Celi, L., Cotner, J.B., Feng, G., Goll, D.S., Hallama, M., Krueger, J., Plassard, C., Rosling, A., Darch, T., Fraser, T., Giesler, R., Richardson, A.E., Tamburini, F., Shand, C.A., Lumsdon, D.G., Zhang, H., Blackwell, M.S.A., Wearing, C., Mezeli, M.M., Almås, Å.R., Audette, Y., Bertrand, I., Beyhaut, E., Boitt, G., Bradshaw, N., Brearley, C.A., Bruulsema, T.W., Ciais, P., Cozzolino, V., Duran, P.C., Mora, M.L., de Menezes, A.B., Dodd, R.J., Dunfield, K., Engl, C., Frazão, J.J., Garland, G., González Jiménez, J.L., Graca, J., Granger, S.J., Harrison, A.F., Heuck, C., Hou, E.Q., Johnes, P.J., Kaiser, K., Kjær, H.A., Klumpp, E., Lamb, A.L., Macintosh, K.A., Mackay, E.B., McGrath, J., McIntyre, C., McLaren, T., Mészáros, E., Missong, A., Mooshammer, M., Negrón, C.P., Nelson, L.A., Pfahler, V., Pobleto-Grant, P., Randall, M., Seguel, A., Seth, K., Smith, A.C., Smits, M.M., Sobarzo, J.A., Spohn, M., Tawarayama, K., Tibbett, M., Voroney, P., Wallander, H., Wang, L., Wasaki J., Haygarth, P.M., 2018. Organic phosphorus in the terrestrial environment: a

- perspective on the state of the art and future priorities. *Plant and Soil* 427(1), 191–208.
- German, D.P., Marcelo, K.R., Stone, M.M., Allison, S.D., 2012. The Michaelis-Menten kinetics of soil extracellular enzymes in response to temperature: a cross-latitudinal study. *Global Change Biology* 18(4), 1468–1479.
- Graham, J.H., Duda, J.J., 2011. The humpbacked species richness-curve: a contingent rule for community ecology. *International Journal of Ecology* 11: 1–16.
- Gu, S., Hu, Q., Cheng, Y., Bai, L., Liu, Z., Xiao, W., Gong, Z., Wu, Y., Feng, K., Deng, Y., Tan, L., 2019. Application of organic fertilizer improves microbial community diversity and alters microbial network structure in tea (*Camellia sinensis*) plantation soils. *Soil and Tillage Research* 195, 104356.
- Harris, D.J., 2016. Inferring species interactions from co-occurrence data with Markov networks. *Ecology* 97(12), 3308–3314.
- Hou, E., Chen, C., Luo, Y., Zhou, G., Kuang, Y., Zhang, Y., Heenan, M., Lu, X., Wen, D., 2018. Effects of climate on soil phosphorus cycle and availability in natural terrestrial ecosystems. *Global Change Biology* 24(8), 3344–3356.
- Hu, Y., Xia, Y., Sun, Q., Liu, K., Chen, X., Ge, T., Zhu, B., Zhu, Z., Zhang, Z., Su, Y., 2018. Effects of long-term fertilization on phoD-harboring bacterial community in Karst soils. *Science of The Total Environment* 628, 53–63.
- Hui, D., Mayes, M.A., Wang, G., 2013. Kinetic parameters of phosphatase: a quantitative synthesis. *Soil Biology and Biochemistry* 65, 105–113.
- Kathuria, S., Martiny, A.C., 2011. Prevalence of a calcium-based alkaline phosphatase associated with the marine cyanobacterium *Prochlorococcus* and other ocean bacteria. *Environmental Microbiology* 13(1), 74–83.
- Kinkel, L.L., Schlatter, D.C., Xiao, K., Baines, A.D., 2014. Sympatric inhibition and niche differentiation suggest alternative coevolutionary trajectories among *Streptomyces*. *The ISME Journal* 8(2), 249–256.
- Layeghifard, M., Hwang, D.M., Guttman, D.S., 2017. Disentangling Interactions in the Microbiome: A Network Perspective. *Trends in Microbiology* 25(3): 217–228.

- Li, C., Li, Y., Ma, J., 2011. Spatial heterogeneity of soil chemical properties at fine scales induced by *Haloxylon ammodendron* (Chenopodiaceae) plants in a sandy desert. *Ecological Research* 26(2), 385–394.
- Liu, S., Zhang, X., Dungait, J.A., Quine, T.A., Razavi, B.S., 2021. Rare microbial taxa rather than *phoD* gene abundance determine hotspots of alkaline phosphomonoesterase activity in the karst rhizosphere soil. *Biology and Fertility of Soils* 57(2), 257–268.
- Liu, J.S., Ma, Q., Hui, X.L., Ran, J.Y., Ma, Q.X., Wang, X.S., Wang, Z.H., 2020. Long-term high-P fertilizer input decreased the total bacterial diversity but not *phoD*-harboring bacteria in wheat rhizosphere soil with available-P deficiency. *Soil Biology and Biochemistry* 149,107918.
- Luo, F., Zhong, J., Yang, Y., Scheuermann, R.H., Zhou, J., 2006. Application of random matrix theory to biological networks. *Physics Letters A* 357(6), 420 – 423.
- Luo, G., Ling, N., Nannipieri, P., Chen, H., Raza, W., Wang, M., Guo, S., Shen, Q. 2017. Long-term fertilisation regimes affect the composition of the alkaline phosphomonoesterase encoding microbial community of a vertisol and its derivative soil fractions. *Biology and Fertility of Soils* 53(4), 375–388.
- Ma, B., Wang, H., Dsouza, M., Lou, J., He, Y., Dai, Z., Brookes, P.C., Xu, J., Gilbert, J.A., 2016. Geographic patterns of co-occurrence network topological features for soil microbiota at continental scale in eastern China. *The ISME Journal* 10(8), 1891 – 1901.
- Martens-Habbena, W., Berube, P.M., Urakawa, H., José, R., Stahl, D.A., 2009. Ammonia oxidation kinetics determine niche separation of nitrifying Archaea and Bacteria. *Nature* 461(7266), 976–979.
- Matsuoka, S., Iwasaki, T., Sugiyama, Y., Kawaguchi, E., Doi, H., Osono, T., 2019. biogeographic patterns of ectomycorrhizal fungal communities associated with *castanopsis sieboldii* across the Japanese archipelago. *Frontiers in Microbiology* 10: 2656.
- Michaelis, L., Menten, M.L., 1913. The kinetics of the inversion effect. *Biochemistry Zeitschrift* 49, 333–369.

- Nannipieri, P., Giagnoni, L., Landi, L., Renella, G., 2011. Role of phosphatase enzymes in soil. In *Phosphorus in Action*. Springer, Berlin, Heidelberg, pp. 215–243.
- Neal, A.L., Rossmann, M., Brearley, C., Akkari, E., Guyomar, C., Clark, I.M., Allen, E., Hirsch, P.R., 2017. Land-use influences phosphatase gene microdiversity in soils. *Environmental Microbiology* 19(7), 2740–2753.
- Nedoma, J., Van Wambeke, F., Štrojsová, A., Štrojsová, M., Duhamel, S., 2007. Affinity of extracellular phosphatases for ELF97 phosphate in aquatic environments. *Marine and Freshwater Research* 58(5), 454–460.
- Ohno, T., Zibilske, L.M., 1991. Determination of low concentrations of phosphorus in soil extracts using malachite green. *Soil Science Society of America Journal* 55(3), 892–895.
- Olander, L.P., Vitousek, P.M., 2000. Regulation of soil phosphatase and chitinase activity by N and P availability. *Biogeochemistry* 49(2), 175–191.
- Olsen, S.R., 1954. Estimation of available phosphorus in soils by extraction with sodium bicarbonate (No. 939). US Department of Agriculture.
- Pérez-Gutiérrez, R.A., López-Ramírez, V., Islas, A., Alcaraz, L.D., Hernández-González, I., Olivera, B.C.L., Santillán, M., Eguiarte, L.E., Souza, V., Travisano, M., Olmedo-Alvarez, G., 2013. Antagonism influences assembly of a *Bacillus* guild in a local community and is depicted as a food-chain network. *The ISME journal* 7(3), 487–497.
- Pilar, M.C., Ortega, N., Perez-Mateos, M., Busto, M.D., 2003. Kinetic behaviour and stability of *Escherichia coli* ATC27257 alkaline phosphatase immobilised in soil humates. *Journal of the Science of Food and Agriculture* 83(3), 232–239.
- Ponisio, L.C., Valdovinos, F.S., Allhoff, K.T., Gaiarsa, M.P., Barner, A., Guimaraes, P.R., Hembry, D.H., Morrisong, B., Gillespie, R., 2019. A network perspective for community assembly. *Frontiers in Ecology and Evolution* 7: 103.
- Ponce-Soto, G.Y., Aguirre-von-Wobeser, E., Eguiarte, L.E., Elser, J.J., Lee, Z.M.P., Souza, V., 2015. Enrichment experiment changes microbial interactions in an ultra-oligotrophic environment. *Frontiers in Microbiology* 6, 246.

- Ragot, S.A., Kertesz, M.A., Bünemann, E.K., 2015. *phoD* alkaline phosphatase gene diversity in soil. *Applied and Environmental Microbiology* 81(20), 7281–7289.
- Ragot, S.A., Kertesz, M.A., Mészáros, É., Frossard, E., Bünemann, E.K., 2017. Soil *phoD* and *phoX* alkaline phosphatase gene diversity responds to multiple environmental factors. *FEMS Microbiology Ecology* 93(1), 118–120.
- Richardson, A.E., Simpson, R.J., 2011. Soil microorganisms mediating phosphorus availability update on microbial phosphorus. *Plant physiology* 156(3), 989–996.
- Sakurai, M., Wasaki, J., Tomizawa, Y., Shinano, T., Osaki, M., 2008. Analysis of bacterial communities on alkaline phosphatase genes in soil supplied with organic matter. *Soil Science and Plant Nutrition* 54(1), 62–71.
- Sattari, S.Z., Bouwman, A.F., Giller, K.E., van Ittersum, M.K., 2012. Residual soil phosphorus as the missing piece in the global phosphorus crisis puzzle. *Proceedings of the National Academy of Sciences* 109(16), 6348–6353.
- Shi, Y., Li, Y., Xiang, X., Sun, R., Yang, T., He, D., Zhang, K.P., Ni, Y.Y., Zhu, Y.G., Adams, J.M., Chu, H., 2018. Spatial scale affects the relative role of stochasticity versus determinism in soil bacterial communities in wheat fields across the North China Plain. *Microbiome* 6(1), 1–12.
- Straka, L.L., Meinhardt, K.A., Bollmann, A., Stahl, D.A., Winkler, M.K., 2019. Affinity informs environmental cooperation between ammonia-oxidizing archaea (AOA) and anaerobic ammonia-oxidizing (Anammox) bacteria. *The ISME Journal* 13(8), 1997–2004.
- Sun, F., Song, C., Wang, M., Lai, D.Y., Tariq, A., Zeng, F., Zhong, Q., Wang, F., Li, Z., Peng, C., 2020. Long-term increase in rainfall decreases soil organic phosphorus decomposition in tropical forests. *Soil Biology and Biochemistry* 151, 108056.
- Sun, H., Wu, Y., Zhou, J., Bing, H., Zhu, H., 2020. Climate influences the alpine soil bacterial communities by regulating the vegetation and the soil properties along an altitudinal gradient in SW China. *Catena* 195, 104727.
- Sun, Q., Qiu, H., Hu, Y., Wei, X., Chen, X., Ge, T., Wu, J., Su, Y., 2019. Cellulose and lignin regulate partitioning of soil phosphorus fractions and alkaline



- phosphomonoesterase encoding bacterial community in phosphorus-deficient soils. *Biology and Fertility of Soils* 55(1), 31–42.
- Tan, H., Barret, M., Mooij, M.J., Rice, O., Morrissey, J.P., Dobson, A., Griffiths, B., O'gara, F., 2013. Long-term phosphorus fertilisation increased the diversity of the total bacterial community and the *phoD* phosphorus mineraliser group in pasture soils. *Biology and Fertility of Soils* 49(6), 661–672.
- Tao, J., Meng, D., Qin, C., Liu, X., Liang, Y., Xiao, Y., Liu, Y., Gu, Y., Li, J., Yin, H., 2018. Integrated network analysis reveals the importance of microbial interactions for maize growth. *Applied Microbiology and Biotechnology* 102(8), 3805–3818.
- Tarafdar, J.C., Yadav, R.S., Meena, S.C., 2001. Comparative efficiency of acid phosphatase originated from plant and fungal sources. *Journal of Plant Nutrition and Soil Science* 164(3), 279–282.
- Team, R.C., 2014. R: A Language and Environment for Statistical Computing. Vienna: R Core Team. *R. Found. Statistics and Computing* 1, 409.
- Thingstad, T.F., Skjoldal, E.F., Bohne, R.A., 1993. Phosphorus cycling and algal-bacterial competition in Sandsfjord, western Norway. *Marine ecology-progress series*, 99, 239-259.
- Tilman, D., 1982. *Resource Competition and Community Structure*. Princeton University Press. pp. 296.
- Tu, Q.C., Deng, Y., Yan, Q.Y., Shen, L.N., Lin, L., He, Z.L., Wu, L.Y., Van Nostrand, J.D., Buzzard, V., Michaletz, S.T., Enquist, B.J., Weiser, M.D., Kaspari, M., Waide, R.B., Brown, J.H., 2016. Biogeographic patterns of soil diazotrophic communities across six forests in the North America. *Molecular Ecology* 25(12): 2937-2948.
- Van Der Gast, C.J., Walker, A.W., Stressmann, F.A., Rogers, G.B., Scott, P., Daniels, T.W., Carroll, M.P., Parkhill, J., Bruce, K.D., 2011. Partitioning core and satellite taxa from within cystic fibrosis lung bacterial communities. *The ISME Journal* 5(5), 780–791.
- Wei, X., Hu, Y., Razavi, B.S., Zhou, J., Shen, J., Nannipieri, P., Wu, J., Ge, T., 2019. Rare taxa of alkaline phosphomonoesterase-harboring microorganisms mediate soil phosphorus mineralization. *Soil Biology and Biochemistry* 131, 62–70.

- Wu, X., Xu, H., Liu, G., Ma, X., Mu, C., Zhao, L., 2017. Bacterial communities in the upper soil layers in the permafrost regions on the Qinghai-Tibetan plateau. *Applied Soil Ecology* 120, 81–88.
- Xie, Y., Wang, F., Wang, K., Yue, H., Lan, X., 2020. Responses of bacterial *phoD* gene abundance and diversity to crop rotation and feedbacks to phosphorus uptake in wheat. *Applied Soil Ecology* 154, 103604.
- Zhou, J., Deng, Y., Shen, L., Wen, C., Yan, Q., Ning, D., Qin, Y.J., Xue, K., Wu, L.Y., He, Z.L., Voordeckers, J.W., Van Nostrand, J.D., Buzzard, V., Michaletz, S.T., Enquist, B.J., Weiser, M.D., Kaspari, M., Waide, R., Yang, Y.F., Brown, J.H., 2016. Temperature mediates continental-scale diversity of microbes in forest soils. *Nature Communications* 7(1), 1–10.
- Zhu, J., Li, M., Whelan, M., 2018. Phosphorus activators contribute to legacy phosphorus availability in agricultural soils: A review. *Science of the Total Environment* 612, 522–537.

Figures

Fig. 1

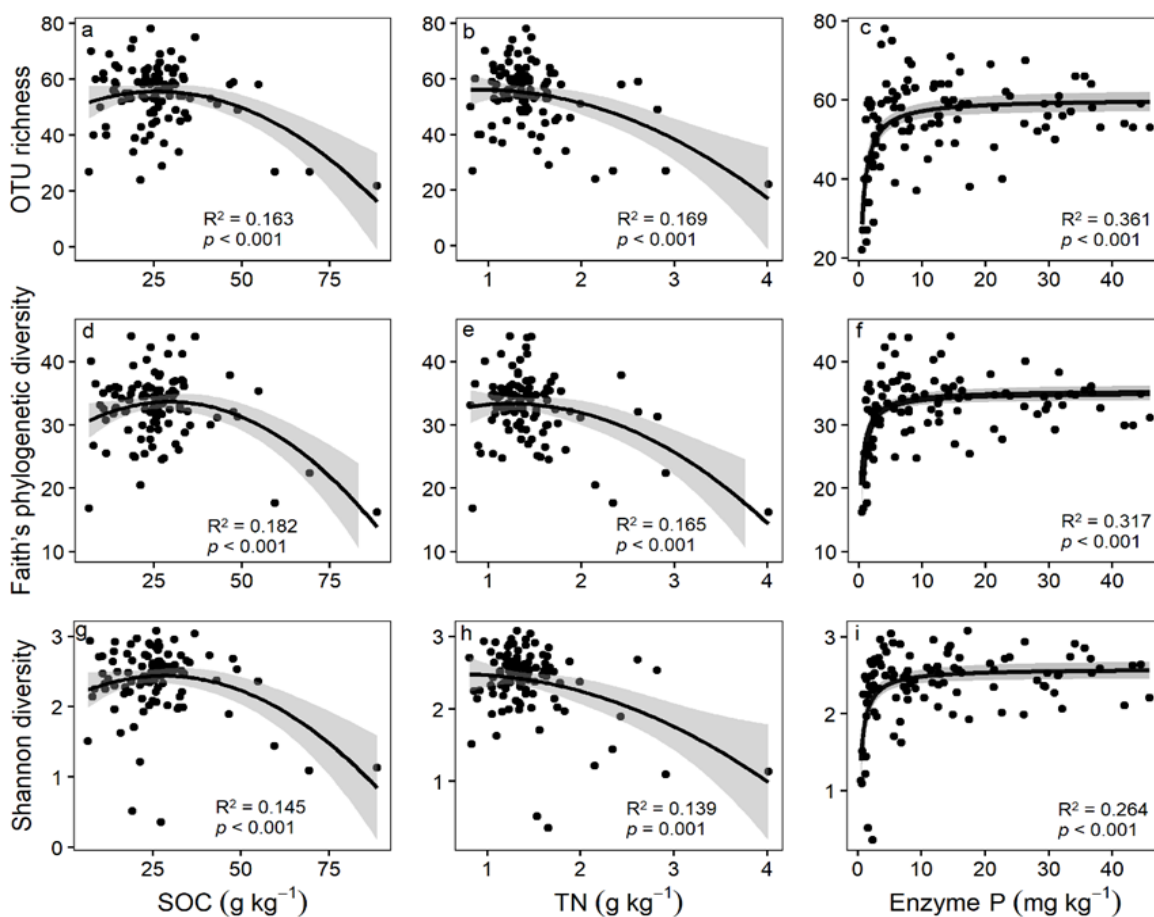


Fig. 2

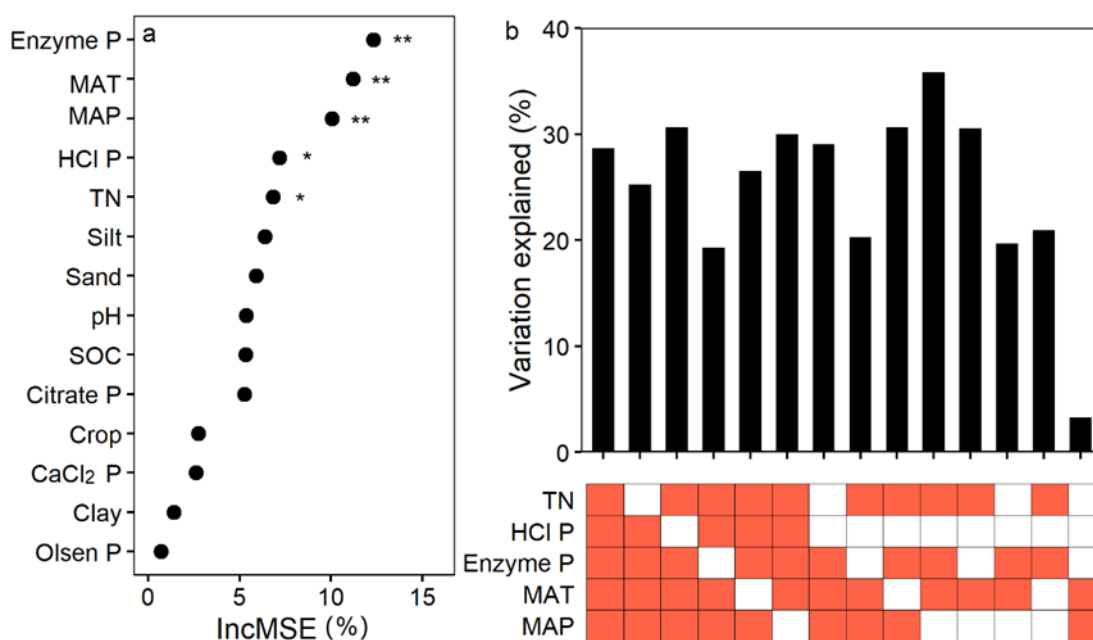


Fig. 3

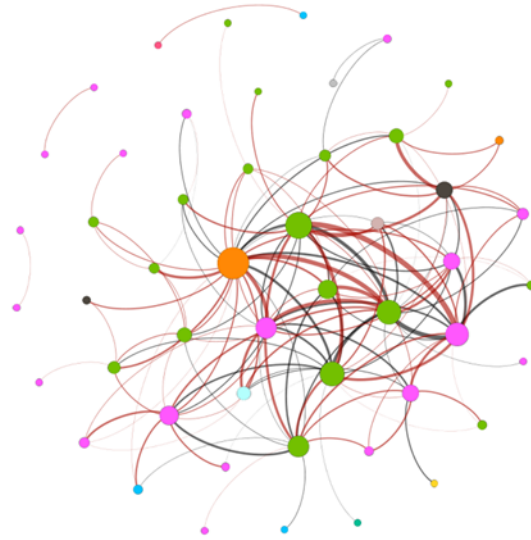
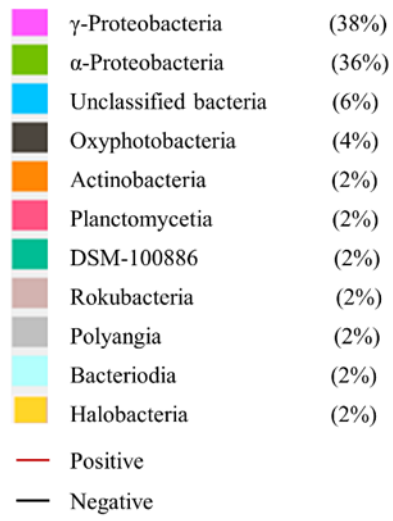


Fig. 4

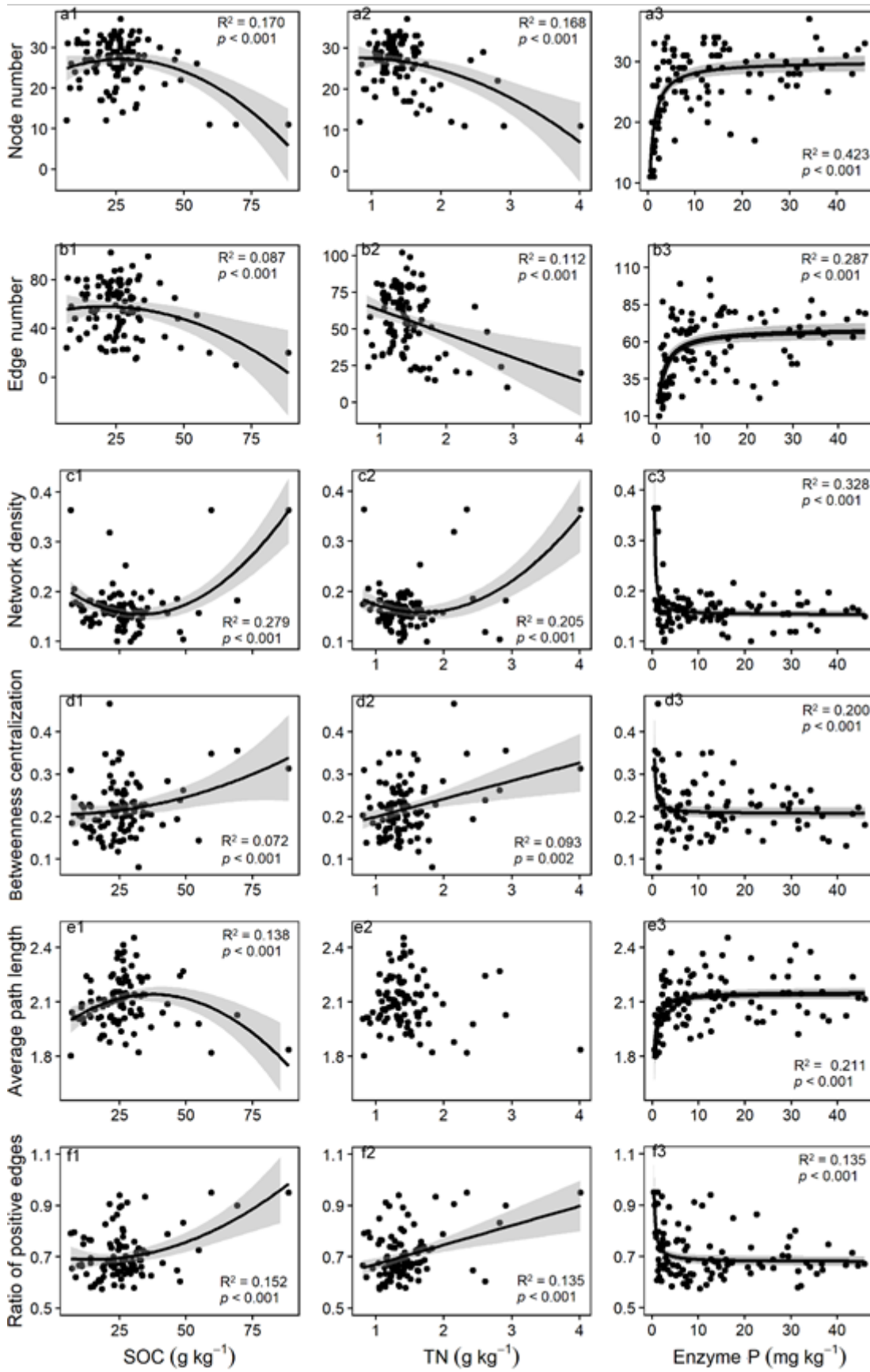
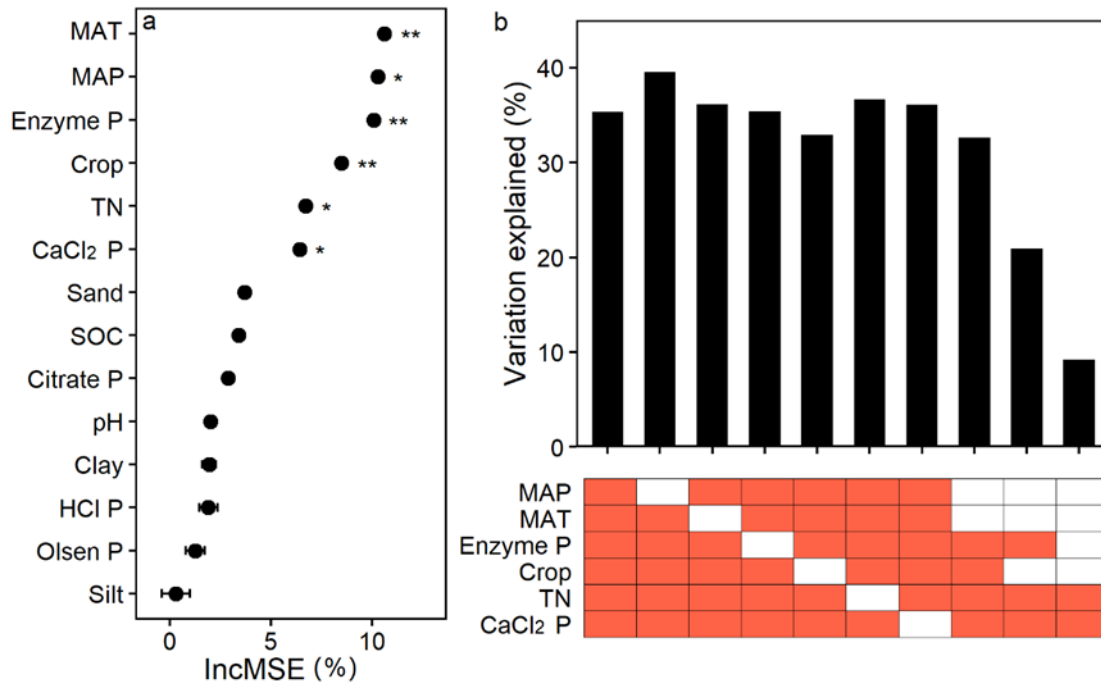


Fig. 5



### Figure Legends

**Fig. 1** Regressions of the observed OTUs (a-c), Faith's phylogenetic diversity (d-f) and Shannon index (g-i) of the phoD-harboring bacteria to soil organic C (SOC; a, d, g), total nitrogen (TN; b, e, g) and available Po (Enzyme P; c, f, i) as fitted to optimal models suggested by the Second-order Akaike information criterion values (AICc) among linear, quadric and Michaelis-Menten patterns. The AICc values are shown in Table S1.

**Fig. 2** Full (a) and sparse (b) model of random forest analysis predicting the effect of soil properties, climate factors and crop species on the diversity of phoD-harboring bacteria. The bar plot in figure b indicates the explanation on diversity variation of each sparse model; red colored boxes below each bar indicate the variables marked at left are used in the model, while the empty boxes indicate the variables are not used. Significant factors are marked using the asterisks. \*,  $p < 0.05$ ; \*\*,  $p < 0.01$ .

**Fig. 3** Co-occurrence network between OTUs of phoD-harboring bacteria. The nodes are colored by class. The size of each nodes indicates the number of connections (degree) and the width of the edges indicates the correlation strength of the connection (weight).

**Fig. 4** Regressions of the node number (a1-a3), edge number (b1-b3), network density (c1-c3), betweenness centrality (d1-d3), average path length (e1-e3), and the ratio of positive edges (f1-f3) of the phoD-harboring bacterial network to soil organic C (SOC; a1-f1), total

nitrogen (TN; a2-f2) and available organic P (Enzyme P; a3-f3) as fitted to optimal models suggested by the Second-order Akaike information criterion values (AICc) among linear, quadric and Michaelis-Menten patterns. The AICc values are shown in Table S3.

**Fig. 5** Full (a) and sparse (b) model of random forest analysis predicting the effect of soil properties, climate factors and crop species on the network topological features of phoD-harboring bacteria. The bar plot in figure b indicates the explanation on diversity variation of each sparse model; red colored boxes below each bar indicate the variables marked at left are used in the model, while the empty boxes indicate the variables are not used. Significant factors are marked using the asterisks. \*,  $p < 0.05$ ; \*\*,  $p < 0.01$ .

## Study 3—Supplementary material

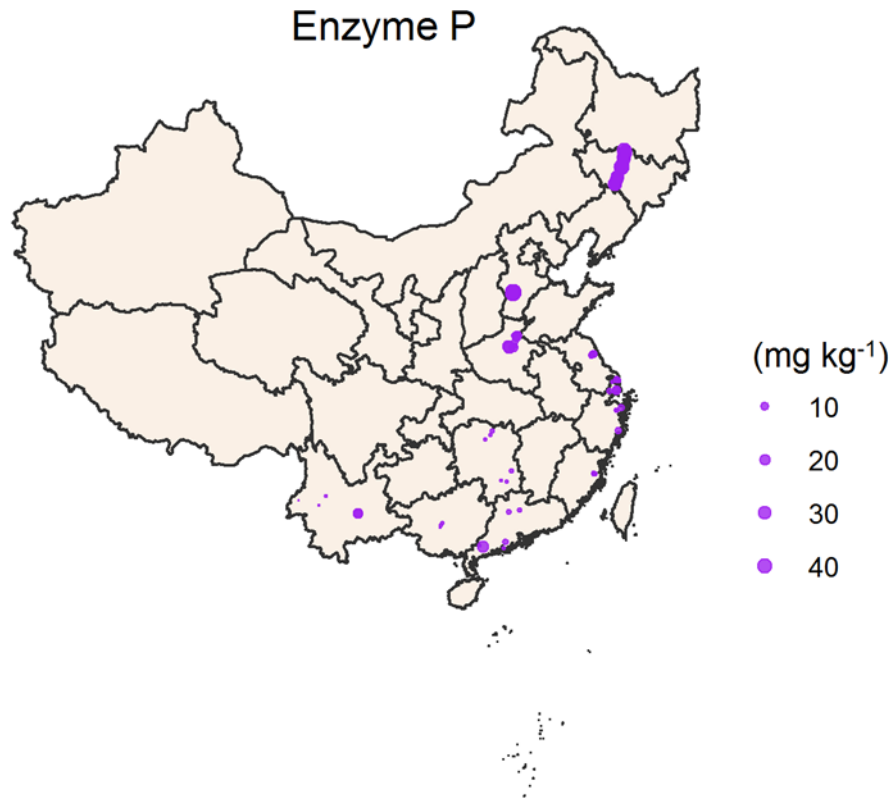


Fig. S1 Geographical distribution of our sampling sites. The size of the circles indicates the enzyme P content of each site.

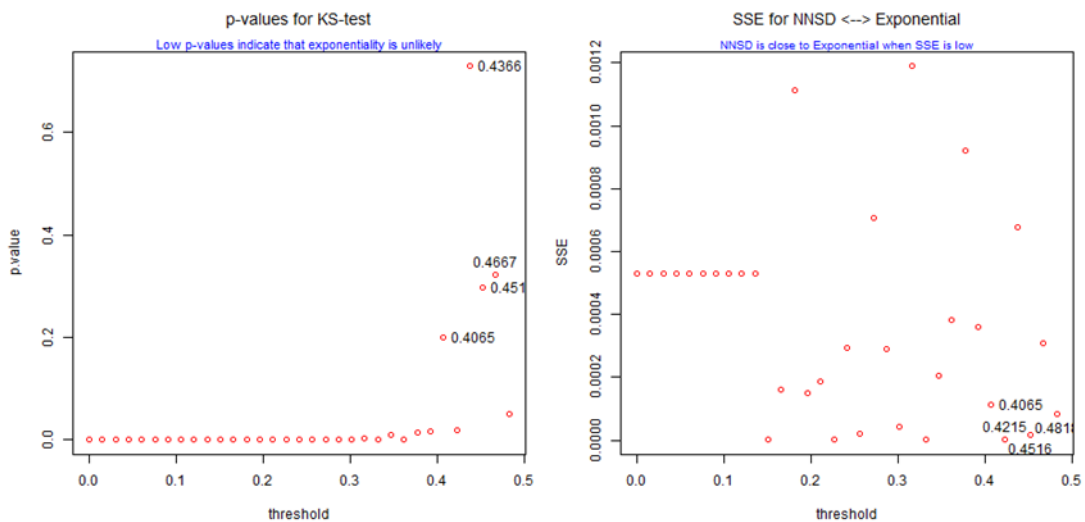


Fig. S2 P value for the KS, SSE, and NNSD tests of the exponential distribution generated by random matrix theory.



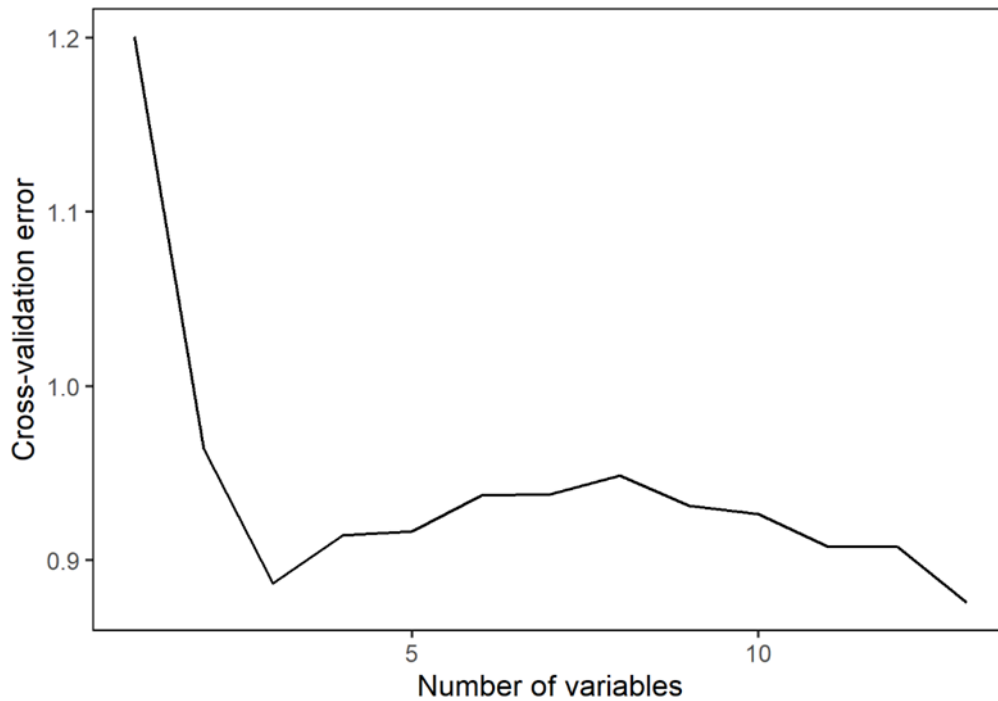


Fig. S3 Five-fold cross-validation error of the diversity of phoD-harboring bacteria as number of variables increasing.

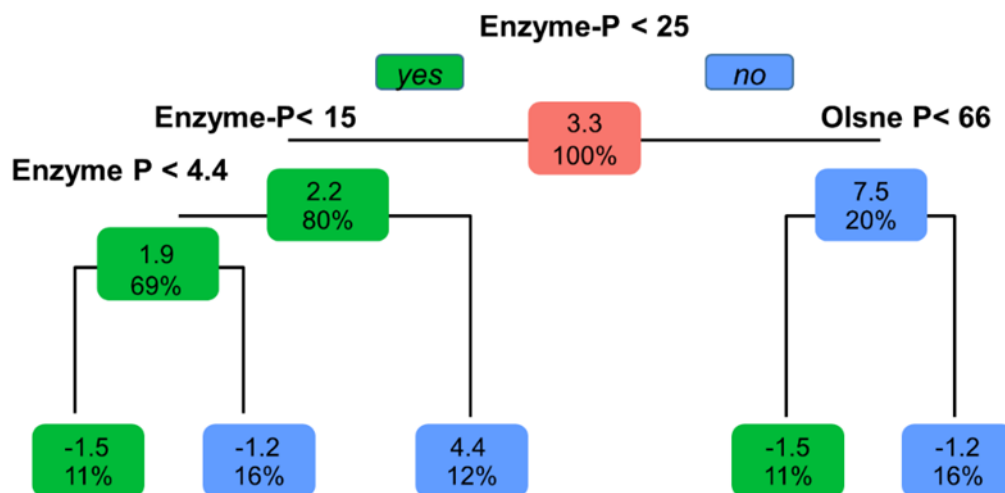


Fig. S4 Multivariate regression tree (MRT) analysis indicating soil enzyme extractable P content constrains on the diversity indices including OTU richness, phylogenetic diversity and Shannon diversity of phoD-harboring bacteria.

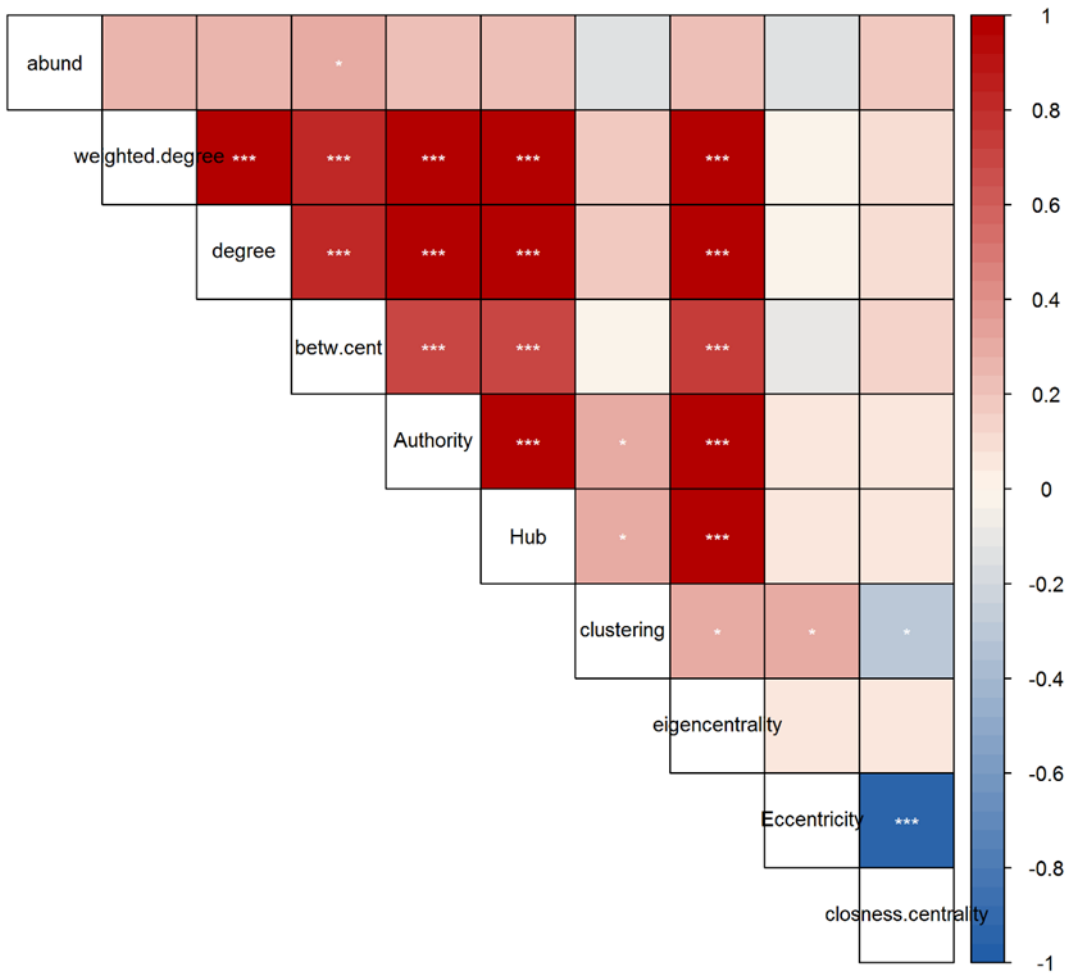


Fig. 5 Pearson correlation between the relative abundance (abund) and network features including weighted degree, unweighted degree (degree), betweenness centrality (betw.cent), authority centralization (Authority), hub centralization (Hub), clustering centralization (Clustering), eigenvector centrality (eigencentrality), Eccentricity Centrality (Eccentricity), and closeness centrality of phoD-harboring bacteria identified as nodes in the global co-occurrence network.

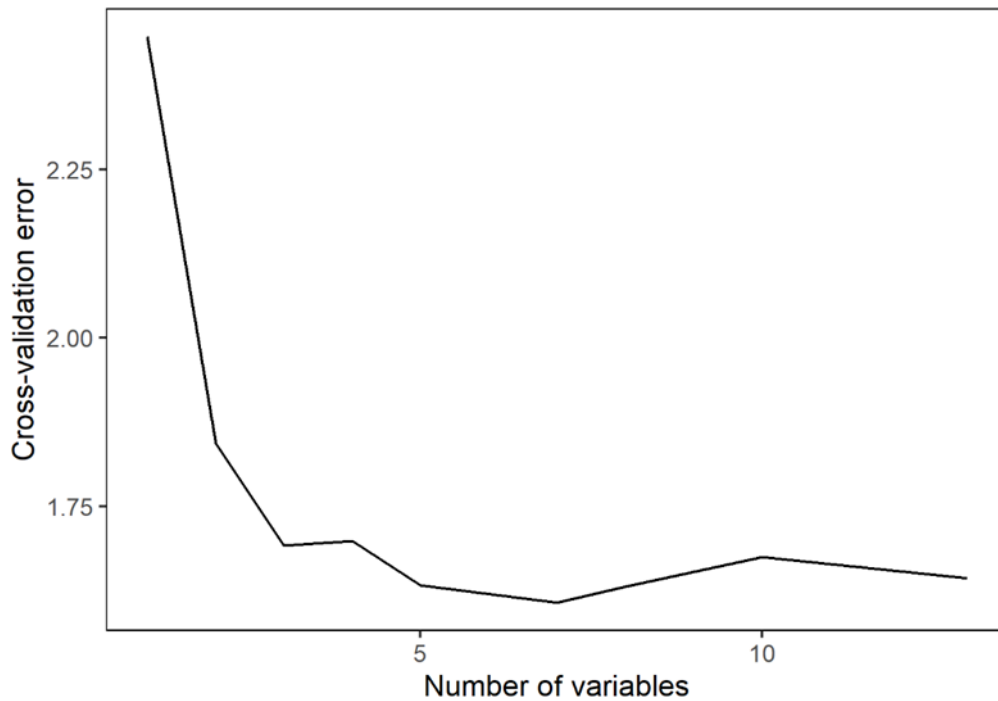


Fig. S6 Five-fold cross-validation error of the network topological features of phoD-harboring bacteria as number of variables increasing.

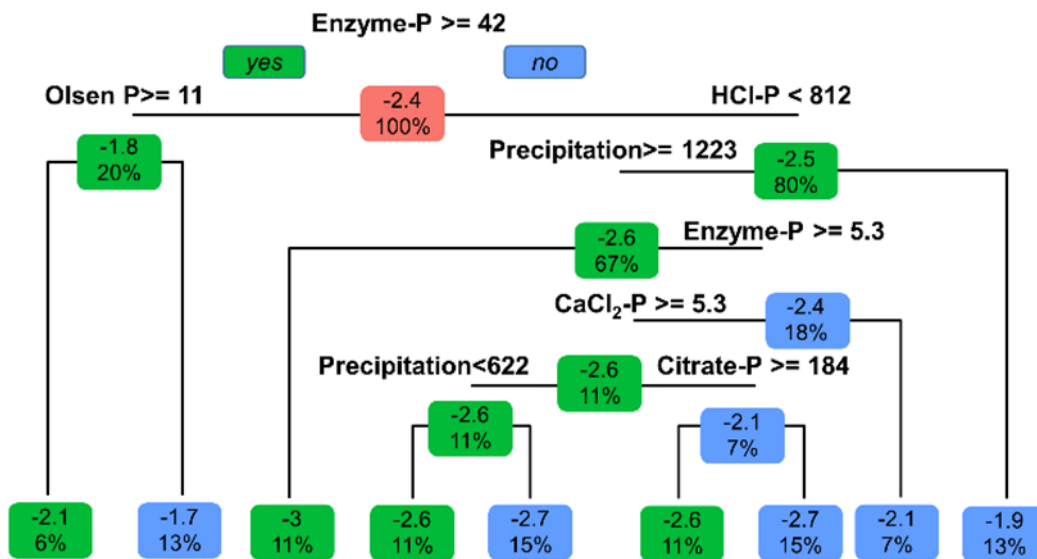


Fig. S7 Multivariate regression tree (MRT) analysis indicating available organic P (Enzyme P) constraints on node number, edge number, network density, betweenness centrality, average path length, and the ratio of positive edges of phoD-harboring bacterial network

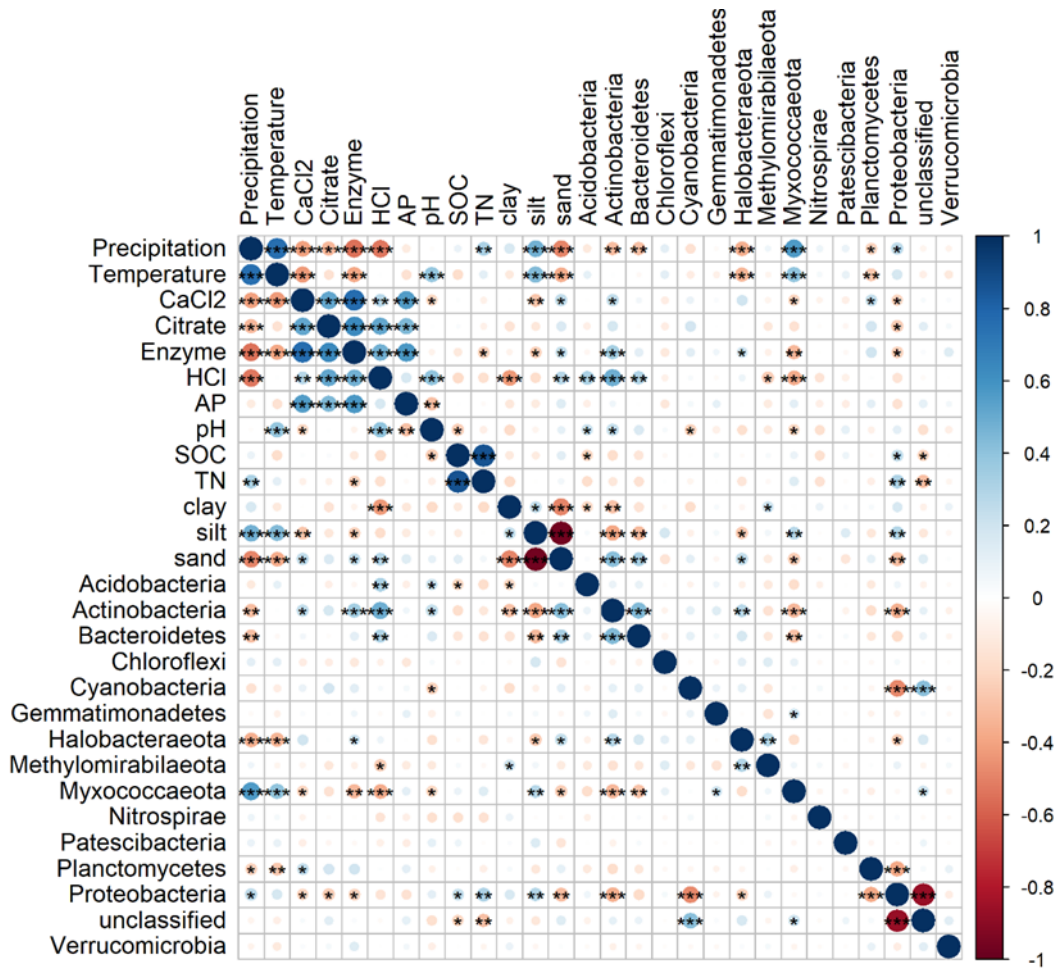


Fig. S8 Pearson correlation between environmental factors and the relative abundance of the main phyla of phoD-harboring bacteria.

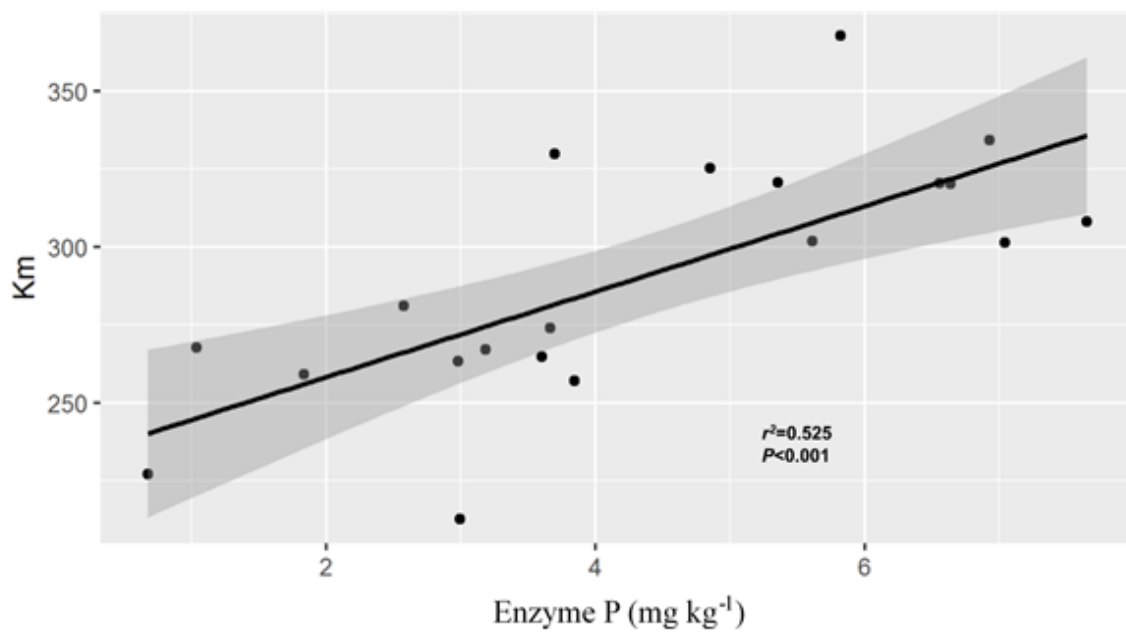


Fig. S9 Relationship between the phosphatase mineable P (Enzyme P) and km of alkaline phosphomonoesterase.

## 5 General Discussion

### 5.1 SOM mineralization of labile and stable organic compounds

Microorganisms, as organic C turnover drivers, play an essential role in the C cycle by decomposing organic matter to release CO<sub>2</sub> into the atmosphere (catabolism) and promoting C fixation in the form of microbe-derived C for plant residues and other organic matters entering the soil (anabolism) (Liang et al., 2017; Zheng et al., 2021). SOM comprises several organic compounds characterized by a continuum of differently stable and chemically unique organic compounds in the form of abundant and stable macromolecular biomacromolecules such as lignin, continuously released labile root exudates, organic N, and organic P compounds (Chen et al., 2018; Zhang et al., 2019; Wei et al., 2021). SOM composition is related to microbial growth, metabolism, and death and can be broken down at different decomposition stages after death (Lehmann and Kleber, 2015; Liang et al., 2017; Fig.1.2).

Labile organic compounds (such as root exudates) and recalcitrant organic compounds (such as lignin) were tested in the first and second experiments. In the first experiment, artificial root exudates were added in three different substrate-nutrient stoichiometry ratios to the paddy field soil for incubation. The composition of root exudates was simulated by combining different amounts of glucose, oxalic acid, and alanine to characterize low molecular weight organic compound (sugars, organic acids, and amino acids) mineralization (Study 1, Fig. 7). Simulated root exudates at all different substrate-nutrient stoichiometry ratios also stimulated microbial activity, increasing CO<sub>2</sub> emission from the soil compared to that from the control soil. Low substrate-nutrient stoichiometry ratios in root exudates accelerated labile C mineralization (Study 1, Fig. 1 and 5). A high C- and N-acquiring enzyme activities associated with the low substrate-nutrient stoichiometry ratios (and CO<sub>2</sub> evolution) indicates a prominent catabolic pathway (Study 1, Fig 4a). The supply of root exudates caused a C-rich condition that increased the microbial activity. The root exudates with different substrate-nutrient stoichiometry ratios offer a labile substrate for microorganisms to maintain the elemental stoichiometric demands, indicating a positive correlation between microbial biomass ratios (MBC/MBN) and C use efficiency (CUE)

(Study 1, Fig. 4d). Sinsabaugh et al. (2013) have stated that enzyme stoichiometry and microbial biomass element stoichiometry are essential indicators for microbial growth. CUE in the first study was from 0.52 to 0.81 (Study 1, Fig.1.2b), which is consistent with the results of previous studies (Spohn et al., 2016; Buckeridge et al., 2020; Du et al., 2020; Widdig et al., 2020). A high CUE indicates increased organic C uptake by microorganisms for biomass synthesis, while low CUE indicates increased C emission to the atmosphere as CO<sub>2</sub> (Study 1, Fig. 1 and 2). The magnitude of microbial CUE is influenced by soil substrate content and environmental conditions (Sinsabaugh et al., 2013; Spohn et al., 2016; Chen et al., 2020). Previous studies have shown that microorganisms consume a large amount of energy at low soil substrate content to obtain more C and N, and the fraction allocated to their growth is reduced, thus decreasing microbial CUE (Ågren et al., 2001; Spohn et al., 2016). In addition, the substrate-nutrient stoichiometry ratios affect microbial CUE (Creamer et al., 2014; Liu et al., 2020; Du et al., 2020). A high soil C/N ratio usually leads to low microbial CUE because when nutrients are restricted, C uptake exceeds the need for microbial biomass synthesis, prompting enhanced microbial respiration (Creamer et al., 2014; Liu et al., 2020). Conversely, low soil C/N ratios could mitigate nutrient limitation, increasing microbial CUE (Manzoni et al., 2012b; Du et al., 2020). Differences in soil substrate content and nutrient elemental stoichiometry ratios inevitably cause microbial CUE differences.

In contrast to low molecular weight root exudates, lignin is characterized as a structural plant constituent with high stability against microbial decomposition. In study 2, I investigated the mineralization and decomposition of this rather recalcitrant biomacromolecule under anaerobic and aerobic conditions in a 390-days incubation experiment employing <sup>13</sup>C-labeled lignin. CO<sub>2</sub> emission during the incubation period showed positive priming first, followed by negative priming during the entire anaerobic condition. Lignin decomposition was proven by the presence of <sup>13</sup>C in emitted CO<sub>2</sub> (after 20% non-lignin is decomposed), indicating that microorganisms decomposed the added organic substrates.

Microbial decomposition requires nutrition supp'y for microbial growth (Hessen et al., 2004; Craine et al., 2007). The addition of organic materials (such as root exudates and lignin) stimulate nutrient demand for microbial growth, increase microbial biomass, and promote their metabolic processes (Wild et al., 2014; Duboc et al., 2014; Ferlian et al., 2017; Liang et al., 2017). In addition, the water saturation of soils also affects microbial activity.

Numerous studies have shown that flooded soils inhibit organic C mineralization and have higher microbial biomass than dry soils (Devêvre and Horwáth, 2000; Kögel-Knabner et al., 2010; Qiu et al., 2017). We observed that both  $^{13}\text{C}$ -DOC and  $^{13}\text{C}$ -MBC were higher in water-saturated soils than those in upland soils (moisture content 40%), while the organic C mineralization rate was lower than that in water-unsaturated soils (Study 2, Fig. 4 and Fig. 7). This indicates that the microbial activity increases if the microorganisms secrete extracellular enzymes in a substrate-controlled manner, which promotes the organic matter decomposition, thus contributing to faster SOM mineralization rates in water-unsaturated than those in water-saturated soils. Furthermore, the  $^{13}\text{C}$ -lignin-respired C under water-unsaturated conditions was significantly higher in upland soil than that in water-saturated soil (Study 2, Fig. 3), indicating that lignin conversion is susceptible to water-unsaturated environmental changes and implying that water-saturated soil is conducive to lignin accumulation.

## **5.2 SOM accumulation under anaerobic conditions**

Generally, anaerobic soils such as paddy field soils are widely accepted as having high C sequestration potential due to their reducing conditions under prolonged flooding (Pan et al., 2004). In water-saturated soils, redox-sensitive processes that lead to metal mineral adsorption or dissolution occur, which changes in response to temporal fluctuations in soil moisture (Du et al., 2009). Moreover, paddy field soils are not completely anaerobic and can form a particular oxidized layer about one cm deep due to the diffusion of dissolved oxygen in the water (Kögel-Knabner et al., 2010). Due to its high redox potential, this layer enables C and N oxidation–reduction processes that stimulate the growth of specific microbial populations, affecting SOM accumulation and stabilization through microbial activity and microbial residue formation (Husson, 2013; Hall et al., 2015). The addition of organic materials, such as low molecular weight compounds of root exudates, and stable polymeric lignin biomacromolecules, effectively promotes SOM accumulation in agricultural systems (Baudoin et al., 2003; Chen et al., 2018). I observed a continuous DOC accumulation in anaerobic and aerobic soils, which was higher in anaerobic soils than that in aerobic soils under anaerobic conditions (Study 2, Fig.7a). This suggests that the change from anaerobic to aerobic conditions increases C mineralization rate and is thus part of the water-soluble compounds consumed by microbial activity, thus reducing DOC concentrations in aerobic soils. Oxygen concentration is one of the critical environmental factors affecting microbial



activity during SOM transformation (Noll et al., 2019; Qian et al., 2022). Aeration can increase oxygen content and nutrient conversion, thus affecting the diversity and function of bacterial communities (Qian et al., 2022). At different oxygen concentrations, soil microbial activity leads to different microbial community structures (Sierra et al., 2015; Moche et al., 2015; Ebrahimi and Or, 2016).

Organic matter accumulation and fate in the soil depend largely on microbial decomposition and anabolic activities (Cotrufo et al., 2013; Geyer et al., 2016; Liang et al., 2017). I observed that MBC content increased under anaerobic conditions and decreased in aerobic drying soils, suggesting that anaerobic soils are more conducive to producing a relatively active microbial biomass and promoting microbial C sequestration than aerobic soils. This may be due to the accumulation of intermediate metabolites of water-soluble organic matter under long-term flooding and anaerobic conditions, forming a relatively stress anaerobic environment and promoting the growth of many anaerobic microorganisms (D'Angelo and Reddy, 2003). The microbial community in anaerobic soils was relatively more stable than that in aerobic soils because of the long-term exposure to high CO<sub>2</sub> concentration in soil (Panikov, 1999; Oppermann et al., 2010). However, the anaerobic microorganisms die rapidly in aerobic soil environment, thus reducing the microbial biomass in the aerobic condition. Redox sensitivity may also affect the reductive dissolution of Fe oxides and the release of organic matter (Schwertmann, 1991; Borch et al., 2010). We observed that <sup>13</sup>C-MBC and <sup>13</sup>C-DOC accumulation in anaerobic soils is higher than that in aerobic soils (Study 2, Fig 7). This may be due to organic matter (e.g., lignin) in anaerobic soils, promoting microbial Fe<sub>o</sub> reduction and dissolving Fe<sub>o</sub> oxides. During long-term anaerobic conditions, the continually and gradually produced microbe-derived C induces an entombing effect resulting from increased <sup>13</sup>C-MBC concentrations in anaerobic soils, indicating that microorganisms selectively preserve cellular components and their degradation products (Liang et al. 2017). The soil microorganisms under anaerobic conditions obtain a high proportion of organic matter from the soil to maintain their biomass, increasing microbe-derived C deposition through the anabolic pathway (such as in vivo turnover), thus contributing to higher SOM accumulation under anaerobic environment than that under aerobic environments.

### **5.3 Effects of nutrients on microbial activities**

C turnover processes frequently happen in association with nutrients such as N and P.

However, the proportions of C, N, and P in SOM are different. The addition of root exudates (particularly N-containing) significantly increased both total soil CO<sub>2</sub> and CO<sub>2</sub> released from the organic N source (Study 1, Fig. 2), indicating that the application of N-containing root exudates enhanced microbial SOM mineralization (Meier., 2017; Liu et al., 2020; Du et al., 2020). This is because N is a limiting element for microbial growth, and the microbial demand for N increases microbial activity and promotes SOM mineralization (Mooshammer et al., 2014; Fisk et al., 2015). I found that artificial root exudates with CN6 substrate-nutrient stoichiometry ratio (high N content) stimulated more CO<sub>2</sub> emission than those with CN80 substrate-nutrient stoichiometry ratio (low N content) (Study 1, Table 1, and Fig. 1). N-acquiring extracellular enzyme (NAG) activity increased in C-rich soil (N limit at high C/N ratio), indicating that N demand modifies microbial activity. This result is consistent with that reported by Kelley et al. (2011), who showed that NAG enzyme activity increases significantly with CO<sub>2</sub> emission, representing an increase in N demand. The same results were also reported by Zeglin et al. (2013), who showed that microbial respiration increased with N nutrients associated with increased NAG enzyme activities in the forest soil. However, our results were in contrast to those of Liu et al. (2020), who observed that increased N resource decreased NAG enzyme activity. These differences are due to the different forms of N nutrients [(NH<sub>4</sub>)<sub>2</sub>SO<sub>4</sub> versus alanine] added and the stoichiometric ratios in the soil. The microbial community structure is also affected by N form, which preferentially uses ammonium N (Geisseler and Scow, 2014). Olander and Vitousek (2000) found that N addition inhibited NAG enzyme activity, which decreased with increasing soil N, only in the youngest N-limited soils.

Microbial biomass and extracellular enzyme activity are mainly regulated by N and P content in decomposed SOM, which changes SOM mineralization rate (Zhu et al., 2018). Organic P is a major but limited component in SOM. The third experiment aimed to quantify the bioavailability of organic P in agricultural soil using the Michaelis–Menten equation to verify that the diversity of *phoD*-harboring bacteria shaped by enzyme-P follows the metabolic theory. In this experiment, 102 agricultural soil samples covering large latitude gradients for SOC, TN, and organic P were collected, and *phoD* gene amplification sequencing on the soil samples was performed. The results show that SOC, TN, and organic P availability are critical parameters for regulating the microbial community structure (e.g., *PhoD*-function gene). The changes in SOC, TN, and organic P (enzyme-P) concentrations followed the same pattern as those of the *phoD*-harboring bacterial community shaping

(Study 3, Fig. 4). This result indicates that the SOC, TN, and enzyme-P are critical elements that accurately reflect the bacterial community composition. SOC concentration can affect microbial community structure and biomass (Stone et al., 2014; Zhang et al., 2016). At high SOC content, the substrate can promote microbial growth, while at low SOC content, it can stimulate competition between microorganisms to change the community structure by increasing the ratio of saturated fatty acids to monounsaturated fatty acids (Kieft et al., 1994; Liu et al., 2012; Blagodatskaya et al., 2014). The shaping of bacterial community structure is also driven by enzymatic reactions (enzyme-P) and follows the Michaelis–Menten model of ecological metabolic theory (Study 3, Fig. 1, and Table S1). A positive relationship was observed between Michaelis–Menten constant ( $km$ ) and enzyme-P, indicating that  $Km$  increase is accompanied by enzymatic hydrolysis depletion (German et al., 2012; Hui et al., 2013). Compared with that of other P forms (Study 3, Fig. 2. CaCl<sub>2</sub>-P, Citrate-P, HCl-P, and Olsen-P), the availability of enzyme-P is more suitable for shaping microbial metabolism-mediated community structure, but its mechanism still needs to be further explored.

## 6 Conclusion and Outlook

In this thesis, I have evaluated the processes of SOM mineralization and accumulation in agricultural soils based on microbial biomass, microbial CUE, extracellular enzyme activity, microbial community structure, and organic C, TN, and organic P availability. In addition, SOM bioavailability and metabolic synthesis was examined by investigating the fate of labile organic substrates (such as root exudates and organic P) and more stable structural compounds (such as lignin) associated with redox control in agricultural soils.

I found that adding root exudates and lignin accelerates CO<sub>2</sub> emission from agricultural soils. The promoted microbial activities and metabolism caused by rapidly available plant exudates promote SOM mineralization than those caused by lignin application. However, the microorganisms degraded the recalcitrant lignin compounds under anaerobic condition via a metabolic pathway of lignin decomposition, and lignin decomposition at anaerobic conditions also leads to negative priming. Priming at both anaerobic and aerobic conditions indicated that microbial biomass was strongly affected by redox and nutrient limitations. Anaerobic water-saturated conditions are conducive to producing a relatively active microbial biomass and induces an entombing effect that promotes microbe-derived C sequestration in anaerobic soil than that in aerobic soil. Organic N and P species promote soil organic C turnover, therefore benefiting the *phoD*-harboring bacteria community structure. The enzyme-P (organic P) shaped the *phoD*-harboring bacteria community, followed by the Michaelis–Menten model from the metabolic theory. In conclusion, the comprehensive datasets provide an overview of SOM turnover on the microbial metabolic processes, which includes mineralization and accumulation of labile (root exudates) and stable organic compounds (lignin) under complex environmental conditions (anaerobic wetting and aerobic drying) in agricultural soils.

In future, RNA/DNA-SIP probes should be used to quantify the microbial community structural changes during SOM transformation under anaerobic and aerobic environment. Further, the genomics and metatranscriptomics of specific function enzymes under both conditions can be explored to understand the microbial metabolic mechanisms involved in SOM turnover.

## Bibliography

- Ågren, G.I., Bosatta, E., Magill, A.H., 2001. Combining theory and experiment to understand effects of inorganic nitrogen on litter decomposition. *Oecologia* 128, 94–98.
- Allison, S.D., Vitousek, P.M., 2005. Responses of extracellular enzymes to simple and complex nutrient inputs. *Soil Biology and Biochemistry* 37, 937–944.
- Anderson, K.A., Downing, J.A., 2006. Dry and wet atmospheric deposition of nitrogen, phosphorus and silicon in an agricultural region. *Water Air Soil Pollut* 176, 351–374.
- Atashgahi, S., Hornung, B., van der Waals, M.J., da Rocha, U.N., Hugenholtz, F., Nijse, B., Molenaar, D., van Spanning, R., Stams, A.J.M., Gerritse, J., Smidt, H., 2018. A benzene-degrading nitrate-reducing microbial consortium displays aerobic and anaerobic benzene degradation pathways. *Scientific reports* 8, 4490.
- Austin, A.T., Méndez, M.S., Ballaré, C.L., 2016. Photodegradation alleviates the lignin bottleneck for carbon turnover in terrestrial ecosystems. *Proceedings of the National Academy of Sciences* 113, 4392–4397.
- Baldock, J.A., Skjemstad, J.O., 2000. Role of the soil matrix and minerals in protecting natural organic materials against biological attack. *Organic Geochemistry* 31, 697–710.
- Baudoin, E., Benizri, E., Guckert, A., 2003. Impact of artificial root exudates on the bacterial community structure in bulk soil and maize rhizosphere. *Soil Biology and Biochemistry* 35, 1183–1192.
- Billings, A.F., Fortney, J.L., Hazen, T.C., Simmons, B., Davenport, K.W., Goodwin, L., Ivanova, N., Kyrpides, N.C., Mavromatis, K., Woyke, T., DeAngelis, K.M., 2015. Genome sequence and description of the anaerobic lignin-degrading bacterium *Tolumonas lignolytica* sp. nov. *Standards in genomic sciences* 10, 106.
- Blagodatskaya, E., Blagodatsky, S., Anderson, T.-H., Kuzyakov, Y., 2014. Microbial Growth and Carbon Use Efficiency in the Rhizosphere and Root-Free Soil. *PLoS ONE* 9.

- Boodt, M. de, Hayes, M.H.B., Herbillon, A., North Atlantic Treaty Organization (Eds.), 1990. Soil colloids and their associations in aggregates, NATO ASI series. Presented at the NATO Advanced Research Workshop on Soil Colloids and Their Associations in Aggregates, Plenum Press, New York.
- Borch, T., Kretzschmar, R., Kappler, A., Cappellen, P.V., Ginder-Vogel, M., Voegelin, A., Campbell, K., 2010. Biogeochemical Redox Processes and their Impact on Contaminant Dynamics. *Environmental science & technology* 44, 15–23.
- Borken, W., Matzner, E., 2009. Reappraisal of drying and wetting effects on C and N mineralization and fluxes in soils. *Global Change Biology* 15, 808–824.
- Brookes, P.C., Cayuela, M.L., Contin, M., De Nobili, M., Kemmitt, S.J., Mondini, C., 2008. The mineralisation of fresh and humified soil organic matter by the soil microbial biomass. *Waste Management* 28, 716–722.
- Brown, J.H., Gillooly, J.F., Allen, A.P., Savage, V.M., West, G.B., 2004. Toward a metabolic theory of ecology. *Ecology* 85, 1771–1789.
- Brown, R.W., Mayser, J.P., Widdowson, C., Chadwick, D.R., Jones, D.L., 2021. Dependence of thermal desorption method for profiling volatile organic compound (VOC) emissions from soil. *Soil Biology and Biochemistry* 160, 108313.
- Buckeridge, K.M., Mason, K.E., McNamara, N.P., Ostle, N., Puissant, J., Goodall, T., Griffiths, R.I., Stott, A.W., Whitaker, J., 2020. Environmental and microbial controls on microbial necromass recycling, an important precursor for soil carbon stabilization. *Communications Earth and Environment* 1, 36.
- Buée, M., De Boer, W., Martin, F., van Overbeek, L., Jurkevitch, E., 2009. The rhizosphere zoo: An overview of plant-associated communities of microorganisms, including phages, bacteria, archaea, and fungi, and of some of their structuring factors. *Plant and Soil* 321, 189–212.
- Burdon, J., 2001. Are the traditional concepts of the structures of humic substances realistic?. *Soil Science* 166, 752–769.
- Carter, M.R. and Gregorich, E.G., 2007. Soil sampling and methods of analysis. CRC press. Boca Raton.

- Chen, X., Hu, Y., Feng, S., Rui, Y., Zhang, Z., He, H., He, X., Ge, T., Wu, J., Su, Y., 2018. Lignin and cellulose dynamics with straw incorporation in two contrasting cropping soils. *Scientific reports* 8, 1633.
- Chen, X., Xia, Y., Rui, Y., Ning, Z., Hu, Y., Tang, H., He, H., Li, H., Kuzyakov, Y., Ge, T., Wu, J., Su, Y., 2020. Microbial carbon use efficiency, biomass turnover, and necromass accumulation in paddy soil depending on fertilization. *Agriculture, Ecosystems and Environment* 292, 106816.
- Chung, H., Grove, J.H., Six, J., 2008. Indications for Soil Carbon Saturation in a Temperate Agroecosystem. *Soil Science Society of America Journal* 72, 1132–1139.
- Coppens, F., Garnier, P., De Gryze, S., Merckx, R., Recous, S., 2006. Soil moisture, carbon and nitrogen dynamics following incorporation and surface application of labelled crop residues in soil columns. *European Journal of Soil Science* 57, 894–905.
- Cotrufo, M.F., Wallenstein, M.D., Boot, C.M., Denef, K., Paul, E., 2013. The Microbial Efficiency-Matrix Stabilization (MEMS) framework integrates plant litter decomposition with soil organic matter stabilization: do labile plant inputs form stable soil organic matter? *Global Change Biology* 19, 988–995.
- Creamer, C.A., Jones, D.L., Baldock, J.A., Farrell, M., 2014. Stoichiometric controls upon low molecular weight carbon decomposition. *Soil Biology and Biochemistry* 79, 50–56.
- Craine, J.M., Morrow, C., Fierer, N., 2007. microbial nitrogen limitation increases decomposition. *Ecology* 88, 2105–2113.
- Conant, Richard T., Keith Paustian, and Edward T. Elliott. 2001. Grassland management and conversion into grassland: effects on soil carbon. *Ecological Applications* 11 (2): 343–55.
- Curtin, D., Beare, M.H., Qiu, W., Sharp, J., 2019. Does Particulate Organic Matter Fraction Meet the Criteria for a Model Soil Organic Matter Pool? *Pedosphere* 29, 195–203.
- Dalal, R.C., 1998. Soil microbial biomass—what do the numbers really mean? *Australian Journal of Experimental Agriculture* 38, 649.

- D'Angelo, E., Reddy, K.R., 2003. Effect of Aerobic and Anaerobic Conditions on Chlorophenol Sorption in Wetland Soils. *Soil Science Society of America Journal* 67, 787–794.
- Davidson, E.A., Trumbore, S.E., Amundson, R., 2000. Soil warming and organic carbon content. *Nature* 408, 789–790.
- Devêvre, O.C., Horwáth, W.R., 2000. Decomposition of rice straw and microbial carbon use efficiency under different soil temperatures and moistures. *Soil Biology and Biochemistry* 32, 1773–1785.
- Drotz, S.H., Sparman, T., Nilsson, M.B., Schleucher, J., Oquist, M.G., 2010. Both catabolic and anabolic heterotrophic microbial activity proceed in frozen soils. *Proceedings of the National Academy of Sciences* 107, 21046–21051.
- Duboc, O., Dignac, M.-F., Djukic, I., Zehetner, F., Gerzabek, M.H., Rumpel, C., 2014. Lignin decomposition along an Alpine elevation gradient in relation to physicochemical and soil microbial parameters. *Global Change Biology* 20, 2272–2285
- Du, L., Zhu, Z., Qi, Y., Zou, D., Zhang, G., Zeng, X., Ge, T., Wu, J., Xiao, Z., 2020. Effects of different stoichiometric ratios on mineralisation of root exudates and its priming effect in paddy soil. *Science of The Total Environment* 743, 140808.
- Du Laing, G., Rinklebe, J., Vandecasteele, B., Meers, E., Tack, F.M.G., 2009. Trace metal behaviour in estuarine and riverine floodplain soils and sediments: A review. *Science of The Total Environment* 407, 3972–3985.
- Dunham-Cheatham, S.M., Zhao, Q., Obrist, D., Yang, Y., 2020. Unexpected mechanism for glucose-primed soil organic carbon mineralization under an anaerobic–aerobic transition. *Geoderma* 376, 114535.
- Ebrahimi, A., Or, D., 2016. Microbial community dynamics in soil aggregates shape biogeochemical gas fluxes from soil profiles - upscaling an aggregate biophysical model. *Global Change Biology* 22, 3141–3156.
- Francesca Cotrufo, M., Lavallee, J.M., Zhang, Y., Hansen, P.M., Paustian, K.H., Schipanski, M., Wallenstein, M.D., 2021. In -N- O ut: A hierarchical framework to understand



and predict soil carbon storage and nitrogen recycling. *Global Change Biology* 27, 4465–4468.

Friedlingstein, P., Jones, M.W., O’Sullivan, M., Andrew, R.M., Bakker, D.C.E., Hauck, J., Le Quéré, C., Peters, G.P., Peters, W., Pongratz, J., Sitch, S., Canadell, J.G., Ciais, P., Jackson, R.B., Alin, S.R., Anthoni, P., Bates, N.R., Becker, M., Bellouin, N., Bopp, L., Chau, T.T.T., Chevallier, F., Chini, L.P., Cronin, M., Currie, K.I., Decharme, B., Djeutchouang, L., Dou, X., Evans, W., Feely, R.A., Feng, L., Gasser, T., Gilfillan, D., Gkritzalis, T., Grassi, G., Gregor, L., Gruber, N., Gürses, Ö., Harris, I., Houghton, R.A., Hurtt, G.C., Iida, Y., Ilyina, T., Luijkx, I.T., Jain, A.K., Jones, S.D., Kato, E., Kennedy, D., Klein Goldewijk, K., Knauer, J., Korsbakken, J.I., Körtzinger, A., Landschützer, P., Lauvset, S.K., Lefèvre, N., Lienert, S., Liu, J., Marland, G., McGuire, P.C., Melton, J.R., Munro, D.R., Nabel, J.E.M.S., Nakaoka, S.-I., Niwa, Y., Ono, T., Pierrot, D., Poulter, B., Rehder, G., Resplandy, L., Robertson, E., Rödenbeck, C., Rosan, T.M., Schwinger, J., Schwingshackl, C., Séférian, R., Sutton, A.J., Sweeney, C., Tanhua, T., Tans, P.P., Tian, H., Tilbrook, B., Tubiello, F., van der Werf, G., Vuichard, N., Wada, C., Wanninkhof, R., Watson, A., Willis, D., Wiltshire, A.J., Yuan, W., Yue, C., Yue, X., Zaehle, S., Zeng, J., 2021. Global Carbon Budget 2021 (preprint). *Antroposphere Energy and Emissions*.

Friedlingstein, P., O’Sullivan, M., Jones, M.W., Andrew, R.M., Hauck, J., Olsen, A., Peters, G.P., Peters, W., Pongratz, J., Sitch, S., Le Quéré, C., Canadell, J.G., Ciais, P., Jackson, R.B., Alin, S., Aragão, L.E.O.C., Arneeth, A., Arora, V., Bates, N.R., Becker, M., Benoit-Cattin, A., Bittig, H.C., Bopp, L., Bultan, S., Chandra, N., Chevallier, F., Chini, L.P., Evans, W., Florentie, L., Forster, P.M., Gasser, T., Gehlen, M., Gilfillan, D., Gkritzalis, T., Gregor, L., Gruber, N., Harris, I., Hartung, K., Haverd, V., Houghton, R.A., Ilyina, T., Jain, A.K., Joetzjer, E., Kadono, K., Kato, E., Kitidis, V., Korsbakken, J.I., Landschützer, P., Lefèvre, N., Lenton, A., Lienert, S., Liu, Z., Lombardozzi, D., Marland, G., Metzl, N., Munro, D.R., Nabel, J.E.M.S., Nakaoka, S.-I., Niwa, Y., O’Brien, K., Ono, T., Palmer, P.I., Pierrot, D., Poulter, B., Resplandy, L., Robertson, E., Rödenbeck, C., Schwinger, J., Séférian, R., Skjelvan, I., Smith, A.J.P., Sutton, A.J., Tanhua, T., Tans, P.P., Tian, H., Tilbrook, B., van der Werf, G., Vuichard, N., Walker, A.P., Wanninkhof, R., Watson, A.J., Willis, D., Wiltshire, A.J., Yuan, W., Yue, X.,

- Zaehle, S., 2020. Global Carbon Budget 2020. *Earth System Science Data* 12, 3269–3340.
- Frimmel, F.H. and Christman, R.F., 1988. Humic substances and their role in the environment: report of the Dahlem Workshop on Humic. New York
- Fisk, L.M., Barton, L., Jones, D.L., Glanville, H.C., Murphy, D.V., 2015. Root exudate carbon mitigates nitrogen loss in a semi-arid soil. *Soil Biology and Biochemistry* 88, 380–389.
- Geisseler, D., Scow, K.M., 2014. Long-term effects of mineral fertilizers on soil microorganisms – A review. *Soil Biology and Biochemistry* 75, 54–63.
- German, D.P., Marcelo, K.R.B., Stone, M.M., Allison, S.D., 2012. The Michaelis-Menten kinetics of soil extracellular enzymes in response to temperature: a cross-latitudinal study. *Global Change Biology* 18, 1468–1479.
- Geyer, K.M., Kyker-Snowman, E., Grandy, A.S., Frey, S.D., 2016. Microbial carbon use efficiency: accounting for population, community, and ecosystem-scale controls over the fate of metabolized organic matter. *Biogeochemistry* 127, 173–188.
- Gillespie, A.W., Farrell, R.E., Walley, F.L., Ross, A.R.S., Leinweber, P., Eckhardt, K.-U., Regier, T.Z., Blyth, R.I.R., 2011. Glomalin-related soil protein contains non-mycorrhizal-related heat-stable proteins, lipids and humic materials. *Soil Biology and Biochemistry* 43, 766–777.
- Glaser, B., Turrión, M.-B., Alef, K., 2004. Amino sugars and muramic acid—biomarkers for soil microbial community structure analysis. *Soil Biology and Biochemistry* 36, 399–407.
- Gommers, P.J.F., van Schie, B.J., van Dijken, J.P., Kuenen, J.G., 1988. Biochemical limits to microbial growth yields: An analysis of mixed substrate utilization. *Biotechnology and bioengineering* 32, 86–94.
- Guan, H.L., Fan, J.W., Lu, X., 2022. Soil specific enzyme stoichiometry reflects nitrogen limitation of microorganisms under different types of vegetation restoration in the karst areas. *Applied Soil Ecology* 169, 104253.

- Guenet, B., Leloup, J., Raynaud, X., Bardoux, G., Abbadie, L., 2010. Negative priming effect on mineralization in a soil free of vegetation for 80 years. *European Journal of Soil Science* 61, 384–391.
- Guggenberger, G., 2005. Humification and Mineralization in Soils, in: Varma, A., Buscot, F. (Eds.), *Microorganisms in Soils: Roles in Genesis and Functions*, Soil Biology. Springer-Verlag, Heidelberg, Berlin.
- Hafner, S.D., Groffman, P.M., Mitchell, M.J., 2005. Leaching of dissolved organic carbon, dissolved organic nitrogen, and other solutes from coarse woody debris and litter in a mixed forest in New York State. *Biogeochemistry* 74, 257–282.
- Hai, L., Li, X.G., Li, F.M., Suo, D.R., Guggenberger, G., 2010. Long-term fertilization and manuring effects on physically-separated soil organic matter pools under a wheat–wheat–maize cropping system in an arid region of China. *Soil Biology and Biochemistry* 42, 253–259.
- Hall, S.J., Silver, W.L., Timokhin, V.I., Hammel, K.E., 2015. Lignin decomposition is sustained under fluctuating redox conditions in humid tropical forest soils. *Global Change Biology* 21, 2818–2828.
- Hamer, U., Marschner, B., Brodowski, S., Amelung, W., 2004. Interactive priming of black carbon and glucose mineralisation. *Organic Geochemistry* 35, 823–830.
- Hanke, A., Cerli, C., Muhr, J., Borken, W., Kalbitz, K., 2013. Redox control on carbon mineralization and dissolved organic matter along a chronosequence of paddy soils: Redox control on carbon turnover. *European Journal of Soil Science* 64, 476–487.
- Hasibeder, Roland, Lucia Fuchslueger, Andreas Richter, and Michael Bahn. 2015. ‘Summer Drought Alters C Allocation to Roots and Root Respiration in Mountain Grassland’. *New Phytologist* 205 (3): 1117–27
- Hazen, T.C., Dubinsky, E.A., DeSantis, T.Z., Andersen, G.L., Piceno, Y.M., Singh, N., Jansson, J.K., Probst, A., Borglin, S.E., Fortney, J.L., Stringfellow, W.T., Bill, M., Conrad, M.E., Tom, L.M., Chavarria, K.L., Alusi, T.R., Lamendella, R., Joyner, D.C., Spier, C., Baelum, J., Auer, M., Zemla, M.L., Chakraborty, R., Sonnenthal, E.L., D’haeseleer, P., Holman, H.-Y.N., Osman, S., Lu, Z., Van Nostrand, J.D., Deng, Y.,

- Zhou, J., Mason, O.U., 2010. Deep-Sea Oil Plume Enriches Indigenous Oil-Degrading Bacteria. *Science* 330, 204–208.
- Hessen, D.O., Ågren, G.I., Anderson, T.R., Elser, J.J., de Ruiter, P.C., 2004. Carbon sequestration in ecosystems: the role of stoichiometry. *Ecology* 85, 1179–1192.
- Hettiaratchi, J.P.A., Jayasinghe, P.A., Bartholameuz, E.M., Kumar, S., 2014. Waste degradation and gas production with enzymatic enhancement in anaerobic and aerobic landfill bioreactors. *Bioresource Technology* 159, 433–436.
- Hill, B.H., Elonen, C.M., Seifert, L.R., May, A.A., Tarquinio, E., 2012. Microbial enzyme stoichiometry and nutrient limitation in US streams and rivers. *Ecological Indicators* 18, 540–551.
- Hryniewicz, K., Baum, C., Leinweber, P., 2009. Mycorrhizal community structure, microbial biomass P and phosphatase activities under *Salix polaris* as influenced by nutrient availability. *European Journal of Soil Biology* 45, 168–175.
- Huang, Y., Guenet, B., Wang, Y.L., Ciais, P., 2021. Global Simulation and Evaluation of Soil Organic Matter and Microbial Carbon and Nitrogen Stocks Using the Microbial Decomposition Model Orchimic v2.0. *Global Biogeochemical Cycles* 35.
- Husson, O., 2013. Redox potential (Eh) and pH as drivers of soil, plant, microorganism systems: a transdisciplinary overview pointing to integrative opportunities for agronomy. *Plant and Soil* 362, 389–417.
- Joos, F., Spahni, R., 2008. Rates of change in natural and anthropogenic radiative forcing over the past 20,000 years. *Proceedings of the National Academy of Sciences* 105, 1425–1430.
- Kallenbach, C.M., Frey, S.D., Grandy, A.S., 2016. Direct evidence for microbial-derived soil organic matter formation and its ecophysiological controls. *Nature Communications* 7, 13630.
- Kelleher, Brian.P., Simpson, Andre.J., 2006. Humic Substances in Soils: Are They Really Chemically Distinct? *Environmental Science and Technology* 40, 4605–4611.

- Kelley, A.M., Fay, P.A., Polley, H.W., Gill, R.A., Jackson, R.B., 2011. Atmospheric CO<sub>2</sub> and soil extracellular enzyme activity: a meta-analysis and CO<sub>2</sub> gradient experiment. *Ecosphere* 2(8), art96.
- Kieft, T.L., Ringelberg, D.B., White, D.C., 1994. Changes in Ester-Linked Phospholipid Fatty Acid Profiles of Subsurface Bacteria during Starvation and Desiccation in a Porous Medium. *Applied and Environmental Microbiology* 60, 3292–3299.
- Kimura, M., Asakawa, S., 2006. Comparison of community structures of microbiota at main habitats in rice field ecosystems based on phospholipid fatty acid analysis. *Biology and Fertility of Soils* 43, 20–29.
- Kindler, R., Siemens, J., Kaiser, K., Walmsley, D.C., Bernhofer, C., Buchmann, N., Cellier, P., Eugster, W., Gleixner, G., Grünwald, T., Heim, A., Ibrom, A., Jones, S.K., Jones, M., Klumpp, K., Kutsch, W., Larsen, K.S., Lehuger, S., Loubet, B., McKenzie, R., Moors, E., Osborne, B., Pilegaard, K., Reibmann, C., Saunders, M., Schmidt, M.W.I., Schrumpf, M., Seyfferth, J., Skiba, U., Soussana, J.-F., Sutton, M.A., Tefs, C., Vowinckel, B., Zeeman, M.J., Kaupenjohann, M., 2011. Dissolved carbon leaching from soil is a crucial component of the net ecosystem carbon balance: Dissolved carbon leaching. *Global Change Biology* 17, 1167–1185.
- Kirkby, C.A., Richardson, A.E., Wade, L.J., Conyers, M., Kirkegaard, J.A., 2016. Inorganic Nutrients Increase Humification Efficiency and C-Sequestration in an Annually Cropped Soil. *PLoS ONE* 11, e0153698.
- Kögel-Knabner, I., Amelung, W., Cao, Z., Fiedler, S., Frenzel, P., Jahn, R., Kalbitz, K., Kölbl, A., Schloter, M., 2010. Biogeochemistry of paddy soils. *Geoderma* 157, 1–14.
- Kong, Angela Y. Y., Johan Six, Dennis C. Bryant, R. Ford Denison, and Chris van Kessel. 2005. The Relationship between C Input, Aggregation, and Soil Organic C Stabilization in Sustainable Cropping Systems. *Soil Science Society of America Journal* 69 (4): 1078–85
- Kononova, M.M., 1966. *Soil Organic Matter*. Pergamon.
- Kramer, C., Gleixner, G., 2006. Variable use of plant- and soil-derived carbon by microorganisms in agricultural soils. *Soil Biology and Biochemistry* 38, 3267–3278.

- Kuzyakov, Y., 2010. Priming effects: Interactions between living and dead organic matter. *Soil Biology and Biochemistry* 42, 1363–1371.
- Kuzyakov, Y., Mason-Jones, K., 2018. Viruses in soil: Nano-scale undead drivers of microbial life, biogeochemical turnover and ecosystem functions. *Soil Biology and Biochemistry* 127, 305–317.
- La Manna, L., Tarabini, M., Gomez, F., Rostagno, C.M., 2021. Changes in soil organic matter associated with afforestation affect erosion processes: The case of erodible volcanic soils from Patagonia. *Geoderma* 403, 115265.
- Lal, R., 2002. Soil carbon dynamics in cropland and rangeland. *Environmental Pollution* 116, 353–362.
- Lal, R., Follett, R.F., Kimble, J. and Cole, C.V., 1999. Managing US cropland to sequester carbon in soil. *Journal of Soil and Water Conservation* 54(1),374-381.
- Lehmann, J., Kleber, M., 2015. The contentious nature of soil organic matter. *Nature* 528, 60–68.
- Lehmann, J., Skjemstad, J., Sohi, S., Carter, J., Barson, M., Falloon, P., Coleman, K., Woodbury, P., Krull, E., 2008. Australian climate–carbon cycle feedback reduced by soil black carbon. *Nature Geoscience* 1, 832–835.
- Li, T., Peng, C., Bu, Z., Zhu, Q., Song, H., Guo, X., Wang, M., 2021. Woody plants reduce the sensitivity of soil extracellular enzyme activity to nutrient enrichment in wetlands: A meta-analysis. *Soil Biology and Biochemistry* 159, 108280.
- Liang, C., Schimel, J.P., Jastrow, J.D., 2017. The importance of anabolism in microbial control over soil carbon storage. *Nature Microbiology* 2, 17105.
- Liu, L., Gundersen, P., Zhang, T., Mo, J., 2012. Effects of phosphorus addition on soil microbial biomass and community composition in three forest types in tropical China. *Soil Biology and Biochemistry* 44, 31–38.
- Liu, Y., Shahbaz, M., Ge, T., Zhu, Z., Liu, S., Chen, L., Wu, X., Deng, Y., Lu, S., Wu, J., 2020. Effects of root exudate stoichiometry on CO<sub>2</sub> emission from paddy soil. *European Journal of Soil Biology* 101, 103247.

- Lorenz, K., Lal, R., 2009. Biogeochemical C and N cycles in urban soils. *Environment International* 35, 1–8.
- Luo, Z., Wang, E., Sun, O.J., 2010. Soil carbon change and its responses to agricultural practices in Australian agro-ecosystems: A review and synthesis. *Geoderma* 155, 211–223.
- Luo, Zhongkui, Enli Wang, and Osbert Jianxin Sun. 2010. Soil C Change and Its Responses to Agricultural Practices in Australian Agro-Ecosystems: A Review and Synthesis. *Geoderma* 155 (3–4): 211–23
- Lützw, M. v., Kögel-Knabner, I., Ekschmitt, K., Matzner, E., Guggenberger, G., Marschner, B., Flessa, H., 2006. Stabilization of organic matter in temperate soils: mechanisms and their relevance under different soil conditions - a review: Mechanisms for organic matter stabilization in soils. *European Journal of Soil Science* 57, 426–445.
- Lynam, M.M., Dvonch, J.T., Hall, N.L., Morishita, M., Barres, J.A., 2014. Spatial patterns in wet and dry deposition of atmospheric mercury and trace elements in central Illinois, USA. *Environmental Science and Pollution Research* 21, 4032–4043.
- Ma, S., Chen, G., Tang, W., Xing, A., Chen, X., Xiao, W., Zhou, L., Zhu, J., Li, Y., Zhu, B., Fang, J., 2021. Inconsistent responses of soil microbial community structure and enzyme activity to nitrogen and phosphorus additions in two tropical forests. *Plant and Soil* 460, 453–468.
- Manzoni, S., Taylor, P., Richter, A., Porporato, A., Ågren, G.I., 2012b. Environmental and stoichiometric controls on microbial carbon-use efficiency in soils. *New Phytologist* 196, 79–91.
- Marzaioli, F., Lubritto, C., Galdo, I.D., D’Onofrio, A., Cotrufo, M.F., Terrasi, F., 2010. Comparison of different soil organic matter fractionation methodologies: Evidences from ultrasensitive <sup>14</sup>C measurements. *Nuclear Instruments and Methods in Physics Research Section B: Beam Interactions with Materials and Atoms* 268, 1062–1066.
- Meier, I.C., Finzi, A.C., Phillips, R.P., 2017. Root exudates increase N availability by stimulating microbial turnover of fast-cycling N pools. *Soil Biology and Biochemistry* 106, 119–128.

- Midwood, A.J., Hannam, K.D., Gebretsadikan, T., Emde, D., Jones, M.D., 2021. Storage of soil carbon as particulate and mineral associated organic matter in irrigated woody perennial crops. *Geoderma* 403, 115185.
- Miltner, A., Bombach, P., Schmidt-Brücken, B., Kästner, M., 2012. SOM genesis: microbial biomass as a significant source. *Biogeochemistry* 111, 41–55.
- Moche, M., Gutknecht, J., Schulz, E., Langer, U., Rinklebe, J., 2015. Monthly dynamics of microbial community structure and their controlling factors in three floodplain soils. *Soil Biology and Biochemistry* 90, 169–178.
- Mooshammer, M., Wanek, W., Hämmerle, I., Fuchslueger, L., Hofhansl, F., Knoltsch, A., Schnecker, J., Takriti, M., Watzka, M., Wild, B., Keiblinger, K.M., Zechmeister-Boltenstern, S., Richter, A., 2014. Adjustment of microbial nitrogen use efficiency to carbon:nitrogen imbalances regulates soil nitrogen cycling. *Nature Communications* 5, 3694.
- Mylotte, R., Verheyen, V., Reynolds, A., Dalton, C., Patti, A.F., Chang, R.R., Burdon, J., Hayes, M.H.B., 2015. Isolation and characterisation of recalcitrant organic components from an estuarine sediment core. *Journal of Soils and Sediments* 15, 211–224.
- Nakamura, A., Tun, C.C., Asakawa, S., Kimura, M., 2003. Microbial community responsible for the decomposition of rice straw in a paddy field: estimation by phospholipid fatty acid analysis. *Biology and Fertility of Soils* 38, 288–295.
- Olander, L.P., Vitousek, P.M., 2000. Regulation of soil phosphatase and chitinase activity by N and P availability. *Biogeochemistry* 49, 175–191.
- Olk, D.C., Cassman, K.G., Schmidt-Rohr, K., Anders, M.M., Mao, J.-D., Deenik, J.L., 2006. Chemical stabilization of soil organic nitrogen by phenolic lignin residues in anaerobic agroecosystems. *Soil Biology and Biochemistry* 38, 3303–3312.
- Oppermann, B.I., Michaelis, W., Blumenberg, M., Frerichs, J., Schulz, H.M., Schippers, A., Beaubien, S.E., Krüger, M., 2010. Soil microbial community changes as a result of long-term exposure to a natural CO<sub>2</sub> vent. *Geochimica et Cosmochimica Acta* 74, 2697–2716.



- Ossohou, M., Galy-Lacaux, C., Yoboué, V., Adon, M., Delon, C., Gardrat, E., Konaté, I., Ki, A., Zouzou, R., 2021. Long-term atmospheric inorganic nitrogen deposition in West African savanna over 16 year period (Lamto, Côte d'Ivoire). *Environmental Research Letters* 16, 015004.
- Pan, G., Li, L., Wu, L., Zhang, X., 2004. Storage and sequestration potential of topsoil organic carbon in China's paddy soils. *Global Change Biology* 10, 79–92.
- Panikov, N.S., 1999. Understanding and prediction of soil microbial community dynamics under global change. *Applied Soil Ecology* 11, 161–176.
- Perli, T., Vos, A.M., Bouwknecht, J., Dekker, W.J.C., Wiersma, S.J., Mooiman, C., Ortiz-Merino, R.A., Daran, J.-M., Pronk, J.T., 2021. Identification of Oxygen-Independent Pathways for Pyridine Nucleotide and Coenzyme A Synthesis in Anaerobic Fungi by Expression of Candidate Genes in Yeast. *mBio* 12.
- Poeplau, C., Helfrich, M., Dechow, R., Szoboszlay, M., Tebbe, C.C., Don, A., Greiner, B., Zopf, D., Thumm, U., Korevaar, H., Geerts, R., 2019. Increased microbial anabolism contributes to soil carbon sequestration by mineral fertilization in temperate grasslands. *Soil Biology and Biochemistry* 130, 167–176.
- Qian, Z., Zhuang, S., Gao, J., Tang, L., Harindintwali, J.D., Wang, F., 2022. Aeration increases soil bacterial diversity and nutrient transformation under mulching-induced hypoxic conditions. *Science of The Total Environment* 817, 153017
- Qiu, H., Zheng, X., Ge, T., Dorodnikov, M., Chen, X., Hu, Y., Kuzyakov, Y., Wu, J., Su, Y., Zhang, Z., 2017. Weaker priming and mineralisation of low molecular weight organic substances in paddy than in upland soil. *European Journal of Soil Biology* 83, 9–17.
- Rimmer, D.L., 2006. Free radicals, antioxidants, and soil organic matter recalcitrance: Antioxidants and organic matter recalcitrance. *European Journal of Soil Science* 57, 91–94.
- Rodionov, A., Amelung, W., Peinemann, N., Haumaier, L., Zhang, X., Kleber, M., Glaser, B., Urusevskaya, I., Zech, W., 2010. Black carbon in grassland ecosystems of the world. *Global Biogeochemical Cycles* 24(3).

- Rodríguez, A., Durán, J., Rey, A., Boudouris, I., Valladares, F., Gallardo, A., Yuste, J.C., 2019. Interactive effects of forest die-off and drying-rewetting cycles on C and N mineralization. *Geoderma* 333, 81–89.
- Rosinger, C., Rousk, J., Sandén, H., 2019. Can enzymatic stoichiometry be used to determine growth-limiting nutrients for microorganisms? - A critical assessment in two subtropical soils. *Soil Biology and Biochemistry* 128, 115–126.
- Schimel, J., 2003. The implications of exoenzyme activity on microbial carbon and nitrogen limitation in soil: a theoretical model. *Soil Biology and Biochemistry* 35, 549–563.
- Schimel, J.P., Schaeffer, S.M., 2012. Microbial control over carbon cycling in soil. *Frontiers in Microbiology* 3.
- Schmidt, M.W.I., Torn, M.S., Abiven, S., Dittmar, T., Guggenberger, G., Janssens, I.A., Kleber, M., Kögel-Knabner, I., Lehmann, J., Manning, D.A.C., Nannipieri, P., Rasse, D.P., Weiner, S., Trumbore, S.E., 2011. Persistence of soil organic matter as an ecosystem property. *Nature* 478, 49–56.
- Schurig, C., Smittenberg, R.H., Berger, J., Kraft, F., Woche, S.K., Goebel, M.-O., Heipieper, H.J., Miltner, A., Kaestner, M., 2013. Microbial cell-envelope fragments and the formation of soil organic matter: a case study from a glacier forefield. *Biogeochemistry* 113, 595–612.
- Schwertmann, U., 1991. Solubility and dissolution of iron oxides. *Plant and Soil* 130, 1–25.
- Sierra, C.A., Trumbore, S.E., Davidson, E.A., Vicca, S., Janssens, I., 2015. Sensitivity of decomposition rates of soil organic matter with respect to simultaneous changes in temperature and moisture. *Journal of Advances in Modeling Earth Systems* 7, 335–356.
- Silva-Olaya, A.M., Mora-Motta, D.A., Cherubin, M.R., Grados, D., Somenahally, A., Ortiz-Morea, F.A., 2021. Soil enzyme responses to land use change in the tropical rainforest of the Colombian Amazon region. *PLoS ONE* 16, e0255669.
- Sinsabaugh, R.L., Follstad Shah, J.J., 2012. Ecoenzymatic Stoichiometry and Ecological Theory. *Annual Review of Ecology, Evolution, and Systematics* 43, 313–343

- Sinsabaugh, R.L., Manzoni, S., Moorhead, D.L., Richter, A., 2013. Carbon use efficiency of microbial communities: stoichiometry, methodology and modelling. *Ecology Letters* 16, 930–939.
- Six, J., Elliott, E.T., Paustian, K., Doran, J.W., 1998. Aggregation and Soil Organic Matter Accumulation in Cultivated and Native Grassland Soils. *Soil Science Society of America Journal* 62, 1367-1377.
- Skjemstad, J., Clarke, P., Taylor, J., Oades, J., McClure, S., 1996. The chemistry and nature of protected carbon in soil. *Soil Research*. 34, 251.
- Sohi, S.P., Krull, E., Lopez-Capel, E., Bol, R., 2010. A review of biochar and its use and function in soil. *Advances in Agronomy*. 105, 47–82.
- Sokol, N.W., Bradford, M.A., 2019. Microbial formation of stable soil carbon is more efficient from belowground than aboveground input. *Nature Geoscience* 12, 46–53.
- Sollins, P., Homann, P., Caldwell, B.A., 1996. Stabilization and destabilization of soil organic matter: mechanisms and controls. *Geoderma* 74, 65–105.
- Song, N., Xu, H., Yan, Z., Yang, T., Wang, C., Jiang, H.-L., 2019. Improved lignin degradation through distinct microbial community in subsurface sediments of one eutrophic lake. *Renewable Energy* 138, 861–869.
- Spaccini, R., 2002. Increased soil organic carbon sequestration through hydrophobic protection by humic substances. *Soil Biology and Biochemistry* 34, 1839–1851.
- Sperlich, D., Barbeta, A., Ogaya, R., Sabaté, S., Peñuelas, J., 2016. Balance between carbon gain and loss under long-term drought: impacts on foliar respiration and photosynthesis in *Quercus ilex* L. *Journal of Experimental Botany* 67, 821–833.
- Spohn, M., Klaus, K., Wanek, W., Richter, A., 2016. Microbial carbon use efficiency and biomass turnover times depending on soil depth – Implications for carbon cycling. *Soil Biology and Biochemistry* 96, 74–81.
- Stevenson, F.J., 1994. *Humus chemistry: genesis, composition, reactions*, 2nd ed. Wiley, New York.
- Stevenson, F.J., Cole, M.A., 1999. *Cycles of soil: carbon, nitrogen, phosphorus, sulfur, micronutrients*, second ed. Wiley, New York.

- Stewart, C.E., Paustian, K., Conant, R.T., Plante, A.F., Six, J., 2008. Soil carbon saturation: Evaluation and corroboration by long-term incubations. *Soil Biology and Biochemistry* 40, 1741–1750.
- Stone, M.M., DeForest, J.L., Plante, A.F., 2014. Changes in extracellular enzyme activity and microbial community structure with soil depth at the Luquillo Critical Zone Observatory. *Soil Biology and Biochemistry* 75, 237–247.
- Suetsugu, A., Sato, T., Kaneta, Y., Sato, A., 2005. Effects of Organo-mineral Complexes on Flocculation, Settlement and Vertical Distribution of Bioelements in Soil Suspensions. *Soil Science and Plant Nutrition* 51, 323–331.
- Sumner, M.E. (Ed.), 2000. *Handbook of soil science*. CRC Press, Boca Raton, Fla.
- Sun, Y., Zang, H., Splettstößer, T., Kumar, A., Xu, X., Kuzyakov, Y., Pausch, J., 2021. Plant intraspecific competition and growth stage alter carbon and nitrogen mineralization in the rhizosphere. *Plant, Cell and Environment* 44, 1231–1242.
- Tagami, K., Twining, J.R., Wasserman, M.A.V., 2012. Terrestrial Radioecology in Tropical Systems, in: *Radioactivity in the Environment*. Elsevier, 18 155–230.
- Tangyu, M., Muller, J., Bolten, C.J., Wittmann, C., 2019. Fermentation of plant-based milk alternatives for improved flavour and nutritional value. *Appl Microbiol Biotechnol* 103, 9263–9275.
- Tate, R.L., 1987. *Soil organic matter: biological and ecological effects*. Wiley, New York.
- Trumbore, S.E., 1997. Potential responses of soil organic carbon to global environmental change. *Proceedings of the National Academy of Sciences* 94, 8284–8291.
- Ueki, A., Kaku, N., Ueki, K., 2018. Role of anaerobic bacteria in biological soil disinfection for elimination of soil-borne plant pathogens in agriculture. *Applied microbiology and biotechnology* 102, 6309–6318.
- Vanni, M.J., McIntyre, P.B., 2016. Predicting nutrient excretion of aquatic animals with metabolic ecology and ecological stoichiometry: a global synthesis. *Ecology* 97, 3460–3471.

- Viscarra Rossel, R.A., Webster, R., Bui, E.N., Baldock, J.A., 2014. Baseline map of organic carbon in Australian soil to support national carbon accounting and monitoring under climate change. *Global Change Biology* 20, 2953–2970.
- Wang, Y., Shahbaz, M., Zhran, M., Chen, A., Zhu, Z., Galal, Y.G.M., Ge, T., Li, Y., 2021. Microbial Resource Limitation in Aggregates in Karst and Non-Karst Soils. *Agronomy* 11, 1591.
- Wei, X., Hu, Y., Cai, G., Yao, H., Ye, J., Sun, Q., Veresoglou, S.D., Li, Yaying, Zhu, Z., Guggenberger, G., Chen, X., Su, Y., Li, Yong, Wu, J., Ge, T., 2021. Organic phosphorus availability shapes the diversity of phoD-harboring bacteria in agricultural soil. *Soil Biology and Biochemistry* 161, 108364.
- Widdig, M., Schleuss, P.-M., Biederman, L.A., Borer, E.T., Crawley, M.J., Kirkman, K.P., Seabloom, E.W., Wragg, P.D., Spohn, M., 2020. Microbial carbon use efficiency in grassland soils subjected to nitrogen and phosphorus additions. *Soil Biology and Biochemistry* 146, 107815.
- Wiesenberg, G., Schwarzbauer, J., Schmidt, M., Schwark, L., 2004. Source and turnover of organic matter in agricultural soils derived from n-alkane/n-carboxylic acid compositions and C-isotope signatures. *Organic Geochemistry* 35, 1371–1393.
- Wild, B., Schnecker, J., Alves, R.J.E., Barsukov, P., Bárta, J., Čapek, P., Gentsch, N., Gittel, A., Guggenberger, G., Lashchinskiy, N., Mikutta, R., Rusalimova, O., Šantrůčková, H., Shibistova, O., Urich, T., Watzka, M., Zrazhevskaya, G., Richter, A., 2014. Input of easily available organic C and N stimulates microbial decomposition of soil organic matter in arctic permafrost soil. *Soil Biology and Biochemistry* 75, 143–151
- Woo, H.L., Ballor, N.R., Hazen, T.C., Fortney, J.L., Simmons, B., Davenport, K.W., Goodwin, L., Ivanova, N., Kyrpides, N.C., Mavromatis, K., Woyke, T., Jansson, J., Kimbrel, J., DeAngelis, K.M., 2014. Complete genome sequence of the lignin-degrading bacterium *Klebsiella* sp. strain BRL6-2. *Standards in Genomic Sciences* 9, 19.
- Xiao, W., Chen, X., Jing, X., Zhu, B., 2018. A meta-analysis of soil extracellular enzyme activities in response to global change. *Soil Biology and Biochemistry* 123, 21–32.

- Xu, Z., Zhang, T., Wang, S., Wang, Z., 2020. Soil pH and C/N ratio determines spatial variations in soil microbial communities and enzymatic activities of the agricultural ecosystems in Northeast China: Jilin Province case. *Applied Soil Ecology* 155, 103629.
- Yang, J., Yang, Y., Wu, W.-M., Zhao, J., Jiang, L., 2014. Evidence of Polyethylene Biodegradation by Bacterial Strains from the Guts of Plastic-Eating Waxworms. *Environmental Science and Technology* 48, 13776–13784.
- Yang, Y., Liang, C., Wang, Y., Cheng, H., An, S., Chang, S.X., 2020. Soil extracellular enzyme stoichiometry reflects the shift from P- to N-limitation of microorganisms with grassland restoration. *Soil Biology and Biochemistry* 149, 107928.
- Yao, L., Rashti, M.R., Brough, D.M., Burford, M.A., Liu, W., Liu, G., Chen, C., 2019. Stoichiometric control on riparian wetland carbon and nutrient dynamics under different land uses. *Science of The Total Environment* 697, 134127.
- Youssef, N.H., Couger, M.B., Struchtemeyer, C.G., Ligginstoffer, A.S., Prade, R.A., Najjar, F.Z., Atiyeh, H.K., Wilkins, M.R., Elshahed, M.S., 2013. The Genome of the Anaerobic Fungus *Orpinomyces* sp. Strain C1A Reveals the Unique Evolutionary History of a Remarkable Plant Biomass Degrader. *Applied and Environmental Microbiology* 79, 4620–4634.
- Yu, P., Davis, S.M., Toon, O.B., Portmann, R.W., Bardeen, C.G., Barnes, J.E., Telg, H., Maloney, C., Rosenlof, K.H., 2021. Persistent Stratospheric Warming Due to 2019–2020 Australian Wildfire Smoke. *Geophysical Research Letters* 48(7).
- Zeglin, L.H., Kluber, L.A., Myrold, D.D., 2013. The importance of amino sugar turnover to C and N cycling in organic horizons of old-growth Douglas-fir forest soils colonized by ectomycorrhizal mats. *Biogeochemistry* 112, 679–693.
- Zhang, Qian, Wu, J., Yang, F., Lei, Y., Zhang, Quanfa, Cheng, X., 2016. Alterations in soil microbial community composition and biomass following agricultural land use change. *Scientific Reports* 6, 36587.
- Zhang, X., Dippold, M.A., Kuzyakov, Y., Razavi, B.S., 2019. Spatial pattern of enzyme activities depends on root exudate composition. *Soil Biology and Biochemistry* 133, 83–93.

- Zheng, Jufeng, Chen, J., Pan, G., Wang, G., Liu, X., Zhang, X., Li, L., Bian, R., Cheng, K., Zheng, Jinwei, 2017. A long-term hybrid poplar plantation on cropland reduces soil organic carbon mineralization and shifts microbial community abundance and composition. *Applied Soil Ecology* 111, 94–104.
- Zheng, T., Xie, H., Thompson, G.L., Bao, X., Deng, F., Yan, E., Zhou, X., Liang, C., 2021. Shifts in microbial metabolic pathway for soil carbon accumulation along subtropical forest succession. *Soil Biology and Biochemistry* 160, 108335.
- Zhu, Z., Ge, T., Luo, Y., Liu, S., Xu, X., Tong, C., Shibistova, O., Guggenberger, G., Wu, J., 2018. Microbial stoichiometric flexibility regulates rice straw mineralization and its priming effect in paddy soil. *Soil Biology and Biochemistry* 121, 67–76.

## Acknowledgments

I sincerely thank my supervisor, Professor. Georg Guggenberger has always been highly encouraged, supported, and organized throughout my Ph.D. During these four years of study in Hanover, his foresight and ardor for research have inspired me, and I have greatly benefited from his professional suggestions, wit, and wisdom. Without his guidance and support, most of my work would be impossible to complete.

I am deeply indebted to my second supervisor (as I define it), Dr. Leopold Sauheidl, who has always been highly instructive, caring, and enthusiastic in organizing the work in the lab during my Ph.D. His kind help always made my experiment run smoothly, and his advice made my mind clear. Finally, I am very grateful to Dr. Norman Gentsch for his kind help with the soil samples collected from the field and for showing me the first statistic analysis in R.

I deeply cherished working with all laboratory members, especially Anne Katrin Herwig, Elke Eichmann–Prusch, Silke Bokeloh, Roger–Michael Klatt, Viola Rünzi, Pieter Wiese, Ulrike Pieper. You always provided me with some practical tips and support when I worked in the laboratory. I want to thank my colleagues Dr. Olga Shibistova, Dr. Katharina Leiber–Sauheidl, Dr. Susanne Woche, Dr. Jens Boy, Dr. Jannis Florian Carstens Dr. Alberto Andrino de la Fuente, PD Dr. Stenfan Dultz, who always gives me expert advice when I have a scientific question.

I am thankful to the members of the chemistry group of our institute, especially Aline Fernandes Figueiredo, Carolina Urbina Malo, Elisa Diaz Garica, Jiem Krüger, Katharina Schreider, Markus Koch, Oliver Donnerhack, Partrick Liebmann, Reyhane Eslamikhah. I am thrilled and blessed to have you all with me during my Ph.D. study in Hannover.

Finally, I would like to thank my family and friends who have supported me in spirit and cheered me on during the past four years. I would also like to mention my little nieces, who always bring a lot of birdsong laughter to my daily life and make the study career exceptionally enjoyable.

I am sincerely grateful to have had such a memorable and cherished time with you all during my Ph.D. in Hannover, Germany.

26<sup>th</sup> October 2021



## Curriculum vitae and publications

### Cai Guan

Glünderstr. 8, 30167, Hannover, Germany

E-mail: [guanajs@gmail.com](mailto:guanajs@gmail.com)

Date and place of birth: 19<sup>th</sup> September 1992, Changsha, China

#### Educational experience:

- 2017.11-a.p. Dissertation. Institute of Soil Science, Leibniz University Hannover, Hannover 30419, Germany
- 2015.8-2017.10 Master study. Key Laboratory of Agro-Ecological Processes in Subtropical Region, Institute of Subtropical Agriculture, Chinese Academy of Sciences, Changsha 410125, China
- 2014.9-2015.7 Master study, College of Bioscience and Biotechnology, Hunan Agricultural University, Changsha 410128, China
- 2010.9-2014.6 Undergraduate study, College of Orient Science & Technology, Hunan Agricultural University, Changsha 410128, China
- 2007.9-2010.6 Full Middle Education, in NO.21 Middle School, Changsha 410007, China

#### Research:

- 2014.9-a.p. Soil organic matter cycling in response to land use and environmental change, <sup>13</sup>C isotope signature technology, Microbiology, Lignin degradation, Soil phosphorus, Soil enzyme, Dissolved organic matter.

#### Publications:

- 2022 **Guan Cai**, Norman Gentsch, Tida Ge, Jiří Bárta, Karin Pritsch, Olga Shibistova, Leopold Sauheitl, Georg Guggenberger. (2022). "Lignin degradation during anaerobic and aerobic processes in wetland". *In preparation*.
- 2022 **Guan Cai**, Muhammad Shahbaz, Zhenke Zhu, Yajun Hu, Yuhuai Liu,

- Olga Shibistova, Leopold Sauheitl, Jinshui Wu, Georg Guggenberger, Tida Ge. (2022). "Different root exudates C/N ratios accelerate CO<sub>2</sub> emission from paddy soil". *Land Degradation and Development* <https://doi.org/10.1002/ldr.4198>.
- 2021 Wei, Xiaomeng, Yajun Hu, **Guan Cai**, Huaiying Yao, Jun Ye, Qi Sun, Stavros D. Veresoglou, Yaying Li, Zhenke Zhu, Georg Guggenberger, Xiangbi Chen, Yirong Su, Yong Li, Jinshui Wu, Tida Ge. "Organic phosphorus availability shapes the diversity of phoD-harboring bacteria in agricultural soil." *Soil Biology and Biochemistry* (2021): 108364. <https://doi.org/10.1016/j.soilbio.2021.108364>.